"FEDERICO II" UNIVERSITY OF NAPLES

SCHOOL OF MEDICINE

PhD PROGRAM IN NEUROSCIENCE

XXXI cycle

Role of the lysosomal channel
Transient Receptor Potential Mucolipin 1 (TRPML1)
in the functional coupling between endoplasmic reticulum and
lysosomes in experimental models of brain ischemia

Tutor:

Prof. Agnese Secondo

PhD Student:

Dr. Valentina Tedeschi

Coordinator:

Prof. Maurizio Taglialatela

Academic year 2017/2018

SUMMARY

ABSTRACT

A growing interest has been recently devoted to the role of intracellular Ca^{2+} stores in brain ischemia. For instance, disturbances of Ca^{2+} content in the endoplasmic reticulum (ER), the main intracellular Ca^{2+} store, have been reported as one of the main mechanisms underlying this neurological disease. Interestingly, lysosomes are emerging as other important Ca^{2+}-storing organelles, cooperating with the ER in the handling of intracellular Ca^{2+} concentration ($[Ca^{2+}]_i$). One of the main regulators of lysosomal Ca^{2+} homeostasis is represented by *Transient Receptor Potential Mucolipin 1* (TRPML1), a non-selective cation channel releasing lysosomal Ca^{2+} into the cytosol.

In this study we investigated the role of ER/lysosome Ca^{2+} coupling and the contribution of TRPML1 in brain ischemia. Our results showed that under physiological conditions TRPML1 activation induced by its specific agonist ML-SA1 or by lysosomal v-ATPase inhibitor bafilomycin A1 significantly increased $[Ca^{2+}]_i$ in cortical neurons. ML-SA1-induced Ca^{2+} leak from lysosomes strongly reduced ER Ca^{2+} content, whereas the TRPML1 inhibitor *trans*-Ned19 or channel knocking down increased ER Ca^{2+} levels. However, this interplay was disrupted under hypoxic conditions produced by exposing cortical neurons to oxygen and glucose deprivation (OGD) followed by reoxygenation (Rx). Indeed, during OGD/Rx both ER and lysosomal Ca^{2+} levels were significantly impaired. Interestingly, the administration of *trans*-Ned19 during the reoxygenation phase prevented dysfunctional lysosomal Ca^{2+} homeostasis and neuronal death. In consideration of the role played by lysosomes in autophagy regulation, we showed that *trans*-Ned19 hampered the autophagic flux during hypoxia thus protecting neurons. Moreover, we found that in ischemic rats subjected to the transient occlusion of the middle cerebral artery (tMCAO) the intracerebroventricular (icv) administration of this drug at the onset of reperfusion was able to reduce the brain ischemic

volume, ameliorated the general and focal deficits, and promoted a protective blockade of the autophagic flux.

Collectively, the results presented in my PhD thesis demonstrate the detrimental role of TRPML1 dysfunction in the neurodegeneration associated to brain ischemia, thus identifying a novel potential therapeutic target that could be pharmacologically modulated, together with other relevant mechanisms, to induce neuroprotection.

1. INTRODUCTION

1.1 Lysosome: the cell's recycling centre

Lysosomes are membrane-enclosed intracellular organelles, identified and characterized by the Belgian cytologist and biochemist Christian de Duve in 1955 using a cell fractionation technique (de Duve C. *et al.*, 1955). The term "lysosomes" originated from the Greek words λύσις/*lysis*, which means dissolution or destruction, and σῶμα/*soma*, which means body, thus reflecting the ability of these organelles to degrade specific substrates within the cell. Lysosomes can be found in almost all animal cells with the exception of very few, highly specialized cell types, including red blood cells (Allison A. *et al.*, 1967). Each mammalian cell normally contains several hundreds of lysosomes, which comprise up to 5% of the intracellular volume. They are heterogeneous in size and morphology; indeed, their canonical diameter ranges from 50 nm to 500 nm and, although they often show a globular shape, sometimes they can be tubular. Moreover, they often contain electron-dense deposits within their lumen and sometimes multilamellar membrane whorls. Lysosomal size and number can vary in cells following different pathophysiological stimuli. For instance, the accumulation of undigested materials within their lumen leads to a dramatic increase in both their size and number. By contrast, upon nutrient starvation, lysosomal number is drastically reduced to <50 per cell, and their size is increased up to 1500 nm as a result of membrane fusion events (Alberts B. *et al.*, 1994; Luzio J.P. *et al.*, 2007; Saftig P. and Klumperman J., 2009; Appelqvist H. *et al.*, 2013; Xu H. and Ren D., 2015).

Lysosomes are characterized by an acidic lumen (pH ~4.5) and contain more than 60 different soluble hydrolytic enzymes, including proteases, glycosidases, nucleases, lipases, sulfatases, and phosphatases. Each kind of hydrolase degrades a specific target substrate at acidic pH, and, collectively, these enzymes ensure the degradation of all types of macromolecules. The breakdown products derived from the degradation process are usually

exported to the cytoplasm, where they become available for metabolic reuse (Bainton D.F., 1981; Luzio J.P. *et al.*, 2007; Appelqvist H. *et al.*, 2013). The best-characterized class of lysosomal hydrolases is represented by the cathepsin family of proteases. In humans several members of cathepsin family have been identified. They have been classified into three distinct groups, based on the amino acid found in their active site: serine (cathepsin A, and G), cysteine (cathepsin B, C, F, H, K, L, O, S, V, W, and X), and aspartic cathepsins (cathepsin D, and E). The aspartic cathepsin D and some of the cysteine cathepsins (including cathepsins B, C, H, and L) are ubiquitous and among the most abundant lysosomal proteases (Appelqvist H. *et al.*, 2013).

To protect the cell from an unwanted degradation, lysosomes are limited by a 7-10 nm single phospholipid-bilayer, poor in cholesterol and extremely rich in carbohydrates (Schulze H. *et al.*, 2009; Saftig P. *et al.*, 2010). The high carbohydrate content is a unique feature of lysosomal membrane and is due to the presence of several integral proteins that are heavily glycosylated within their luminal domains, and hence resist digestion. The most abundant lysosomal glycoproteins include LAMP1 (*lysosomal associated membrane protein 1*), LAMP2 (*lysosomal associated membrane protein 2*), LIMP1 (*lysosomal integral membrane protein 1*)/CD63, and LIMP2 (*lysosomal integral membrane protein 2*). These heavily glycosylated proteins create a continuous and thick (~8 nm) glycocalyx on the inner side of lysosomal membrane, which protects the cell from the luminal acidic environment and from the action of acidic hydrolases (Neiss W.F., 1984; Eskelinen E.L. *et al.*, 2003; Saftig P. *et al.*, 2010).

The acidic pH required for the activation of lysosomal hydrolases and for the regulation of many other lysosomal functions is generated and maintained by the proton-pumping vacuolar H^+-ATPase (or v-ATPase), a transmembrane multimeric complex which is present and active in all types of eukaryotic cells. It uses energy from ATP hydrolysis to actively transport protons, against their electrochemical gradient, from the cytoplasm to the lysosomal lumen; in particular,

two protons are translocated per ATP hydrolyzed (Ohkuma S., *et al.*, 1982; Finbow M.E. and Harrison M.A., 1997; Mindell J.A., 2012).

Materials destined for degradation can reach lysosomes through two main pathways: extracellular materials are taken up from outside the cell and transported to lysosomes by the endocytic pathway, whereas intracellular components are delivered to lysosomal compartments *via* the autophagic pathway (de Duve C., 2005).

1.1.1   The endocytic pathway

Endocytosis is a process mediating the internalization of fluid, external solutes, macromolecules, plasma membrane (PM) components, and particles by the invagination of the PM and the subsequent formation of vesicles and vacuoles through membrane fission events. In metazoan cells, endocytosed cargo includes several biomaterials, such as nutrients and their carriers, receptor-ligand complexes, fluid, solutes, lipids, membrane proteins, extracellular-matrix components, cell-debris, and pathogens (including viruses, bacteria, parasites, and toxins) (Huotari J. and Helenius A., 2011; Grimm C. *et al.*, 2017).

Endocytosis starts with the formation of endocytic vesicles budding from the PM that mediate the entry of cargoes within the cell. Endocytic vesicles then fuse with early endosomes (EEs), the main sorting station in the endocytic pathway (Huotari J. and Helenius A., 2011; Reggiori F. and Klumperman J., 2016). The majority of cargoes delivered during endocytosis, including most receptors, is recycled back to PM through the recycling endosomes (REs). By contrast, the biomaterials destined for degradation are retained in the EEs and, through a multi-step process, reach the lysosomes for digestion (Appelqvist H. *et al.*, 2013). EEs have a complex structure consisting of a vacuolar body with an approximative diameter of 100-500 nm that is associated with cytosolic-facing tubular membrane extensions (Cullen P.J. and Steinberg F., 2018), and are characterized by a luminal pH of 5.9-6.8 (Reggiori F. and Klumperman J., 2016). Within EEs, materials addressed to degradation are incorporated into intraluminal vesicles

(ILVs) which are formed from the endosomal limiting membrane and are essential for efficient cargo sorting. Along the endocytic pathway, EEs, through a process involving exchange of materials and multiple membrane fusion events, are then converted into late endosomes (LEs). LEs are spherical organelles with an approximative diameter of 250-1000 nm and a pH of ~5-6 (Appelqvist H. *et al.*, 2013; Reggiori F. and Klumperman J., 2016). Due to the high content of ILVs, they are often referred to as "multivesicular bodies" (MVBs). *Via* the generation of ILVs, lipids and membranes are delivered to lysosomes in a form that is easily accessible to lysosomal hydrolases for degradation (Appelqvist H. *et al.*, 2013). Once matured, the LE fuses with a lysosome to form an intermediate fusion-hybrid organelle, the endo-lysosome (EL), which mediates the degradation of the incorporated cargoes. Subsequently lysosomes are regenerated from the fusion-hybrid organelles *via* a process known as lysosome biogenesis (Luzio J.P. *et al.*, 2009; Xu H. and Ren D., 2015).
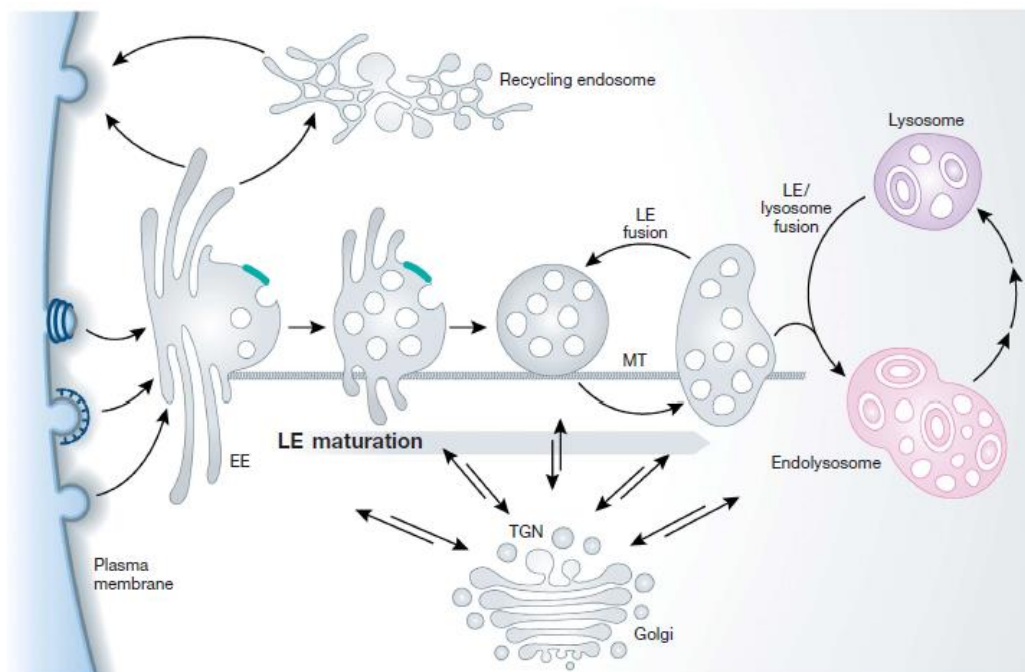
Fig.1 - **The endosome/lysosome system.** The primary endocytic vesicles budding from the PM deliver their cargo to the EEs in the peripheral cytoplasm and fuse with them. However, most of cargo is recycled back to PM through the recycling endosomes. After a period of 8-15 minutes EEs are converted in LEs. The nascent LE carries a selected subset of endocytosed cargo from EE, and newly synthesized lysosomal hydrolases and membrane components derived from the secretory pathway. Following a maturation process, the LE fuses with a lysosome, generating a transient hybrid organelle named endo-lysosome, in which active degradation of cargoes takes place (*modified from Huotari J. and Helenius A., 2011*).

The maturation process from EE to lysosome takes ~40 minutes. During this time, the vesicle undergoes a multitude of changes, including exchange of membrane components, movement to the perinuclear area, formation of ILVs, decrease in luminal pH, acquisition of lysosomal proteins, and changes in morphology (Appelqvist H. *et al.*, 2013). In addition, during endosome maturation, there is a continuously ongoing trafficking between endosomes and *trans*-Golgi network (TGN), which occurs at the level of both EEs and maturing LEs, and probably also after fusion of LEs with lysosomes (Huotari J. and Helenius A., 2011). This process allows the delivery of newly synthesized enzymes and proteins from the TGN to the appropriate endo-lysosomal compartments. Because of the continuous exchange of content between the intermediate compartments participating in the endocytic pathway, it is difficult to identify markers that specifically label a single organelle. Nevertheless, early endosomal antigen 1 (EEA1) and Rab5 are commonly used as markers of EEs. LEs and lysosomes show an overlapping molecular content, including LAMP proteins, and acidic hydrolases (Appelqvist H. *et al.*, 2013). However, lysosomes are characterized by the lack of mannose-6-phosphate receptors (M6PR), a criterion generally used to distinguish these compartments from LEs (Brown W.J. *et al.*, 1986; Appelqvist H. *et al.*, 2013).

At present, the regulation mechanisms of the endocytic pathway are not yet fully understood. However, several proteins have been found to participate in the regulation of endocytosis and intracellular trafficking, e.g. coat proteins, adaptors, retrieval proteins, scission proteins, Rab GTPases, and soluble N-ethylmaleimide sensitive factor attachment protein receptor (SNARE) proteins (Grimm C. *et al.*, 2017).

1.1.2 The autophagic pathway

Autophagy is an evolutionarily conserved cellular process through which cytoplasmic materials, such as proteins or even complete organelles, are directed to lysosomes for degradation. This process allows the clearance of protein aggregates, long-lived proteins,

misfolded proteins and dysfunctional and damaged organelles, and ensures the recycling of their constituents (Ravikumar B. *et al.*, 2010; La Rovere R.M.L. *et al.*, 2016). In mammals autophagy occurs under basal conditions and is implicated in the maintenance of normal cellular homeostasis (Ravikumar B. *et al.*, 2010). However, the process can be stimulated by several physiological and pathological conditions, including starvation, hypoxia, reactive oxygen species (ROS) production, pathogen infection, various diseases, or by treatment with pharmacological agents like rapamycin and torin-1. Under these conditions, the activation of autophagy allows cells to overcome the stress, thus promoting cell survival. However, an impairment in the autophagic process can contribute to the pathogenesis of several human diseases, including neurodegenerative disorders, cancer and infectious diseases (Ravikumar B. *et al.*, 2010; La Rovere R.M.L. *et al.*, 2016). In mammalian cells three major subtypes of autophagy have been described, based on the mechanism by which substrates reach the lysosomal lumen: chaperone-mediated autophagy (CMA), microautophagy, and macroautophagy. Only soluble proteins, but not complete organelles, can be delivered to lysosomes *via* CMA (Cuervo A.M., 2010), whereas micro- and macroautophagy participate in the degradation of both proteins and organelles (Yang Z. and Klionsky D.J., 2009). In more detail, CMA is characterized by the translocation of cytosolic proteins with the pentapeptide KFERQ motif into the lysosomal lumen directly across lysosomal membrane. In this process, protein import is directly mediated by the lysosomal-associated membrane protein type 2A (LAMP2A) translocation complex (Cuervo A.M., 2010; La Rovere R.M.L. *et al.*, 2016). Microautophagy is a constitutive and sometimes selective process by which whole portions of the cytoplasm are engulfed by direct invagination of lysosomal membrane into tubulovesicular structures (Ravikumar B. *et al.*, 2010; Wong W. and Cuervo A.M., 2010; Nixon R.A. and Yang D.S., 2012). Macroautophagy, hereafter referred to as autophagy, is the most extensively studied and the best characterized form of autophagy. During this process, a portion of the cytoplasm, including soluble materials and organelles, is sequestered within a *de novo*-formed

double-membraned structure, the phagophore (also called the isolation membrane). After elongation, phagophore closes upon itself to form a discrete double-membrane autophagic vesicle, the autophagosome, which entraps sequestered cytosolic cargoes. Subsequently, *via* cytoskeleton-dependent motion, autophagosome engages and fuses with lysosome in a calcium (Ca^{2+})-dependent manner, thus forming a fusion-hybrid organelle called autolysosome. Within the autolysosome, lysosomal enzymes degrade cargoes and the resulting macromolecules are transported back to the cytosol for recycling (Yang Z. and Klionsky D.J., 2009; Burman C. and Ktistakis N.T., 2010; Appelqvist H. *et al.*, 2013; Carlsson S.R. and Simonsen A., 2015; La Rovere R.M.L. *et al.*, 2016; Bootman M.D. *et al.*, 2018). When the autophagic process is completed, through lysosome biogenesis, lysosomes are reformed from the fusion-hybrid organelles (Xu H. and Ren D., 2015).

For a long time, autophagy has been considered a non-selective degradative pathway, involved in the degradation of randomly-sequestered cytoplasmic constituents. However, in the last years autophagy has been revealed as a more selective process, leading to the degradation of specific subsets of cellular components. Several targets of selective autophagy have been identified, including aggregated proteins (aggrephagy), lipids (lipophagy), mitochondria (mitophagy), peroxisomes (pexophagy), ribosomes (ribophagy), endoplasmic reticulum (reticulophagy, or ER-phagy) and pathogens (xenophagy) (Ravikumar B. *et al.*, 2010; Stolz A. *et al.*, 2014; Klionsky D.J. *et al.*, 2016).

Autophagy is a highly dynamic multi-step process regulated by approximately 30 autophagy-related proteins (Atg), that coordinate the different steps of the process (initiation, elongation, maturation, autophagosome-lysosome fusion) (La Rovere R.M.L. *et al.*, 2016). Phagophore formation is primarily induced by the assembly and activation of a multiprotein complex, the ULK1 complex, containing ULK1 (*unc-51-like kinase 1*), Atg13, FIP200, and Atg101. This complex can be regulated by two proteins with kinase activity, the cell growth regulator mTOR (*mammalian target of the rapamycin*), and the cell energy sensor AMPK

(*AMP-activated protein kinase*) (Nixon R.A., 2013). Under starvation, AMPK, which responds to reduced cytosolic ATP levels and consequent AMP accumulation, directly activates ULK1 through phosphorylation of Ser317 and Ser777, thus promoting autophagy. By contrast, under normal conditions, high mTOR activity prevents ULK1 activation by phosphorylating this protein in Ser757 and disrupting the interaction between ULK1 and AMPK (Kim J. *et al.*, 2011). Upon AMPK-mediated phosphorylation, ULK1 complex, in turn, phosphorylates AMBRA (*activating molecule in beclin1-regulated autophagy*), a component of the autophagy-specific class III phosphatidylinositol 3-kinase (PI(3)K) complex, containing Vps34 (*vacuolar protein sorting 34*), Vps15 (*vacuolar protein sorting 15*), beclin 1, and Atg14. This event promotes the translocation of PI(3)K complex from cytoskeleton to the phagophore, thus initiating phagophore elongation (Nixon R.A., 2013). Moreover, the phosphorylation of beclin 1 stimulates the local production of phosphatidylinositol 3-phosphate (PI(3)P) by Vps34 activity (Stolz A. *et al.*, 2014). PI(3)P specifically binds to the early autophagic effector proteins WIPI1/2 (*WD repeat domain phosphoinositide-interacting protein 1/2*) and Atg21 (Nixon R.A., 2013; Stolz A. *et al.*, 2014). Another protein essential in this step of autophagy is Atg9, which together with Atg2 and members of the WIPI protein family forms another functional cluster. Atg9 has been reported to localize to different compartments, including recycling endosomes, late endosomes, TGN, and plasma membrane, and dynamically associates with the phagophore (Reggiori F. and Klumperman J., 2016). Although the precise function of Atg9 is still unknown, it has been proposed that it could cycle between endosomes, TGN and the phagophore, carrying some lipid components essential for membrane expansion (Nixon R.A., 2013; Reggiori F. and Klumperman J., 2016). Two ubiquitination-like reactions regulate further elongation and closure of the phagophore. In the first reaction, Atg5 and Atg12 are conjugated to each other in the presence of two additional Atg proteins (Atg7 and Atg10), and subsequently associate with Atg16L. The fully formed complex (containing Atg5, Atg12, and Atg16L) recruits the second ubiquitination-like conjugation system to the phagophore, inducing the conjugation of

phosphatidylethanolamine (PE), a lipid constituent of membranes, to members of microtubule-associated protein light chain 3 (MAP-LC3, hereafter referred to as LC3) protein family (LC3A, LC3B, LC3C). In detail, newly synthesized LC3 (pro-LC3) is post-translationally processed at its C-terminus by the cysteine protease Atg4 to generate the cytosolic non-lipidated form of LC3 (LC3-I). Upon autophagy induction, LC3-I is conjugated to PE on both the inner and outer membrane of the phagophore through the action of Atg7 and Atg5-Atg12-Atg16L complex. The resulting lipidated form of LC3 (LC3-II), together with the Atg5-Atg12-Atg16L complex, is thought to form a protein coat that drives the formation of autophagosomes, possibly by deforming membranes (Reggiori F. and Klumperman J., 2016).
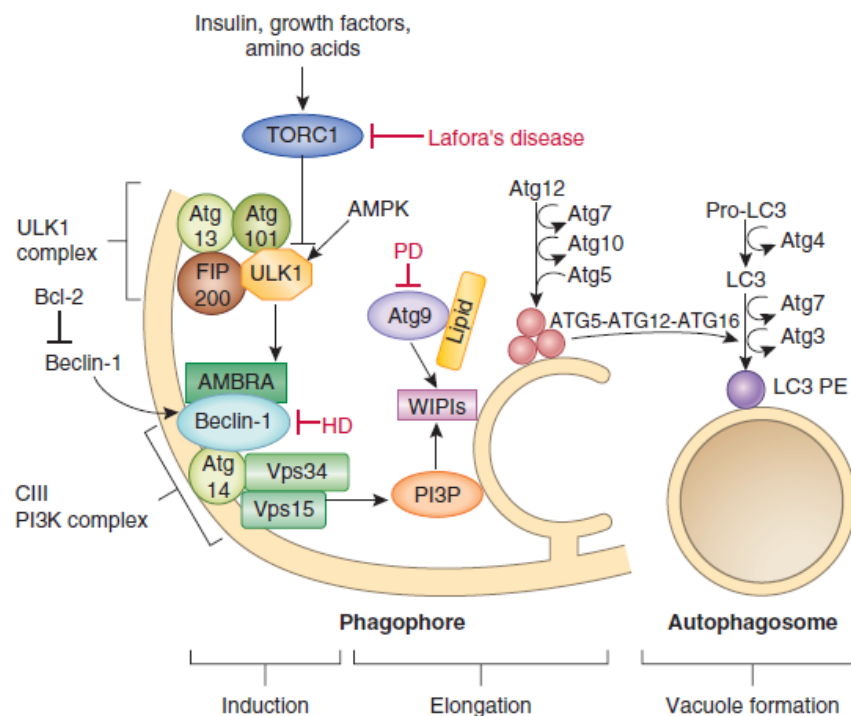
Fig.2 - **Autophagy induction and autophagosome biogenesis.** Schematic depicting the molecular components and protein complexes involved in the induction of autophagy and in the subsequent formation of the autophagosome starting from the phagophore. The steps of the process indicated in red are known to be affected in some neurodegenerative diseases (*modified from Nixon R.A., 2013*).

Another important protein in the autophagic process is SQSTM1/p62, a scaffolding protein that can be considered a linker between autophagy and polyubiquitylated substrates. Indeed, it acts as an autophagy receptor shuttling the polyubiquitylated proteins bound to its ubiquitin associated domain (UBA) to the autophagic machinery, by directly interacting with

LC3-II (Liebl M.P. and Hoppe T., 2016). Interestingly, p62 itself is also a substrate of autophagy: indeed, p62 and p62-bound polyubiquitylated proteins are incorporated into the complete autophagosomes and degraded within autolysosomes, thus serving as an index of autophagic degradation. Since basal autophagy keeps p62 at relatively low levels, an increase in its expression is the result of autophagy inhibition (Klionsky D.J. *et al.*, 2016; Liebl M.P. and Hoppe T., 2016; Yin Y. *et al.*, 2017).
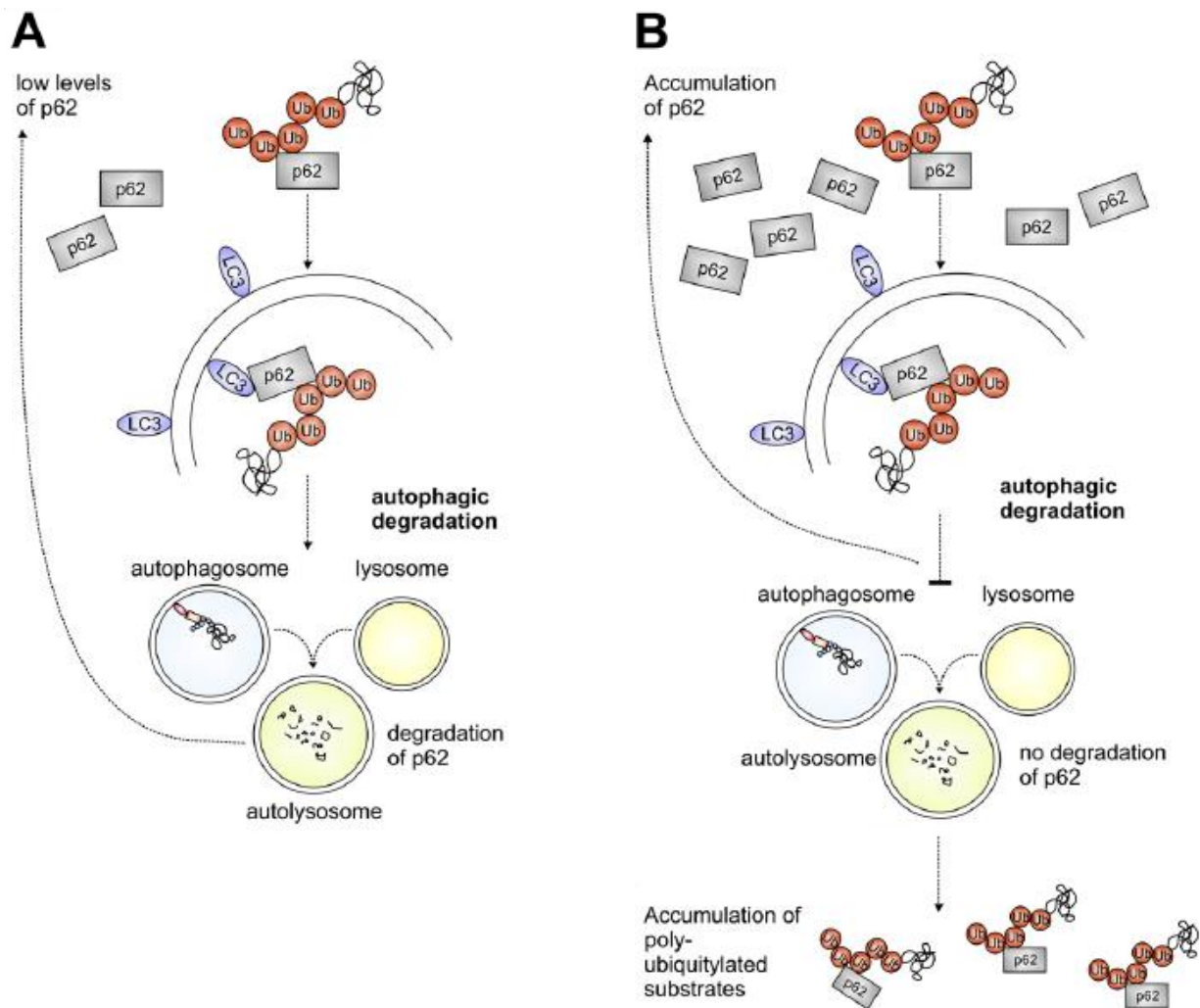
Fig.3 - **p62 links polyubiquitylated substrates to autophagy.** (**A**) Under conditions of productive autophagy, p62 shuttles polyubiquitylated substrates for autophagosomal degradation and is itself a substrate of autophagy. (**B**) When autophagy is impaired, polyubiquitylated substrates accumulate and p62 is not degraded by the autophagic machinery (*modified from Liebl M.P. and Hoppe T., 2016*).

Given that autophagy is a highly dynamic process, the term "autophagic flux" is generally used to refer to the whole process of cargo moving through the autophagic system,

from phagophore to autophagosome formation, including cargo delivery to lysosomes and subsequent cargo breakdown (Klionsky D.J. *et al.*, 2016; Yin Y. *et al.*, 2017). In this case the process may be referred to as "productive" or "complete" autophagy (Klionsky D.J. *et al.*, 2016). However, an accumulation of autophagosomes could reflect a reduction in autophagosome turnover, due, for example, to a block in fusion with lysosomes or to an impairment in the digestive functions of lysosomes, which leads to an inefficient cargo degradation once fusion has occurred. In this scenario, although autophagy is induced, there is no or limited autophagic flux. In these conditions, the block in the autophagic flux is accompanied by an increase in the expression levels of some autophagic markers, including p62 and LC3-II (Klionsky D.J. *et al.*, 2016).
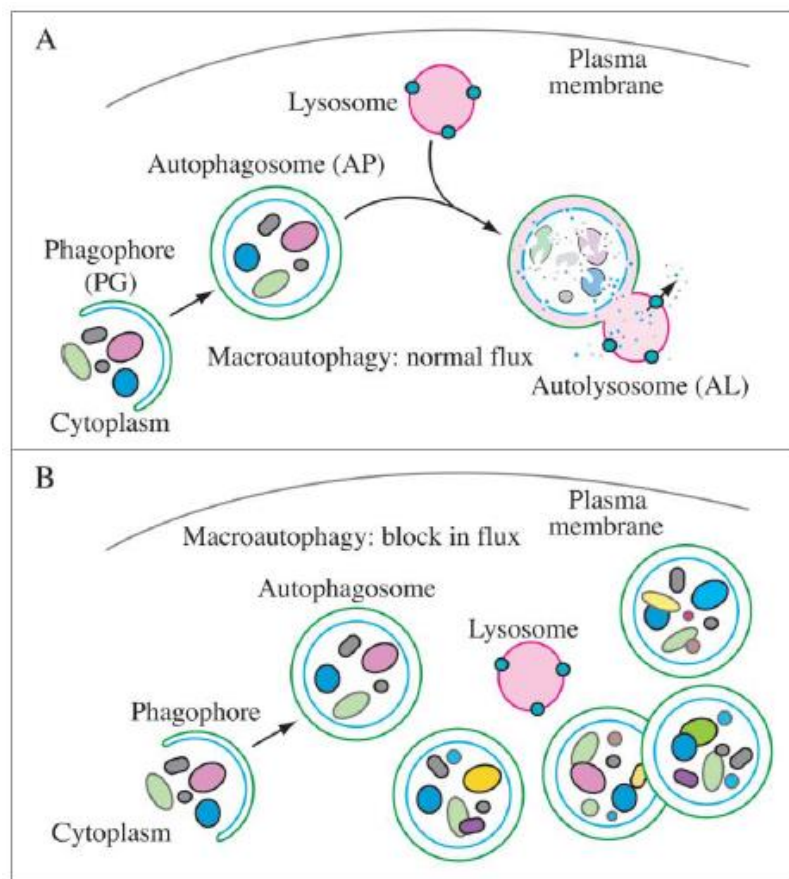
Fig.4 - **Normal versus defective autophagic flux.** (**A**) Autophagy starts with the formation of the phagophore, which subsequently expands to form the autophagosome. To ensure a normal autophagic flux, the completion of the process requires the fusion of the autophagosomes with lysosomes to form autolysosomes, in which cargoes are degraded by lysosomal enzymes. (**B**) A defect in autophagosomes turnover, due to a block in fusion with lysosomes or to an impairment in lysosomal degradation, leads to a block in the autophagic flux, which is accompanied by an increased number of autophagosomes within the cytosol (*modified from Klionsky D.J. et al., 2016*).

1.2 Lysosome: not only a degradative compartment

Traditionally, lysosomes were considered merely to be waste bags involved in the degradation and recycling of cargoes mainly derived from the endocytic and the autophagic pathways (de Duve C., 2005). Recently, it has been reported that, besides their well-known digestive functions, lysosomal compartments are implicated in a plethora of other fundamental processes within the cell, including secretion, plasma membrane repair, signaling, energy metabolism, and immune response, and they are now considered crucial regulators of cell homeostasis (Settembre C. *et al.*, 2013). Intriguingly, it has been also demonstrated that all lysosomal functions are globally regulated at transcriptional level by a lysosomal gene network, named CLEAR (*Coordinated Lysosomal Expression and Regulation*), and by its master gene TFEB (*transcription factor EB*). This lysosomal gene network includes co-regulated lysosomal genes that are involved in several lysosomal processes and functions, such as lysosomal biogenesis, lysosomal acidification, proteolytic activity of lysosomal enzymes, endocytosis, exocytosis, and autophagy. In particular, the master regulator of this network TFEB, belonging to the MiT/TFE (*microphthalmia-transcription factor E*) subfamily of bHLH-LZ (*basic helix-loop-helix leucine-zipper*) transcription factors, promotes the transcription of approximately 500 lysosomal genes by a direct binding to specific sites, called E-boxes, at their promoters (Sardiello M. *et al.*, 2009; Palmieri M. *et al.*, 2011).

Among the lysosomal functions controlled by TFEB, one of the best characterized is lysosomal exocytosis, a two-step Ca^{2+}-dependent process through which lysosomes secrete their luminal content into the extracellular matrix. It initially requires the docking of lysosomes to the close proximity of plasma membrane and then the increase in intracellular Ca^{2+} levels to promote lysosome fusion with the plasma membrane (Medina D.L. *et al.*, 2011; Settembre C. *et al.*, 2013). This process is involved in the elimination of cellular waste products, but it also promotes the release of degradative enzymes and other cargoes that may be essential to the clean-up and maintenance of the extracellular space (LaPlante J.M. *et al.*, 2006). Moreover, it

mediates other important physiological functions, including plasma membrane repair, immune response, and bone resorption. Lysosomal exocytosis is very active in some cell types, such as haematopoietic cells, osteoclasts, and melanocytes. Interestingly, it has been reported that in this process TFEB is able to induce both docking and fusion of lysosomes with the plasma membrane, by raising intracellular Ca^{2+} levels through the activation of the lysosomal Ca^{2+} channel TRPML1 (*Transient Receptor Potential Mucolipin 1*) (Medina D.L. *et al.*, 2011; Settembre C. *et al.*, 2013). Moreover, upon release of lysosomal content, lipids and lysosomal membrane proteins, including LAMP1 and TRPML1, eventually fuse to plasma membrane and then are recycled back through endocytosis (Di Paola S. *et al.*, 2018).

Lysosomes play an important role also in nutrient sensing and in signalling pathways involved in cell metabolism and growth. These organelles sense the nutrient status of the cell through the LYNUS (*lysosome nutrient sensing*) complex, a machinery located to lysosomal surface and made of several interacting protein complexes, including the v-ATPase, Rag GTPases and the mammalian target of rapamycin complex 1 (mTORC1). Its main function is to regulate cell growth and metabolism through mTORC1 signalling pathway; in particular, LYNUS machinery responds to lysosomal amino acid content and signals to the nucleus to adapt to conditions of starvation or plenty (Settembre C. *et al.*, 2013; Settembre C. and Ballabio A., 2014).
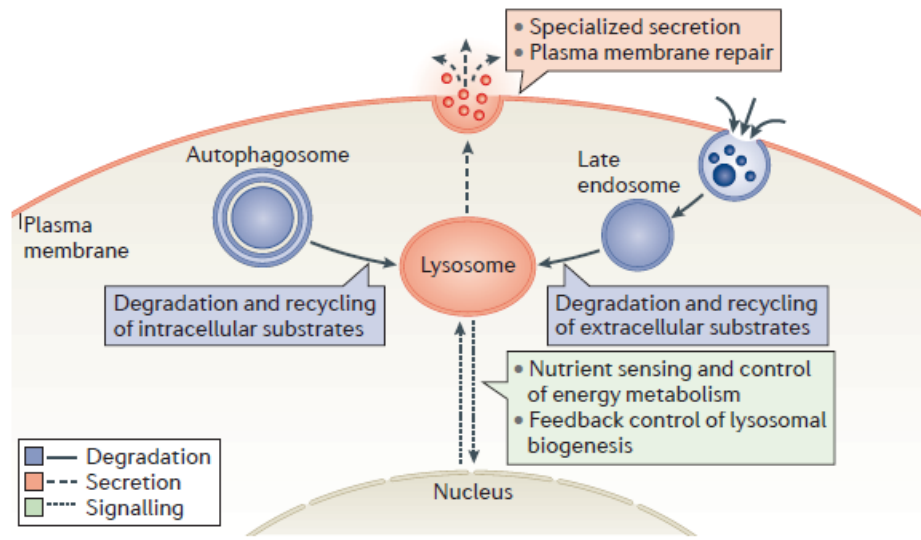
Fig.5 - **Main functions of lysosomes.** Lysosomes are involved in the degradation and recycling of extracellular material (*via* endocytosis) and intracellular components (*via* autophagy). In these processes, they fuse with late endosomes and autophagosomes, respectively. The resulting breakdown products are recycled to generate new cellular components and energy in response to the nutritional needs of the cell. Lysosomes also participates in Ca^{2+}-regulated exocytosis to secrete their content into the extracellular space; this process is particular important in plasma membrane repair. More recently, lysosomes have been identified as signalling organelles that can sense nutrient availability and activate a lysosome-to-nucleus signalling pathway that mediates the starvation response and regulates energy metabolism (*modified from Settembre C. et al., 2013*).

1.3   Lysosome: a novel intracellular Ca^{2+}-storing organelle

In the last years lysosomes have also emerged as important Ca^{2+}-storing compartments. Indeed, the average free calcium concentration within their lumen is approximately 200-600 μM (Christensen K.A. *et al.*, 2002; Lloyd-Evans E. *et al.*, 2008), and is thus comparable to the concentration within the main intracellular Ca^{2+} store, the endoplasmic reticulum (ER) (Bygrave F.L. and Benedetti A., 1996). Due to the high Ca^{2+} concentration within their acidic lumen, lysosomes - together with endosomes, lysosomes-related organelles (LRO), secretory granules, and the more distantly related acidocalcisomes and vacuoles - are often referred to as "acidic Ca^{2+} stores" (Patel S. and Docampo R., 2010).

Despite being smaller in volume than ER, an increasing amount of experimental evidences have demonstrated that lysosomes play a central role in intracellular Ca^{2+} signaling and contribute to the regulation of intracellular Ca^{2+} homeostasis, in both physiological and

pathological conditions (Patel S. and Docampo R., 2010; Morgan A.J. *et al.*, 2011). Under control conditions, Ca^{2+} can be mobilized from lysosomal stores to regulate a lot of Ca^{2+}-dependent functions, including signal transduction, organelle homeostasis and acidification, trafficking and fusion between lysosomes and other compartments, such as late endosomes, autophagosomes, and PM (Xu H. and Ren D., 2015). Furthermore, it has been reported that lysosomal Ca^{2+} signals necessary for the regulation of cellular functions can act locally, through microdomains of Ca^{2+} confined to small (10-100 nm) local areas, or propagate globally throughout the entire cell (Kilpatrick B.S. *et al.*, 2016a). In this respect, it has been proposed that lysosomes can interact with other intracellular organelles, such as the ER, thus triggering a global Ca^{2+} signalling (Patel S. and Docampo R., 2010).

To provide the ionic environment essential for proper lysosomal functions, lysosomal Ca^{2+} concentration is tightly controlled by the activation of several Ca^{2+}-permeable channels and transporters located to lysosomal membrane. In particular, in the last years several Ca^{2+}-release channels have been shown to localize to endo-lysosomal membrane. These include some members of TRP (*Transient Receptor Potential*) channels (e.g. TRPMLs and TRPM2), TPCs (*Two-Pore Channels*) and P2X4 purinoceptor (Patel S. and Cai X., 2015). At present in metazoans little is known about how Ca^{2+} is taken up by the endo-lysosomal system (Brailoiu G.C. and Brailoiu E., 2016).
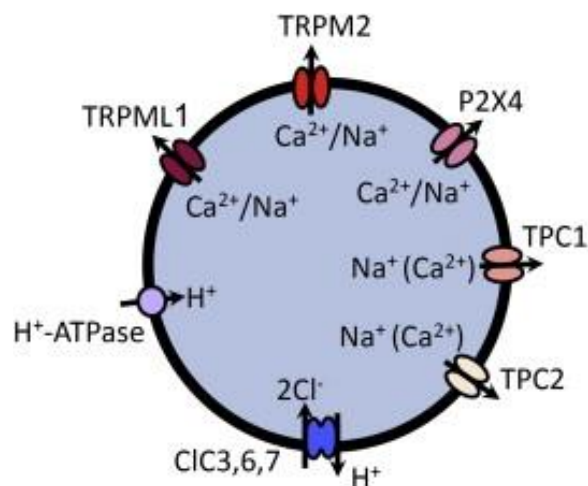
Fig.6 - **Main Ca^{2+}-releasing channels localized to lysosomal membrane** (*modified from Zhong X.Z. and Dong X.P., 2015*).

1.3.1 Ca^{2+} release mechanisms in the endo-lysosomal system

Ca^{2+} release from acidic stores is promoted by a number of Ca^{2+}-permeable channels located to the membranes of the endo-lysosomal system. Among them, a fundamental role is played by TRPML (*Transient Receptor Potential Mucolipin subfamily*) channels (Cheng X. *et al.*, 2010; Grimm C. *et al.*, 2012). However, other channels may contribute to the regulation of endo-lysosomal Ca^{2+} homeostasis, including TPCs (*Two-Pore Channels*) (Calcraft P.J. *et al.*, 2009; Morgan A.J. *et al.*, 2011), TRPM2 (*Transient Receptor Potential Melastatin 2*) (Lange I. *et al.*, 2009; Sumoza-Toledo A. and Penner R., 2011) and P2X4 (Qureshi O.S. *et al.*, 2007; Huang P. *et al.*, 2014).

1.3.1.1 TRPMLs

TRPML channels are members of *Transient Receptor Potential* (TRP) superfamily channels, a large family of cation channels expressed in almost every tissue and cell type. Members of this family exhibit varying degrees of selectivity for different ionic species and play an important role in the regulation of different cell functions, including sensory perception and signal transduction (Nilius B. *et al.*, 2007; Earley S. and Brayden J.E., 2015). Similarly to all other TRPs, TRPMLs contain six transmembrane (6TM) domains, with both the N- and C-termini residing in the cytoplasm and with the pore region occurring between TM5 and TM6 domains (Cheng X. *et al.*, 2010; Grimm C. *et al.*, 2012). However, TRPMLs differ from the other TRP channels, since they have unusually short cytosolic tails, which range from 61 to 72 amino acids (aa), and present a large luminal loop located between TM1 and TM2, which contains several N-glycosylation sites (Puertollano R. and Kiselyov K., 2009). TRPML proteins are also characterized by the presence of multiple positively charged aa residues at their N-terminal end, which seems to be important for channels interaction with phosphoinositides (Dong X.P. *et al.*, 2010). Furthermore, the presence of negatively charged glutamate and aspartate residues within the pore region defines TRPMLs selectivity to cations (Puertollano R.

and Kiselyov K., 2009). In mammals there are three TRPML proteins, TRPML1, TRPML2 and TRPML3 (also referred to as mucolipin 1-3 or MCOLN1-3), encoded by *mcoln1-3* genes. They are relatively small proteins, consisting of <600 aa residues (Nilius B. *et al.*, 2007), which share about 75% of similarity in the aa sequence, especially in the putative pore region between TM5 and TM6 domains (Puertollano R. and Kiselyov K., 2009).
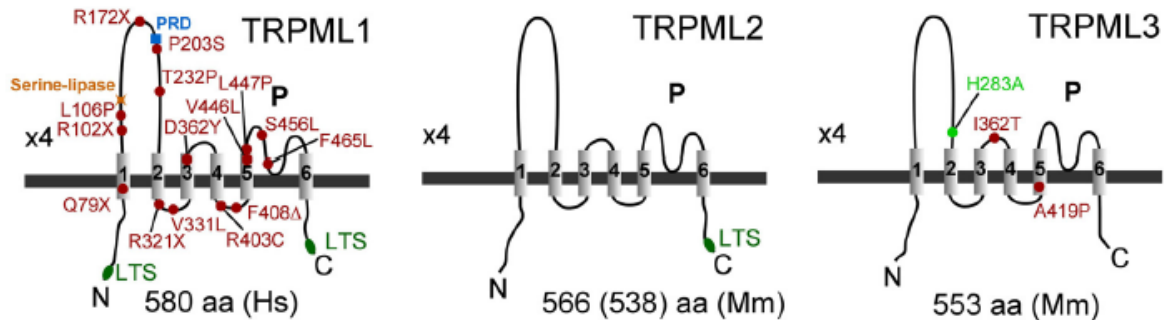
Fig.7 - **Topological structure of TRPML channels.** TRPMLs are 6TM channels, with both N- and C-termini located to the cytosol. They are predicted to form tetramers (4X). The cartoon on the left depicting human TRPML1 structure displays several mutations causing mucolipidosis type IV (MLIV). At present no human diseases have been associated with mutations in TRPML2 and TRPML3 proteins; however, mutations in TRPML3 are responsible for the varitint-waddler (Va) phenotype in mice (*modified from Grimm C. et al., 2012*).

TRPML1 is a ubiquitously expressed protein with the highest expression level in brain, kidney, spleen, liver and heart (Cheng X. *et al.*, 2010). In contrast to TRPML1, the tissue distribution pattern of TRPML2 and TRPML3 proteins is more restricted. Indeed, TRPML2 is predominantly expressed in kidney, liver, heart and in lymphoid organs, such as thymus and spleen (Cheng X. *et al.*, 2010; Sun L. *et al.*, 2015), whereas TRPML3 is mainly detected in cochlea, thymus, kidney, lung, eye, spleen, skin (melanocytes) and in somato-sensory neurons. At subcellular level, TRPML1 is expressed in late endosomes and lysosomes; TRPML2 localized to the membranes of recycling endosomes, late endosomes and lysosomes; TRPML3 is expressed in early endosomes, late endosomes and lysosomes, and also on plasma membrane (Cheng X. *et al.*, 2010). The three mammalian TRPML channels are predicted to form tetramers (Grimm C. *et al.*, 2012). In particular, they were shown to physically interact with each other, thus forming homo- and heteromultimers (Zeevi D.A. *et al.*, 2007; Curcio-Morelli C. *et al.*,

2010a; Venkatachalam K. *et al.*, 2015); however, the protein-protein interactions between endogenous TRPMLs seem to be quite limited (Zeevi D.A. *et al.*, 2009), probably due to the restricted tissue distribution pattern of TRPML2 and TRPML3. It is possible that variable assembly of TRPML proteins, which are differentially expressed in the target tissues, may result in tissue-specific channel characteristics (Curcio-Morelli C. *et al.*, 2010a). Moreover, the biophysical properties and regulation of the heteromultimers may be different from the homomultimers, and this could contribute to the functional diversity of TRPMLs proteins (Venkatachalam K. *et al.*, 2015). In addition, TRPMLs can also physically interact with TPCs, but it has been reported that the two family of channels function independently on endo-lysosomal membranes (Yamaguchi S. *et al.*, 2011).

Functionally, TRPMLs constitute a family of inwardly rectifying (from endo-lysosomal lumen to cytosol) non-selective cation channels, mainly permeable to Ca^{2+}, Na^+ and K^+, but not to H^+ (Cheng X. *et al.*, 2010). In addition, it has been reported that TRPML1 is also permeable to divalent heavy trace metals, such as Fe^{2+} and Zn^{2+} (Dong X.P. *et al.*, 2008; Eichelsdoerfer J.L. *et al.*, 2010; Grimm C. *et al.*, 2012). However, despite their non-selectivity, it has been demonstrated that TRPML channels, and in particular TRPML1, the best characterized protein among this subfamily, play a major role in the regulation of endo-lysosomal Ca^{2+} homeostasis and endo-lysosomal functions, by promoting Ca^{2+} release from acidic organelles (LaPlante J.M. *et al.*, 2002; Abe K. and Puertollano R., 2011). Lysosomal Ca^{2+} release *via* TRPMLs is promoted upon channel stimulation with PI(3,5)P$_2$ (*phosphatidylinositol 3,5-bisphosphate*), a low-abundance endo-lysosomal-specific phosphoinositide, which binds specifically to the positively charged aa residues on the cytoplasmic N-terminus of TRPMLs (Dong X.P. *et al.*, 2010). Moreover, it was shown that TRPML1 is inhibited by the plasma membrane-specific phosphoinositide PI(4,5)P$_2$ (*phosphatidylinositol 4,5-bisphosphate*), which, also binds to the positively charged aa on TRPML1 N-terminus (Zhang X. *et al.*, 2012). It has been suggested

that PI(4,5)P$_2$-mediated inhibition may be a mechanism to prevent the activation of lysosomal TRPML1 in non-native compartments, such as the plasma membrane (Xu H. and Ren D., 2015).

Moreover, some researchers proposed that TRPML1 is also activated by NAADP (*Nicotinic Acid Adenine Dinucleotide Phosphate*) (Zhang F. and Li P.L., 2007; Zhang F. *et al.*, 2009; Zhang F. *et al.*, 2011), the most potent Ca^{2+}-releasing second messenger actually known, which is able to generate intracellular Ca^{2+} signals even at low nanomolar concentrations (Guse A.H. and Lee H.C., 2008). However, in literature some controversies about the activation of TRPML1 by NAADP emerged. Indeed, other researchers suggested that this channel did not participate in NAADP-mediated Ca^{2+} signaling (Pryor P.R. *et al.*, 2006; Yamaguchi S. *et al.*, 2011), corroborating the evidence, already present in literature, that the molecular targets for NAADP action could be the endo-lysosomal TPCs (Brailoiu E. *et al.*, 2009; Calcraft P.J. *et al.*, 2009; Zong X. *et al.*, 2009).

Mutations in *mcoln1* gene are associated with mucolipidosis type IV (MLIV), a devastating lysosomal storage disorder characterized by neurodegeneration (Bargal R. *et al.*, 2000; Bassi T.M. *et al.*, 2000; Sun M. *et al.*, 2000). Moreover, mutations in murine *mcoln3* gene are responsible for the varitint-waddler (Va) phenotype, which is characterized by deafness and pigmentation defects in mice (Di Palma F. *et al.*, 2002). Currently, no mutations in *mcoln2* and *mcoln3* genes have been associated with human diseases.

1.3.1.2 TPCs

TPCs (*Two-Pore Channels*) are a unique family of cation channels containing two repeats of a six transmembrane (2 x 6TM) pore-forming domain. For this structural feature, they represent an evolutionary intermediate between the tetrameric one-domain (6TM) channels – such as voltage-gated K$^+$ channels (K$_v$s), TRPs, and sperm-specific Ca^{2+} channels (CatSpers) – and the monomeric four-domain (4 x 6TM) channels – such as voltage-gated Ca^{2+} channels (Ca$_v$s), and voltage-gated Na$^+$ channels (Na$_v$s) (Xu H. and Ren D., 2015). Each of the

two repeated 6TM domains contains a putative pore-forming region between TM5 and TM6 (Morgan A.J. *et al.*, 2011). Both N- and C-termini are hydrophilic and localizes to the cytoplasm (Ishibashi K. *et al.*, 2000). In animal cells there are three TPC proteins, TPC1, TPC2 and TPC3, encoded by *TPCN1-3* genes and consisting of approximately 800 aa residues (Grimm C. *et al.*, 2012). However, TPC3 protein is absent in many mammals such as mice, rats, and in most primates, including humans; indeed, it has been demonstrated that *TPC3* gene degenerated into a pseudogene in the genomes of humans and other primates (Calcraft P.J. *et al.*, 2009; Brailoiu E. *et al.*, 2010). The primary sequences of the three proteins are quite different from one another (within a given species only ~20% identical, ~35% similar), but each orthologue is quite well conserved across species (40-90% identical, 55-93% similar) (Morgan A.J. *et al.*, 2011).
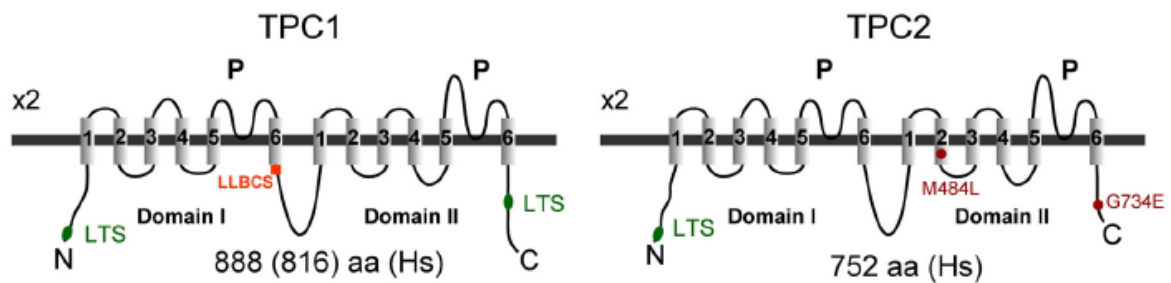
Fig.8 - **Topological structure of TPC channels.** This cartoon shows the structures of human TPC1 and TPC2 protein. They are composed of two repeats of a 6TM pore-forming domains, with both N- and C-termini localized to the cytosol. They are predicted to form dimers (2X). Two polymorphisms in human TPC2 are associated with blond versus brown phenotype (*modified from Grimm C. et al., 2012*).

TPC proteins are ubiquitously expressed, but differentially distributed in the endo-lysosomal system: indeed, TPC1 and TPC3 are predominantly expressed in the endosomal compartments, whereas TPC2 mainly localizes to late endosomes and lysosomes (Calcraft P.J. *et al.*, 2009; Morgan A.J. *et al.*, 2011; Grimm C. *et al.*, 2012). It has been reported that TPC proteins likely assembly in dimers to form one functional pore, thus maintaining the four-fold symmetry typical of voltage-gated ion channels (Patel S. and Cai X., 2015).

TPC channels were traditionally studied for their role in the regulation of endo-lysosomal Ca^{2+} homeostasis; indeed, several papers demonstrated that they promote Ca^{2+} efflux

from endo-lysosomes upon stimulation with the endogenous second messenger NAADP (Brailoiu E. *et al.*, 2009; Calcraft P.J. *et al.*, 2009; Zong X. *et al.*, 2009). However, in the last years some controversies about the ionic permeability and selectivity of endo-lysosomal TPCs have emerged. Indeed, recent evidences suggested that these channels are highly selective for Na^+ (TPC1: P_{Na}/P_K ~100; TPC2: P_{Na}/P_K ~30) (Wang X. *et al.*, 2012; Cang *et al.*, 2013; Kintzer A.F. and Stroud R.M., 2018). In particular, it has been proposed that TPC1 and TPC3 are voltage-gated cation channels, whereas TPC2 is a ligand-gated cation channel, activated by $PI(3,5)P_2$ and potentially by NAADP (Kintzer A.F. and Stroud R.M., 2018). However, the ionic selectivity of TPC channels is still a matter of debate.

To date, no disease-related mutations are known for human or rodent TPCs (Grimm C. *et al.*, 2012). However, polymorphisms in human TPC2 have been associated to the control of hair pigmentation (Chao Y.K. *et al.*, 2017).

1.3.1.3 TRPM2

TRPM2 (*Transient Receptor Potential Melastatin 2*) is a non-selective, Ca^{2+}-permeable cation channel belonging to the melastatin subfamily of TRP channels. Like other TRPs, its structure comprises 6TM domains, with intracellular N- and C-termini and a pore-forming loop between TM5 and TM6 domains (Sumoza-Toledo A. and Penner R., 2011). Interestingly, the channel contains a unique adenosine diphosphate ribose (ADPR) hydrolase domain (Nudix-like domain) in its C-terminus, by virtue of which it is considered a "chanzyme" – a channel with enzymatic activity (Perraud A.L. *et al.*, 2001; Patel S. and Docampo R., 2009). In humans, the ~6.5 kb TRPM2 transcript encodes a protein of ~1500 aa. This protein is expressed at high levels in the brain, but it has been also detected in other tissues, including bone marrow, spleen, heart, liver and lung, and in different cell types such as pancreatic β-cells, endothelial cells, microglia, neurons, cardiomyocytes and immune cells (Sumoza-Toledo A. and Penner R., 2011). Although it is primarily expressed at the plasma membrane, where it mediates Ca^{2+}

influx into the cell, it also localizes to lysosomal membrane, where it acts as a Ca^{2+}-release channel (Lange I. *et al.*, 2009; Sumoza-Toledo A. and Penner R., 2011). Its endogenous activator is the cytosolic second messenger ADPR (*ADP-ribose*) (Perraud A.L. *et al.*, 2001), which binds to the Nudix-like domain in TRPM2 C-terminus and is subsequently hydrolyzed to ribose 5-phosphate and AMP. Since AMP antagonizes ADPR-mediated gating of TRPM2, it has been proposed that the enzymatic activity of the channel may provide a negative feedback inhibition for TRPM2 activity (Sumoza-Toledo A. and Penner R., 2011). Currently, a specific association of lysosomal TRPM2 channel with human diseases has not been found (Sterea A.M. *et al.*, 2018).

1.3.1.4 P2X4

The ionotropic P2X receptors are a family of Ca^{2+}-permeable non-selective cation channels localized to plasma membrane and activated by extracellular ATP (*adenosine 5'-triphosphate*). Among the members of this family, only P2X4 is localized intracellularly to the membranes of late endosomes and lysosomes (Qureshi O.S. *et al.*, 2007; Huang P. *et al.*, 2014). Like other P2X receptors, it contains two transmembrane regions and form trimers (Patel S. and Cai X., 2015; Suurvali J. *et al.*, 2017). P2X4 receptor was found to be localized to lysosomal membrane of some mammalian cells, including rat microglia, macrophages and endothelial cells, where it promotes Ca^{2+} efflux from lysosomes (Qureshi O.S. *et al.*, 2007). Lysosomal P2X4 is activated by luminal ATP (Qureshi O.S. *et al.*, 2007; Huang P. *et al.*, 2014), with an ATP-binding site located within the lysosomal lumen (Morgan A.J. *et al.*, 2011; Patel S. and Cai X., 2015). It has been reported that this channel is regulated by luminal pH: indeed, while the acidic pH (~4.5) at the luminal side inhibits P2X4 activity, an increase in luminal pH in the presence of intra-luminal ATP causes the activation of the channel. This evidence suggests that lysosomal P2X4 is normally inactivated or minimally activated at the resting lysosomal pH (4.5-5.0) (Huang P. *et al.*, 2014).

1.3.2 Ca^{2+} uptake mechanisms in the endo-lysosomal system

To date, a complete knowledge regarding the molecular mechanisms for endo-lysosomal Ca^{2+} uptake in metazoans is still lacking. In these organisms, Ca^{2+} influx within the endo-lysosomal compartments occurs *via* a mechanism poorly characterized, which seems to be dependent on the H^+ gradient generated by the v-ATPase. Indeed, v-ATPase inhibition, by causing an increase in lysosomal pH, leads to lysosomal Ca^{2+} release; by contrast, lysosomal reacidification is accompanied by a lysosomal Ca^{2+} refilling (Christensen K.A. *et al.*, 2002). On the basis of these evidences, it has been proposed that a Ca^{2+}/H^+ exchanger (CAX) could be responsible, at least in part, for pH-dependent Ca^{2+} uptake into lysosomes (Morgan A.J. *et al.*, 2011). This exchanger is known to be involved in the better-characterized mechanism of Ca^{2+} uptake by plant and yeast vacuoles, acidic organelles that are equivalent of lysosomes in animal cells. It uses the proton gradient across the vacuolar membrane to drive Ca^{2+} influx into the lumen (Pittman J.K., 2011). However, CAX genes are not widespread in all metazoan kingdom, and, although the genes related to yeast/plant CAX have been recently described in some vertebrates, including some echinoderm, mollusk, fish, amphibian and non-placental mammals, they are absent in the genome of placental mammals (Melchionda *et al.*, 2016). This evidence suggests that in placental mammals CAX proteins are not involved in lysosomal Ca^{2+} uptake and that in these animals different mechanisms control lysosomal Ca^{2+} uptake, compared with lower order organisms and non placental mammals (Lloyd-Evans E., 2016a). Moreover, in plant and yeast vacuoles lysosomal Ca^{2+} uptake is also mediated by the action of a Ca^{2+}-ATPase, which transports Ca^{2+} against its concentration gradient from the cytosol into the vacuolar lumen (Patel S. and Docampo R., 2010; Pittman J.K., 2011). However, it is unknown whether this pump is also expressed in the endo-lysosomal system of animal cells (Patel S. and Docampo R., 2010). Probably in placental mammals lysosomal Ca^{2+} uptake may not be mediated by a single transporter, but rather it requires the concerted action of putative Na^+/H^+ and Na^+/Ca^{2+} exchangers, acting in series. The net effect of this coupled transport is Ca^{2+} influx into

lysosomal lumen and H^+ efflux from lysosomal lumen (Patel S. and Docampo R., 2010; Morgan A.J. *et al.*, 2011; Brailoiu G.C. and Brailoiu E., 2016).

However, very recently Garrity *et al.* have suggested that Ca^{2+} uptake into lysosomes is not dependent on lysosomal acidification, but the ER seems to be responsible for lysosomal Ca^{2+} refilling. In particular, the authors have shown that the depletion of ER Ca^{2+} stores obtained by using SERCA inhibitors abolished lysosomal Ca^{2+} refilling. Furthermore, the inhibition of IP_3Rs, but not of RyRs, on ER membrane blocked lysosomal Ca^{2+} replenishment by ER (Garrity A.G. *et al.*, 2016).

1.4 TRPML1: the main Ca^{2+} release channel in the lysosome

Among the members of TRPMLs, the most important and the best characterized protein is TRPML1. TRPML1 acts as an inwardly rectifying, non-selective channel permeable to Ca^{2+} and other cations, including Na^+ and K^+ (LaPlante J.M. *et al.*, 2002; Cheng X. *et al.*, 2010; Abe K. and Puertollano R., 2011). Moreover, the channel is also able to mobilize heavy metals, such as Fe^{2+} and Zn^{2+}, from lysosomal lumen to cytosol (Dong X.P. *et al.*, 2008; Eichelsdoerfer J.L. *et al.*, 2010; Grimm C. *et al.*, 2012). Despite being a non-selective cation channel, it is thought that the main physiological function of TRPML1 is to promote Ca^{2+} release from late endosomes and lysosomes (LaPlante J.M. *et al.*, 2002; Abe K. and Puertollano R., 2011).

Human TRPML1 protein is encoded by *mcoln1* gene localized on chromosome 19 (19p13.2-13.3) (Slaugenhaupt S.A. *et al.*, 1999; Bargal R. *et al.*, 2000; Bassi T.M. *et al.*, 2000; Sun M. *et al.*, 2000). TRPML1 is a 580 aa long six-pass transmembrane channel with a molecular weight of ~65 kDa. Similarly to other TRPs, both its N- and C-terminal tails are exposed to the cytosol. Interestingly, the two cytosolic tails contain two independent di-leucine motifs, which regulate TRPML1 delivery to late endosomes and lysosomes. In particular, the N-terminal di-leucine motif ($L^{15}L$) promotes the direct transport of TRPML1 from the TGN to early endosomes and subsequently to lysosomes, through a mechanism that involves the adaptor

protein-1 (AP-1). The C-terminal di-leucine motif (L^{577}L), instead, is involved in the indirect transport of TRPML1 from the TGN to plasma membrane, followed by its internalization and sequential delivery to early endosomes, late endosomes and finally lysosomes; the trafficking of TRPML1 through this indirect route plays a marginal role in TRPML1 delivery to late endosomes and lysosomes and requires the adaptor protein-2 (AP-2). Moreover, some post-translational modifications have been reported to play an important role in the regulation of TRPML1 trafficking and function. For example, the C-terminus of TRPML1 contains three cysteine residues (C^{565}CC) that can be palmitoylated in order to ensure the association of TRPML1 with the late endosomal/lysosomal membranes (Vergarajauregui S. and Puertollano R., 2006). In addition, phosphorylation is an important modification that regulates protein activity. Indeed, protein kinase A (PKA) is able to phosphorylate TRPML1 in its C-terminal tail on S^{557} and S^{559}, thus negatively regulating channel activity. Since these phosphorylation sites are distant from the pore region located between TM5 and TM6 domains, it is possible that phosphorylation affects the interaction between TRPML1 subunits or with other TRP channels (Vergarajauregui S. *et al.*, 2008a). TRPML1 C-terminus can be phosphorylated also by protein kinase D (PKD); this modification seems to be important for the trafficking of TRPML1 from the Golgi apparatus to the lysosomes (Marks D.L. *et al.*, 2012).

Furthermore, the large loop between the first (TM1) and the second (TM2) transmembrane domains contains four N-glycosylation sites. It has been reported that this loop can be cleaved between the second and third glycosylation sites (R^{200}↓P^{201}) by the lysosomal enzyme cathepsin B. The proteolytic cleavage of TRPML1, which occurs late in the biosynthetic pathway at a post-Golgi compartment, is a regulatory mechanism to inhibit TRPML1 channel activity (Kiselyov K. *et al.*, 2005; Miedel M.T. *et al.*, 2006).

Like other members of mucolipin subfamily of TRPs, TRPML1 activity is modulated by phosphoinositides (PIPs): indeed, the channel is strongly activated by the endo-lysosomal-specific phosphoinositide PI(3,5)P$_2$ (Dong X.P. *et al.*, 2010), while it is inhibited by the plasma

membrane-localized phosphoinositide PI(4,5)P$_2$ (Zhang X. *et al.*, 2012). Both the molecules are reported to bind to a stretch of positively charged aa located at the N-terminus of TRPML1; in particular, it seems that aa R^{42}/R^{43}/R^{44} participate in the binding of PI(3,5)P$_2$, while aa R^{61}/K^{62} are involved in the binding of PI(4,5)P$_2$ (Zhang X. *et al.*, 2012). However, also the endogenous second messenger NAADP has been shown to activate the channel (Zhang F. and Li P.L., 2007; Zhang F. *et al.*, 2009; Zhang F. *et al.*, 2011).

1.4.1 Mutations in *mcoln1* gene and mucolipidosis type IV (MLIV)

Loss-of-function mutations in human *mcoln1* gene are responsible for mucolipidosis type IV (MLIV) (OMIM #252650) (Bargal R. *et al.*, 2000; Bassi T.M. *et al.*, 2000; Sun M. *et al.*, 2000), an autosomal recessive lysosomal storage disorder (LSD) first described by Berman and colleagues in 1974 (Berman E.R. *et al.*, 1974). Clinically, the disease is characterized by neurodegeneration, progressive and severe psychomotor retardation, ophthalmological defects, iron deficiency and constitutive achlorhydria (Amir N. *et al.*, 1987; Bach G., 2001; Altarescu G. *et al.*, 2002). Typically, the first symptoms appear early during the childhood (~1-2 years of age), but, after the onset, the clinical progression of the disease is very slow for the first 2-3 decades of life. Individuals with MLIV typically survive to early adulthood and, although their life expectancy is not so clear, patients in their thirties and forties have often been reported (Bach G. *et al.*, 2005). Electron microscopy studies revealed that MLIV cells from every tissue and organ are characterized by the accumulation of enlarged endosomal/lysosomal compartments in which undigested lipid products accumulate; in particular, the storage materials in this disease are more heterogeneous than in the other LSDs, and include sphingolipids (specifically gangliosides), acid mucopolysaccharides, phospholipids, and lipofuscin (Bach G. *et al.*, 1975; Bach G. *et al.*, 1977; Bargal R. and Bach G., 1988; Morgan A.J. *et al.*, 2011). The abnormal accumulation of lipids within MLIV cells is the result of their retention within the acidic organelles, delayed metabolism, and reduced trafficking to the

plasma membrane and Golgi apparatus. Thus, the storage occurring in MLIV is associated with an impairment in lysosomal sorting and/or trafficking of lipids along the late steps of the endocytic pathway, and with defects in lipid metabolism (Bargal R. and Bach G., 1997; Chen C.S. *et al.*, 1998; Jansen S.M. *et al.*, 2001; Venkatachalam K. *et al.*, 2015). However, unlike most other storage diseases, the activity of lysosomal hydrolytic enzymes participating in the catabolism of the stored molecules seems to be unaltered (Chen C.S. *et al.*, 1998).

Concerning the epidemiology of mucolipidosis type IV, the disease is a pan-ethnic disorder that appears rarely in the general population, but it has been observed with a relatively high frequency among Ashkenazi Jewish population; indeed, approximately 70-80% of patients diagnosed with MLIV have Ashkenazi Jewish origin (Raas-Rothschild A. *et al.*, 1999; Bach G., 2001).

In 1999 the gene causing MLIV was mapped to human chromosome 19p13.2-13.3, in a region of approximately 1 cM, by linkage analysis using 13 Ashkenazi Jewish families (Slaugenhaupt S.A. *et al.*, 1999). Later, in 2000, *mcoln1* gene was independently cloned by three research groups, which identified different mutations in *mcoln1* gene, including two major founder mutations causing MLIV in Ashkenazi Jewish population and accounting for ~95% of the mutations in MLIV patients: (1) an A→G transition in the 3' acceptor splice site of intron 3, resulting in an aberrant splicing and in the skipping of exon 4 and 5 (associated with the major Ashkenazi haplotype; ~72% of the alleles); (2) a deletion of ~6000 bp spanning exons 1-6 and the first part of exon 7 (associated with the minor Ashkenazi haplotype; ~23% of the alleles) (Bargal R. *et al.*, 2000; Bassi T.M. *et al.*, 2000; Sun M. *et al.*, 2000). Today, more than 20 different MLIV-causing mutations, including nonsense and missense mutations and an in-frame deletion, have been identified throughout the *mcoln1* gene, in both loops and transmembrane regions of the channel. These mutations can lead to non-functional protein, mislocalized protein, or short versions of the protein (Wakabayashi K. *et al.*, 2011; Grimm C. and Cuajungco M.P., 2014, Venkatachalam K. *et al.*, 2015). Indeed, many patients carry

mutations that introduce premature stop codons in the gene; as a result, the protein is absent or abnormally short, and thus not functional. However, some patients carry single point mutations (i.e. F408Δ and F465L) that make the channel partially inactive on stimulation with endogenous ligands (Chen C.C. *et al.*, 2014).
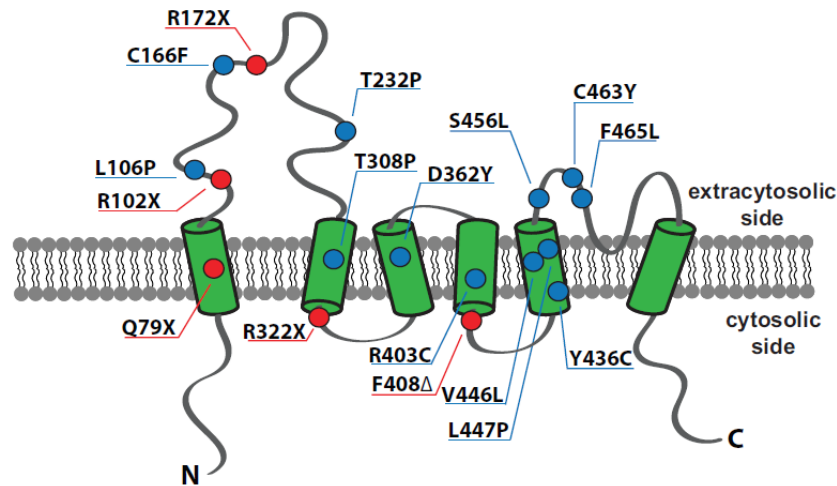

Fig.9 - MLIV-causing mutations in TRPML1 protein. MLIV-causing mutations are reported to occur in the aa residues located in both loops and transmembrane regions. Missense mutations causing amino acid substitution are indicated in blue; mutations causing premature stop codon (X) or in-frame deletion (Δ) are indicated in red (*modified from Venkatachalam K. et al., 2015*).

Mutation number	Nucleotide change	Mutation type	Amino acid change	Mutation ancestry	Primary phenotype
1	g.5534A → G	Splice	–	AJ	
2	c.1406A → G	Splice	454–469del	NJC(CA)	Moderate
3	g.511-6944del	6434-bp deletion	–	AJ	
4	c.163-197del, c.163_197insTCA	Frameshift	–	NJC(G)	
5	c.1221_1223delCTT	aadel	F408del	AJ	Mildest
6	c.473_474delCC	Frameshift	–	NJC(P)	
7	c.1209-1210insT	Frameshift	–	AJ	
8	c.1463_1464insGGCCCAGCAGG	Frameshift	–	NJC	
9	c.304 C → T	Nonsense	R120X	NJC	
10	c.514 C → T	Nonsense	R172X	NJC(CA)	
11	c.964 C → T	Nonsense	R322X	NJ(AD)	
12	c.317 T → C	Missense	L106P	NJC	Milder
13	c.497 G → T	Missense	C166F	AA	Milder
14	c.694A → C	Missense	T232P	NJ	Milder
15	c.1084G → T	Missense	D362Y	NJC	Mild
16	c.1207C → T	Missense	R403C	NJC(CA)	
17	c.1336G → T	Missense	V446L	HA	More severe
18	c.1340T → C	Missense	L447P	NJC	More severe
19	c.1395C → G	Missense	F465L	NJ	More severe
20	c.1388G → A	Missense	C463Y	NJ	More severe
21	c.236_237ins93 from NADH dehydrogenase 5 99–192	31aa Insertion between aa 79–80	In-frame segment of NADH dehydrogenase	NJC(CA)	

Abbreviations: AA = African American, AD = Arab Druze, AJ = Ashkenazi Jewish, CA = Canadian, G = German, HA = Hispanic American, NJ = Non-Jewish, NJC = Non-Jewish Caucasian, P = Polish.

Table 1 - **Mutations identified in patients with MLIV.** Several mutations have been identified in MLIV patients. Most of them are missense mutations, but also frameshift mutations, splice-site mutations, deletions, and insertions have been reported to cause the disease (*modified from Wakabayashi K. et al., 2011*).

Cloning of *mcoln1* gene led to the identification of two additional members of the mucolipin gene family, *mcoln2* and *mcoln3*. Mutations in *mcoln3* gene are reported to cause deafness, circling behaviour, sterility, and pigmentation defects in mice (Di Palma F. *et al.*, 2002). To date, no human diseases have been linked to mutations in *mcoln2* and *mcoln3* genes.

1.4.2 Determination of TRPML1 molecular structure

In the last years, many efforts have been made by researchers in an attempt to determine the molecular structure of TRPML1 protein. Their studies led to the publication of multiple conformations of TRPML1, mainly using electron cryo-microscopy. In the beginning of 2017, Li M. *et al.* have resolved the first high-resolution crystal structure of the long linker between the first two transmembrane segments (TM1 and TM2) of human TRPML1 (Li M. *et al.*, 2017). This region, which constitutes a large part of the channel (more than one-third of the channel's length), is the site of three missense mutations causing MLIV (Wakabayashi K. *et al.*, 2011; Venkatachalam K. *et al.*, 2015). The researchers showed that this linker is able to form a tight tetramer with a highly electronegative central pore which is particularly important in the regulation of TRPML1 by luminal Ca^{2+} and pH. In addition, they demonstrated that the three MLIV-causing mutations in the luminal linker were able to disrupt the structure of the luminal pore and the tetrameric assembly of the full-length channel, thus determining its mislocalization within the cell (Li M. *et al.*, 2017). Moreover, in the same year Schmiege *et al.* have determined the electron cryo-microscopy structure of full-length human TRPML1. They demonstrated that TRPML1 has a topology similar to other TRP channels and forms the canonical homotetrameric assembly in which the ion channel is formed at its centre. Interestingly, the researchers also resolved the structure of the channel in an open conformation, bound to its agonist ML-SA1. They showed that this synthetic compound binds within a hydrophobic pocket created by two TRPML1 subunits, inducing conformational changes that allow Ca^{2+} efflux across the channel (Schmiege P. *et al.*, 2017). Recently, Chen *et al.* resolved the electron cryo-microscopy

structure of mouse TRPML1 channel (91% primary sequence similarity to human TRPML1) embedded in nanodiscs, characterizing the PI(3,5)P$_2$-binding site at the N-terminus of the channel, distal from the pore region (Chen Q. *et al.*, 2017). Finally, Zhang *et al.* presented the structure of mouse TRPML1 in lipid nanodiscs and Amphipols, and, based on their structural analysis, they proposed that the channel is regulated by pH, Ca^{2+} and phosphoinositides in a combined and different manner, depending on its subcellular localization (plasma membrane – late endosomes – lysosomes) along the endocytosis/exocytosis pathways (Zhang S. *et al.*, 2017).

1.4.3 TRPML1 interacting proteins

In recent years, some proteins that physically interact with TRPML1 have been identified. An important TRPML1 interactor is ALG-2 (*Alix-Apoptosis-Linked Gene-2*), a Ca^{2+}-binding protein belonging to the penta-EF hand protein family. This protein, that could act as a lysosomal Ca^{2+} sensor, is able to bind in a Ca^{2+}-dependent manner to a stretch of charged and hydrophobic aa located to the N-terminus of TRPML1. It has been proposed that the binding of ALG-2 to TRPML1 plays an important role in the regulation of the distribution and function of TRPML1 along the late endosomal-lysosomal pathway (Vergarajauregui S. *et al.*, 2009). TRPML1 was also found to interact with the three members of the *Lysosomal-Associated Protein Transmembrane* (LAPTM) family (LAPTM4a, LAPTM4b, and LAPTM5), which participate in the transport of small molecules across intracellular membranes. This association, occurring at the level of the late endosomes and lysosomes, suggested a novel role for LAPTM proteins in the regulation of lysosomal function (Vergarajauregui S. *et al.*, 2011). TRPML1 also associates with Hsc70 and Hsp40, two members of a molecular chaperone complex involved in protein transport into the lysosome during Chaperone-Mediated Autophagy (CMA). It has been hypothesized that the interaction of TRPML1 with these proteins may be required for proper CMA function (Venugopal B. *et al.*, 2009). Furthermore, Spooner *et al.* recently performed a

systematic screen for TRPML1 interactors, identifying some potential proteins that could interact with the channel (i.e. STOML1, Rac2, Cdc42, P5KTI, and NP9). However, further studies are needed to validate the interaction of these candidate interactor proteins with the lysosomal channel (Spooner E. *et al.*, 2013). Finally, TRPML1 has also been reported to interact with TPC channels, although it seems that the two families of channels function independently in lysosomes (Yamaguchi S. *et al.*, 2011).

1.4.4 Lysosomal functions mediated by TRPML1

A growing body of experimental evidences has demonstrated that Ca^{2+} released through TRPML1 channel play a fundamental role in a plethora of lysosomal processes, including lysosomal exocytosis (Medina D.L. *et al.*, 2011; Settembre C. *et al.*, 2013), phagocytosis (Samie M. *et al.*, 2013), lysosomal biogenesis, size and trafficking (Treusch S. *et al.*, 2004; Shen D. *et al.*, 2012; Cao Q. *et al.*, 2017), regulation of autophagy (Medina D.L. *et al.*, 2015; Zhang X. *et al.*, 2016), and lysosomal motility and positioning (Li X. *et al.*, 2016).

1.4.4.1 Lysosomal exocytosis

Different research groups demonstrated that TRPML1 is involved in lysosomal exocytosis. The first evidence suggesting an active role for TRPML1 in this process date back to 2006, when LaPlante *et al.* revealed that lysosomal exocytosis was dramatically impaired in fibroblasts from MLIV patients, carrying loss-of-function mutations in TRPML1. Interestingly, they found that the dysfunction observed could be efficiently corrected by transfecting the MILV cells with the wild-type TRPML1 cDNA (LaPlante J.M. *et al.*, 2006). The involvement of the channel in lysosomal exocytosis was confirmed by another paper, in which the authors showed that lysosomal exocytosis was increased in cells expressing gain-of-function mutations in TRPML1, *via* a mechanism that is dependent on lysosomal Ca^{2+} release (Dong X.P. *et al.*, 2009). These evidences suggest that TRPML1 may promote lysosomal Ca^{2+} release to induce

lysosomal exocytosis. In this regard, the involvement of TRPML1 in this process was further corroborated by the discovery that TFEB, a master regulator of several lysosomal functions, controls not only the gene encoding for TRPML1, but also the process of lysosomal exocytosis. Indeed, in 2011 Medina *et al.* reported that in TFEB-overexpressing cells the silencing of TRPML1 abolished the increase in intracellular Ca^{2+} concentration mediated by TFEB, thus inhibiting lysosomal exocytosis. Accordingly, in human MLIV cells that carried loss-of-function mutation of the channel, Ca^{2+} levels were not affected by TFEB overexpression and lysosomal exocytosis was not induced. Moreover, the depletion of TRPML1 impaired TFEB-mediated fusion of lysosomes with the plasma membrane, and inhibited the secretion of lysosomal enzymes into the extracellular medium. These results suggest that TFEB modulates lysosomal exocytosis by triggering intracellular Ca^{2+} elevation through TRPML1 (Medina D.L. *et al.*, 2011).

1.4.4.2 Phagocytosis

TRPML1 is also involved in the phagocytosis and clearance of large extracellular particles in macrophage cells. Phagocytosis of large particles, such as apoptotic bodies, is known to require the delivery of endosomal and lysosomal membranes to form plasmalemmal pseudopods (Czibener C. *et al.*, 2006). In a recent paper, Samie *et al.* showed that the binding of large particles to macrophages triggered an increase in $PI(3,5)P_2$ levels, which promoted transient Ca^{2+} release through TRPML1, locally at the sites of uptake. This phenomenon contributed to phagosome biogenesis by rapidly delivering lysosomal membrane to nascent phagosomes *via* focal exocytosis, thus leading to the clearance of senescent and apoptotic cells. The involvement of TRPML1 in phagocytosis has been demonstrated by the evidence that both particle ingestion and lysosomal exocytosis were blocked by the pharmacological inhibition of TRPML1 and were defective in macrophages isolated from TRPML1 knock out mice. By

contrast, TRPML1 overexpression or its pharmacological activation facilitated both the processes (Samie M. *et al.*, 2013).

1.4.4.3 Lysosomal biogenesis, size and trafficking

Cells lacking TRPML1 are characterized by profound defects in the late endosomal/lysosomal compartments. Mutations in *cup-5*, the *C.elegans* functional ortholog of the mammalian TRPML1, cause a block/delay in the complete maturation of lysosomes and lead to the accumulation of aberrant large vacuoles that are hybrids of late endosomes and lysosomes (LELs). These alterations indicate a defect in lysosomal biogenesis and reformation from hybrid organelles (Treusch S. *et al.*, 2004). A similar accumulation of enlarged LELs has also been observed in cells from *Drosophila trpml* mutants (Venkatachalam K. *et al.*, 2008) and in cells from TRPML1 knock out mice (Venugopal B. *et al.*, 2007).

It has been proposed that TRPML1 exerts a crucial function also in the control of lysosome size. Indeed, in yeast a pivotal role in the regulation of vacuole size is played by $PI(3,5)P_2$, the endogenous activator of the channel. $PI(3,5)P_2$ deficiency was accompanied by a dramatic increase in vacuole size and defects in multivesicular bodies (MVB) sorting; in contrast, high levels of $PI(3,5)P_2$ caused organelle shrinkage and fragmentation (Efe J.A. *et al.*, 2005). Also in mammals $PI(3,5)P_2$ deficiency led to the enlargement of vacuoles/LELs and to trafficking defects (Dong X.P. *et al.*, 2010). Moreover, TRPML1^{-/-} cells from MLIV patients displayed an accumulation of enlarged endosomal/lysosomal compartments, in which lipids and other biomaterials accumulated, suggesting profound defects in lysosomal biogenesis and trafficking (Chen X. *et al.*, 2010). In 2017 Cao *et al.* have demonstrated the direct involvement of TRPML1 in the regulation of lysosomal size in mammalian cells. Indeed, TRPML1 upregulation, by activating calmodulin, was able to suppress in a Ca^{2+}-dependent manner the formation of enlarged lysosomes/vacuoles induced by the chemical vacuolin-1 or by the activation of P2X4 receptor. These data supported the predominant role of TRPML1 in

lysosome fission. Considering the involvement of lysosome fission in the processes of lysosome biogenesis and reformation, it has been suggested that TRPML1 could mediate the reformation of lysosomes from hybrid organelles formed after fusion with late endosomes or autophagosomes, thus participating in lysosome biogenesis (Cao Q. *et al.*, 2017).

Furthermore, the lack of TRPML1 has also been associated with multiple trafficking defects, including the retrograde transport of some lipid molecules to the TGN and the transport and degradation of different substrates into the lysosomes (Di Paola S. *et al.*, 2018). In particular, the LEL-to-TGN retrograde trafficking is impaired in MLIV cells, since lactosylceramide, a lipid normally localized to the Golgi apparatus, accumulated in lysosomes, thus suggesting that lipid trafficking (the exit of lipids from late endosomes and lysosomes) is impaired in the absence of TRPML1 (Chen C.S. *et al.*, 1998). Moreover, defects in components of the intracellular cholesterol/lipid trafficking pathway are commonly associated with another severe lysosomal storage disorder, the Niemann-Pick type C (NPC) disease (Rosenbaum A.I. and Maxfield F.R., 2011). In 2012 Shen *et al.* reported that the increase in TRPML1 expression and activity was sufficient to correct the lysosomal trafficking defects and reduced cholesterol accumulation in NPC cells (Shen D. *et al.*, 2012).

Collectively, all these evidences suggest that the activation of TRPML1 is required for the regulation of lysosomal biogenesis, size and intracellular trafficking.

1.4.4.4 Regulation of autophagy

Several experimental evidences demonstrated the crucial role of TRPML1 in the regulation of the autophagic process. In human fibroblasts derived from MLIV patients, the impairment of the autophagic pathway induced a significant accumulation of the autophagic markers p62 and LC3-II, as a result of increased autophagosome formation and delayed autophagosome fusion with lysosomes. These alterations led to an inefficient autophagosome degradation (Vergarajauregui S. *et al.*, 2008b). A similar increase in p62 and LC3-II was also

observed in neuronal cells derived from *mcoln1-/-* mouse, a murine model of MLIV. This finding

suggested an accumulation of protein aggregates and a defect in autophagy which could account

for the neurodegeneration occurring in MLIV (Curcio-Morelli C. *et al.*, 2010b). Autophagic

defects have also been described in other animal models of MLIV, including *Drosophila trpml*

mutant and *C.elegans cup-5* null mutant. In particular, the disruption in autophagy observed in

trpml mutant flies, which exhibited a MLIV-like phenotype, was attributable to a reduced

degradation of cargoes following fusion between autophagosomes and lysosomes

(Venkatachalam K. *et al.*, 2008). Similarly, in *C.elegans* mutations in *cup-5* are responsible for

defects in the autophagic pathway. Indeed, in *cup-5* null mutant worms, a variety of autophagic

substrates accumulated in enlarged vacuoles similar to late endosomes and lysosomes, thus

indicating a dysfunction in the proteolytic degradation of autolysosomes (Sun T. *et al.*, 2011).

However, a deepen knowledge about the molecular mechanisms underlying TRPML1-

mediated regulation of autophagy came from recent studies performed in mammalian cells. In

example, in 2015 Medina *et al.* demonstrated that lysosomal Ca^{2+} release through TRPML1, by

activating the Ca^{2+}-dependent Ser/Thr phosphatase calcineurin (CaN), promoted TFEB nuclear

translocation and TFEB-mediated transcription of the autophagic genes. Interestingly, the

inhibition of TRPML1, by preventing the cytoplasm-to-nucleus shuttling of TFEB, hampered

the transcription of the autophagic genes, thus determining a block in the autophagic process

(Medina D.L. *et al.*, 2015). Furthermore, it has been proven that autophagy can also be activated

by lysosomal Ca^{2+} release through TRPML1 in response to oxidative stress conditions. Indeed,

following an elevation in ROS production (for example, due to mitochondrial damage) or an

increase in exogenous oxidants, TRPML1-mediated Ca^{2+} release promoted CaN-dependent

TFEB nuclear translocation, thus enhancing both autophagy and lysosome biogenesis. In this

way, TRPML1 acted as a ROS sensor activated upon elevations in ROS levels, which could

reduce oxidative stress in the cell. Indeed, the subsequent increase in the autophagic flux

mediated by the lysosomal channel could facilitate the elimination of damaged mitochondria and excessive ROS, thus restoring the cellular redox homeostasis (Zhang X. *et al.*, 2016).

1.4.4.5 Lysosomal motility and positioning

In 2016 Li *et al.* have demonstrated that upon nutrient starvation TRPML1 activity is also required to promote Ca^{2+}-dependent centripetal movement of lysosomes towards the perinuclear region of the cell. The authors showed that under resting conditions lysosomes were scattered throughout the cytoplasm, while during autophagy these organelles were recruited to the perinuclear area, where autophagosomes accumulated, in a mechanism mediated by TRPML1. Indeed, TRPML1-mediated Ca^{2+} release activated the Ca^{2+}-binding protein ALG-2, which bound to TRPML1 and, in turn, recruited the dynein-dynactin complex required for centripetal movement of lysosomes. Following their accumulation in close proximity to the nucleus, lysosomes fused with autophagosomes, thus promoting the formation of autolysosomes (Li X. *et al.*, 2016).

1.5 Physical and functional coupling between lysosomes and ER

Accumulating evidences demonstrated the existence of a physical and functional crosstalk between lysosomes and ER in different types of animal cells. Lysosomes/ER interaction seems to occur at membrane contact sites (MCSs), restricted regions between two membranes that are in close proximity (typically less than 30 nm separation). These restricted spaces, functionally referred to as microdomains or nanojunctions, act as platforms for the exchange of small molecules and ions, including Ca^{2+}, between different compartments (Burgoyne T. *et al.*, 2015; Penny C.J. *et al.*, 2015; Aston D. *et al.*, 2017). Interestingly, it has been estimated that 80-100% of lysosomes forms MCSs with the ER, thus suggesting a

functional role for the physical coupling between these two Ca^{2+} stores in the regulation of intracellular Ca^{2+} homeostasis (Burgoyne T. *et al.*, 2015; La Rovere R.M.L. *et al.*, 2016).

Concerning the mechanisms underlying Ca^{2+} exchange between lysosomes and ER, it has been proposed that the two compartments could interact at least in two ways: in a first model, Ca^{2+} released from acidic stores can be sequestered by the ER, priming the latter for enhanced release (Lee H.C. *et al.*, 2012). This mechanism has been proposed to account for the NAADP-induced Ca^{2+} oscillation observed in sea urchin eggs (Churchill G.C. and Galione A., 2001) and the excitation-contraction coupling in guinea-pig atrial myocytes (Collins T.P. *et al.*, 2011). Alternatively, according to the so-called "trigger" hypothesis, the Ca^{2+}-mobilizing second messenger NAADP initiates a small local Ca^{2+} release from acidic Ca^{2+} stores that is subsequently amplified by ER Ca^{2+} release. In particular, it has been proposed that Ca^{2+} released through lysosomal channels (i.e. TPCs) upon stimulation with NAADP (local signalling) could sensitizes the neighbouring ER Ca^{2+} channels (IP$_3$Rs and/or RyRs) to mediate further Ca^{2+} release from ER *via* Ca^{2+}-induced Ca^{2+} release (CICR) mechanism (global signalling) (Cancela J.M. *et al.*, 1999; Patel S. and Docampo R., 2010; Lee H.C. *et al.*, 2012). The crosstalk ("channel chatter") between lysosomal and ER Ca^{2+} channels is responsible for the so-called "anterograde" Ca^{2+} signaling (from lysosomes to ER). This mechanism was proposed to account for the blockage of the cholecystokinin (CKK)-activated and NAADP-dependent Ca^{2+} release in mouse pancreatic acinar cells by antagonists of the RyRs and IP$_3$Rs (Cancela J.M. *et al.*, 1999; Lee H.C. *et al.*, 2012).
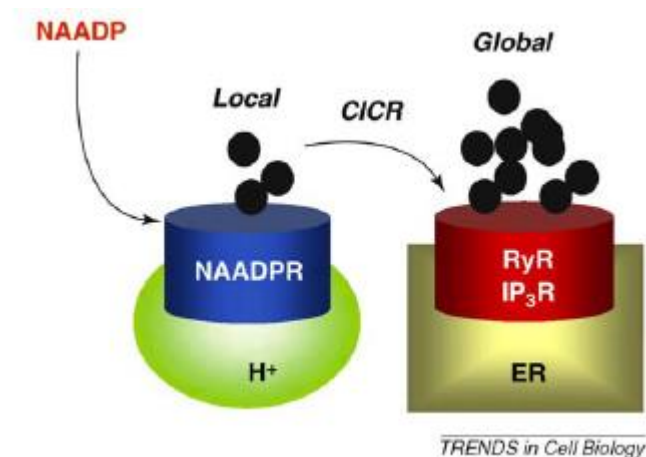
Fig.10 - **NAADP-mediated "channel chatter" between lysosomal and ER Ca^{2+} channels.** Schematic showing the proposed mechanism of action of NAADP, according to the "trigger" hypothesis. The activation of lysosomal Ca^{2+} channels by NAADP generates a local Ca^{2+} signalling from acidic Ca^{2+} stores, which is subsequently amplified by ER Ca^{2+} channels, thus resulting in a global Ca^{2+} signalling (*modified from Patel S. and Docampo R., 2010*).

However, it has been recently demonstrated that the dialogue between the two compartments can be bidirectional. Indeed, in addition to the above-mentioned "anterograde" Ca^{2+} signalling, the communication can also occur in the reverse "retrograde" direction (from ER to lysosomes). The first evidence of a retrograde Ca^{2+} signalling was provided in 2013 by Morgan *et al.*, who discovered this reverse communication in sea urchin eggs. In these cells, ER could signal back to acidic organelles, and Ca^{2+} released from ER through IP$_3$Rs and RyRs could stimulate the NAADP pathway, thus amplifying acidic Ca^{2+} store signalling. The authors proposed that Ca^{2+} released from ER could activate the NAADP pathway in two ways: first, by promoting Ca^{2+}-dependent NAADP synthesis; second, by activating NAADP-sensitive channels on lysosomal stores (Morgan A.J. *et al.*, 2013).

An intimate association between ER and acidic organelles involving Ca^{2+} microdomains has been described in different types of mammalian cells. In particular, in pulmonary artery myocytes it has been found that lysosomes were in close apposition with the sarcoplasmic reticulum (SR), a specialized type of smooth ER found in myocytes. Interestingly, this coupling was able to trigger intracellular Ca^{2+} signalling involving both the compartments (Kinnear N.P. *et al.*, 2008). Furthermore, in 2013 Kilpatrick *et al.* demonstrated the existence of extensive

MCSs between lysosomes and ER also in human fibroblasts (Kilpatrick B.S. *et al.*, 2013). These MCSs were similar to those observed between ER and mitochondria, important for Ca^{2+} dialogue between the two compartments (Csordás G. *et al.*, 2006). The authors suggested a functional role for this physical coupling, since they found that Ca^{2+} mobilization from lysosomes was able to induce complex Ca^{2+} signals within the cell involving Ca^{2+} release from ER, probably *via* IP$_3$Rs. This finding was consistent with the trigger hypothesis for NAADP action (Kilpatrick B.S. *et al.*, 2013).
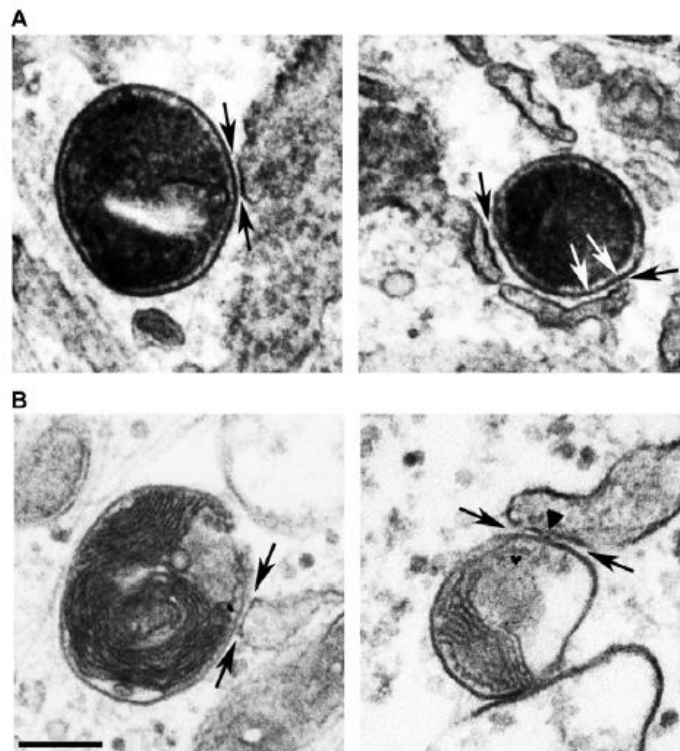

Fig.11 - Physical association between lysosomal and ER membranes in human fibroblasts. (**A,B**) Electron micrographs of human fibroblasts pulsed with horseradish peroxidase (**A**) or BSA-gold (**B**) to label lysosomes. Membrane contact sites (MCSs) between lysosomes and ER are indicated by black arrows. Fibres connecting opposing membranes (white arrows) and regions of very close membrane apposition (arrowhead) are also indicated. Scale bar: 200 nm (*modified from Kilpatrick B.S. et al., 2013*).

In 2016 the same research group has demonstrated that, contrary to the prevailing view, also the activation of the endogenous TRPML1 was able to trigger a global Ca^{2+} signalling in human cells, in a manner similar to the activation of TPCs by NAADP. Indeed, upon stimulation with synthetic agonists, Ca^{2+} release through TRPML1 was followed by Ca^{2+} release from the ER. These results suggested that TRPML1, like other endo-lysosomal Ca^{2+} channels, could

"chatter" with ER Ca^{2+} channels to evoke global Ca^{2+} signals (Kilpatrick B.S. *et al.*, 2016b). Moreover, very recently Aston *et al.* have demonstrated that in rabbit ventricular cardiomyocytes lysosomes were intimately associated with the SR, forming microdomains which allowed functional Ca^{2+} signalling between the two organelles. Indeed, they found that Ca^{2+} release from acidic stores subsequently triggered Ca^{2+} release from SR (Aston D. *et al.*, 2017).

1.6   Lysosomal Ca^{2+} dysfunction in neurodegeneration

Several neurodegenerative diseases, including some lysosomal storage disorders (LSDs) and aging-related diseases, have been recently associated with alterations in lysosomal Ca^{2+} handling. LSDs are a heterogeneous group of approximately 50 childhood rare disorders, most of which characterized by neurodegeneration. A common feature of these diseases is the accumulation (storage) of different types of undegraded macromolecules in the late endocytic/lysosomal system (Morgan A.J. *et al.*, 2011). So far, three LSDs have been associated with defects in lysosomal Ca^{2+} homeostasis: Niemann-Pick type C (NPC) disease (Lloyd-Evans E. *et al.*, 2008), juvenile neuronal ceroid lipofuscinosis (JNCL, also known as Batten disease) (Chandrachud U. *et al.*, 2015), and Chediak-Higashi syndrome (CHS) (Lloyd-Evans E. and Platt F.M., 2011). NPC is the first human disease that has been correlated with a dysregulation in lysosomal Ca^{2+} homeostasis. In this disorder, lysosomes accumulate cholesterol, sphingomyelin, glycosphingolipids, and sphingosine. The disease is also characterized by low Ca^{2+} levels in the acidic stores, caused by defective lysosomal Ca^{2+} uptake and subsequent reduction in lysosomal Ca^{2+} release. In NPC the dysfunction in lysosomal Ca^{2+} leads to an impairment in late endosomes/lysosomes fusion and to a defective lipid trafficking (Lloyd-Evans E. *et al.*, 2008; Lloyd-Evans E. and Platt F.M., 2011). JNCL is characterized by the accumulation of autofluorescent lipofuscin in lysosomes and by abnormalities in the production and clearance of autophagic vacuoles (Lloyd-Evans E. *et al.*, 2016b). Recent studies have

shown that in cerebellar cells from CLN3$^{\Delta ex7/8/\ \Delta ex7/8}$ mouse, an animal model recapitulating the major genetic defects observed in JNCL patients, there was an elevation in lysosomal Ca^{2+} levels (Chandrachud U. *et al.*, 2015; Lloyd-Evans E. *et al.*, 2016b). Moreover, in CHS, an increase in lysosomal Ca^{2+} uptake seems to be responsible for an impairment in lysosomal exocytosis (Styrt B. *et al.*, 1988; Lloyd-Evans E. and Platt F.M., 2011).

Defects in lysosomal Ca^{2+} homeostasis have also been described in other common neurodegenerative diseases, including Alzheimer's disease (AD) and Parkinson's disease (PD). In particular, in a mouse model of familial AD (FAD), loss-of-function mutations in presenilins (PSEN$^{-/-}$) significantly altered lysosomal Ca^{2+} storage and release, especially in hippocampal neurons; as a consequence, lysosomal fusion processes were strongly impaired (Coen K. *et al.*, 2012). It has been proposed that the dysfunction in lysosomal Ca^{2+} observed in PSEN1$^{-/-}$ cells was dependent on the elevation in lysosomal pH, which caused an abnormal Ca^{2+} efflux from lysosomes *via* the hyperactivation of the lysosomal channel TRPML1 (Lee J.H. *et al.*, 2015).

Moreover, increasing evidences demonstrated that deregulated Ca^{2+} signaling and lysosomal dysfunction also underlie the neurodegeneration associated to PD. In particular, mutations in PD-linked genes GBA1 (encoding for the lysosomal enzyme glucocerebrosidase) and LRRK2 (encoding for a protein whose function is still unknown) are responsible for defects in lysosomal Ca^{2+} homeostasis. It has been shown that GBA1 fibroblasts contained lower lysosomal Ca^{2+} levels compared to wild-type cells; in addition, they were characterized by a disrupted endo-lysosomal morphology with enlarged and clustered lysosomes. LRRK2 mutations have been reported to induce hyperactive lysosomal Ca^{2+} signaling and extensive lysosomal morphology defects; moreover, it has been proposed that these mutations could be associated with a reduction in lysosomal Ca^{2+} concentration (Kilpatrick B.S. *et al.*, 2016a).

At present, there is no information about the possible contribution of lysosomal Ca^{2+} in the neurodegeneration associated to brain ischemia.

1.7 Brain ischemia

Stroke is a multifactorial neurological disease which accounts for ~9% of all death around the world and represents the second most common cause of death after ischemic heart disease and the major cause of long-lasting disability worldwide. Because of the ageing of population, the burden of this neurological disease will increase greatly during the next years, especially in the developing countries (Donnan G.A. *et al.*, 2008).

Several neurological defects occur following stroke, including hemiplegia, numbness, balance problems, loss of sensory and vibratory sensation, decreased reflexes, ptosis, visual field defects, aphasia, and apraxia due to neuronal damage. However, the severity of symptoms depends on the brain area affected by the insult (Pandya R.S. *et al.*, 2011; Chen Y. *et al.*, 2014).

There are two main types of stroke: ischemic stroke (also known as brain ischemia, ~85% of cases), resulting from the occlusion of a blood vessel that supplies the brain produced by thrombosis or embolism, and haemorrhagic stroke (~15% of cases), due to the rupture of a cerebral blood vessel (Donnan G.A. *et al.*, 2008; Pandya R.S. *et al.*, 2011). In ischemic stroke the interruption of the blood flow in a portion of the brain cuts off the supply of oxygen and nutrients (and in particular glucose) essential for the normal cerebral functions, thus causing damage to the brain tissue. After the ischemic insult, a complex sequence of pathological events takes place, including disruption of the blood-brain barrier (BBB), energy failure, dysregulation of ion homeostasis (and in particular, increased intracellular Ca^{2+} levels), acidosis, excitotoxicity, free-radical mediated toxicity, generation of arachidonic acid products, cytokine-mediated apoptosis, activation of glial cells, and infiltration of leukocytes (Arumugam T.V. *et al.*, 2009).

Moreover, ischemic stroke can be categorized into two types, based on the origin of the occlusion and the extent of the injured area: global or focal cerebral ischemia. Global cerebral ischemia occurs when cerebral blood flow is reduced throughout most or all the brain. This may be the result of generalized blood flow reduction secondary to severe physiological

derangements, such as persistent hypotension or severe cardiovascular abnormalities. In contrast, in focal ischemia the reduction of blood flow occurs in a specific and restricted brain region (Traystman R.J., 2003; Zhou Z.B. *et al.*, 2016). During focal brain ischemia two different areas are distinguishable in the injured brain: the ischemic "core" and "penumbra". The core is the area of the brain where blood flow is reduced below 10-20% of its normal level; in this area, rapid anoxic depolarization causes loss of membrane potential followed by cellular swelling, loss of membrane integrity and rapid necrotic cell death (Arumugam T.V. *et al.*, 2009). Due to these pathological events, the infarction core results irreversibly damaged (Donnan G.A. *et al.*, 2008). The penumbra is the tissue surrounding the core, where the blood flow is partially preserved due to collateral circulation and diffusion (Arumugam T.V. *et al.*, 2009). Cerebral tissue in this area is functionally impaired, but structurally intact, thus a prompt therapeutic intervention can promote neurological improvement and recovery. Within this tissue, the reduction in blood flow and the resulting loss of oxygen supply trigger a cascade of neurochemical events beginning with energy depletion (Donnan G.A. *et al.*, 2008). In particular, the combination of ATP reduction and the compensatory activation of anaerobic glycolysis leads to an increase in the level of inorganic phosphate, lactate, and H^+, thus resulting in cellular acidification. The decrease in ATP levels also impairs the ability of membrane ATPases to remove Na^+ and Ca^{2+} from the cell, thus causing membrane depolarization, which in turn promotes the activation of synaptic glutamate receptors. Since during ischemia the energy-dependent mechanisms responsible for glutamate re-uptake are impaired, extracellular glutamate accumulates, thus activating glutamate receptors in a prolonged and excessive manner. The effect is a massive Ca^{2+} influx through NMDA (*N-methyl-D-aspartate*) receptors, AMPA (*a-amino-3-hydroxy-5-methyl-4-isoxazolepropionate*) receptors, and voltage-dependent Ca^{2+} channels. Moreover, energy failure and disruption of intracellular Ca^{2+} homeostasis are responsible for mitochondrial impairment. Increased production of free radicals, which damage cellular proteins, DNA, and membrane lipids, results from

mitochondrial dysfunction, Ca^{2+} overload, and activation of enzymes such as cyclooxygenase, and nitric oxide synthase. Ca^{2+} influx induces the activation of two different cysteine proteases: caspases and calpains. These, in turn, cause the degradation of cytoskeletal proteins, membrane receptors, and metabolic enzymes. Moreover, the increase in intracellular Na^+ levels can directly cause cell swelling, oxidative stress, and cell death. When intracellular Na^+, Cl^-, and H_2O levels increase at the same time, cytotoxic edema occurs. Moreover, excessive K^+ efflux and intracellular K^+ depletion play a role in apoptotic cascade, whereas K^+ released from mitochondria contributes to increased reactive oxygen species (ROS) production and ATP depletion. Oxidative stress and caspases activation exacerbate mitochondrial dysfunction that eventually results in apoptotic cell death (Arumugam T.V. *et al.*, 2009).
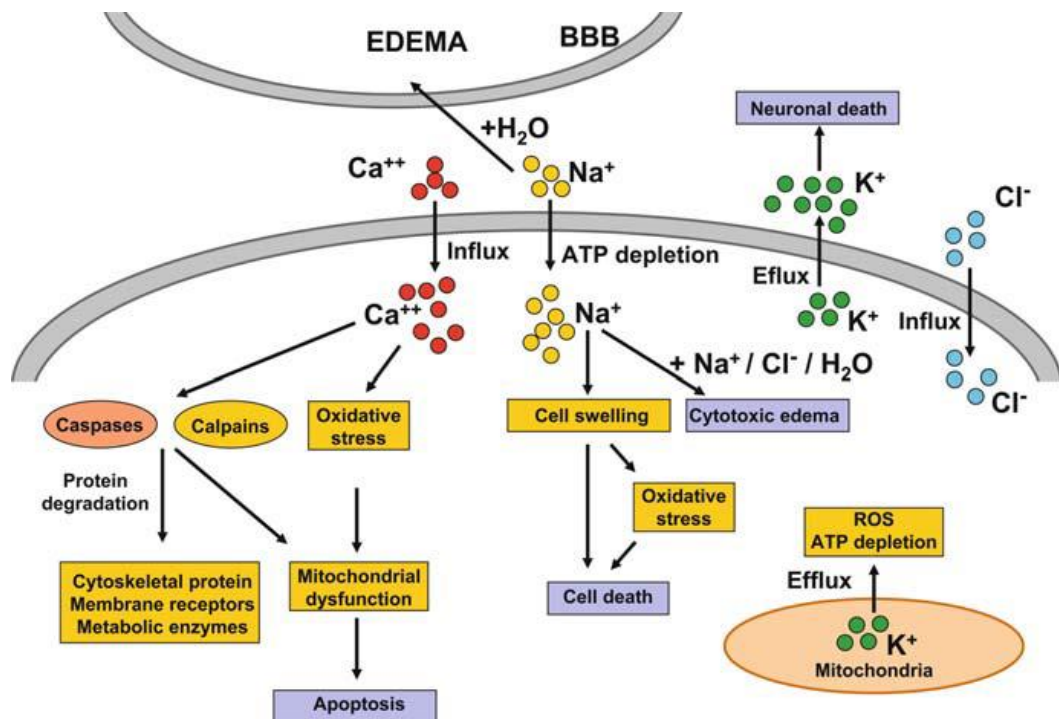

Fig.12 - Pathogenic events dysregulating ionic homeostasis during brain ischemia. Energy depletion occurring during brain ischemia is followed by a cascade of pathological events, including the disruption of ionic homeostasis, Ca^{2+} channel dysfunction, membrane disruption, formation of a cytotoxic edema, protein degradation, oxidative stress, and mitochondrial dysfunction. The combination of all these events ultimately lead to apoptotic neuronal death (*modified from Arumugam T.V. et al., 2009*).

Moreover, upon reperfusion, when the occlusion is removed (spontaneously or pharmacologically) and the blood flow is restored in the infarcted area, oxygen availability

results in a larger increase in ROS and nitric oxide (NO) production, which add up to free radicals produced during ischemia. The resulting oxidative stress causes further neuronal damage and may ultimately result in the initiation of pathways that lead to necrotic and apoptotic cell death (Manzanero S. *et al.*, 2013).

In addition to mitochondria, cerebral ischemia also induces dysfunctions in the ER. Indeed, an increase in the expression of genes encoding ER stress proteins (Paschen W. *et al.*, 2003; Shibata M. *et al.*, 2003; Paschen W. and Mengersdorf T., 2005; Pallast S. *et al.*, 2010) and a marked depletion of Ca^{2+} ions from ER have been observed in cortical neurons after exposure to oxygen and glucose deprivation (OGD) followed by reoxygenation (Sirabella R. *et al.*, 2009), an *in vitro* model to reproduce the pathological events occurring during ischemia/reperfusion.

1.7.1 Brain ischemia and ER dysfunction

Besides Ca^{2+} storage and signalling, a central function of the ER is the folding and processing of newly synthesized proteins, two Ca^{2+}-dependent processes. When these functions are impaired, misfolded and unfolded proteins accumulate in the ER lumen, thus leading to a pathological condition termed "ER stress". To cope with conditions associated with ER impairment, functioning cells activate a high conserved stress response termed "Unfolded Protein Response" (UPR), in an attempt to restore ER functions and assist the correct protein folding. Various proteins play a role in this critical process, including the ER molecular chaperone GRP78 (*glucose-regulated protein 78 kDa*). Indeed, the main purpose of UPR is to increase protein folding and processing capacity, thus reducing the load of misfolded proteins in ER lumen. However, when ER stress is too severe and prolonged, apoptotic cell death is triggered (Paschen W. and Mengersdorf T., 2005; Malhotra J.D. and Kaufman R.J., 2007).

Several experimental evidences showed that ER stress plays a key role in the neurodegeneration associated to brain ischemia. Indeed, it has been reported that the ischemic insult induces the accumulation of misfolded proteins in ER lumen and promotes the expression of several genes involved in ER stress (Paschen W. and Mengersdorf T., 2005; Kim I. *et al.*, 2008). Moreover, reperfusion of the affected tissues triggers oxidative stress, with production of NO, a mediator of protein nitrosylation, and ROS that alter cellular redox-dependent reactions, interfere with protein disulphide bonding, and result in protein misfolding. NO and other reactive molecules may also modify oxidizable residues (cysteine and tyrosine) in ER calcium channels, including RyRs (S-nitrosylation) and SR/ER Ca^{2+}-ATPases (SERCAs) (by tyrosine nitration), thus causing ER Ca^{2+} depletion and, consequently, exacerbating protein misfolding (Kim I. *et al.*, 2008).

1.7.2 Brain ischemia and autophagy

Recently, the role of autophagy in the neurodegeneration associated to cerebral ischemia has been extensively investigated. Several studies have reported that autophagy is activated following the ischemic insult; however, the contribution of this process to neuronal death/survival is still a matter of debate (Chen W. *et al.*, 2014). Newly emerged research indicates that altered autophagy flux functionality is involved in the neurodegeneration of the aging brain, chronic neurological disease, and after acute ischemic brain injury. However, currently there is no unified theory on the role played by autophagy in brain ischemia, and increasing evidence demonstrated that the process is a double-edged sword in this neurological disease (Chen W. *et al.*, 2014; Yin Y. *et al.*, 2017). At present the controversial role of autophagy during ischemia is prevalent across the literature: indeed, some studies conclude that autophagy is neuroprotective and other studies suggest that autophagy leads to cell death. In example, Carloni *et al.* reported a study of ischemia in rats, in which the inhibition of autophagy by 3-MA (*3-methyladenine*) led to a decrease in beclin 1 expression and to increased cell death;

however, they found that the promotion of autophagy by rapamycin reduced cell death and brain injury, suggesting a beneficial role for autophagy (Carloni S. *et al.*, 2010). Conversely, other studies have shown that autophagy is neurotoxic, since it leads to cell death after ischemia. In example, in their study Wen *et al.* demonstrated profound activation of autophagy in rats subjected to permanent middle cerebral artery occlusion (pMCAO) (Wen Y.D. *et al.*, 2008); moreover, the administration of the autophagy inhibitor 3-MA was neuroprotective and prevented neuronal death after ischemia induced in rats by pMCAO and four-vessel occlusion (4-VO) (Wen Y.D. *et al.*, 2008; Xin X.Y. *et al.*, 2011).

Since at present the exact role and the molecular mechanisms of autophagy process during brain ischemia have not yet been elucidated, further studied are required to verify the contribution of this process to the pathophysiological events underlying this neurological disorder.

1.7.3 Pharmacological treatments for brain ischemia

So far, two main approaches have emerged for acute treatment of ischemic stroke. The first strategy targets the insult itself, trying to rapidly restore focal cerebral blood flow by lysing or mechanically removing the arterial thrombus. The second major therapeutic approach involves neuroprotection, which aims to interrupt the cascade of pathophysiological events leading to cell death, thus reducing the vulnerability of the penumbra (Brouns R. and De Deyn P.P., 2009).

At present, the only effective pharmacological treatment for acute ischemic stroke approved by the Food and Drug Administration (FDA) and the European Medicines Agency (EMA) is the early intravenous administration of recombinant tissue plasminogen activator (tPA) (Donnan G.A. et al., 2008; Brouns R. and De Deyn P.P., 2009; Haelewyn B. et al., 2010). This thrombolytic drug is a serine protease that converts the proenzyme plasminogen to the protease plasmin, which is responsible for the degradation of the thrombus (Haelewyn B. et al.,

2010). However, because of its short therapeutic time window (between 3 and 4.5 hours after stroke onset) and the adverse effect of intracerebral haemorrhage (6-7% of cases), the number of patients who might receive treatment and therefore potential benefit is small (Donnan G.A. et al., 2008; Hacke W. et al., 2008; Brouns R. and De Deyn P.P., 2009). In the last decades many drugs have been tested to reduce brain damage following brain ischemia in animal models, but most of them have failed to reach clinical trials or to be efficient in ischemic stroke patients (Haelewyn B. et al., 2010). In particular, the number of studies involving neuroprotective treatments has increased exponentially since elucidation of the molecular mechanisms of stroke in the 1970s. Although the great number of preclinical and clinical studies have further improved the understanding of the pathophysiological mechanisms underlying ischemic stroke, great challenges remain in identifying agents with significant therapeutic efficacy.

Figure 13 summarizes some neuroprotective therapeutic approaches that have been evaluated in a variety of preclinical or clinical trials. These strategies include the administration of voltage-gated Ca^{2+} channels inhibitors, a number of NMDA and AMPA receptors inhibitors to reduce glutamate excitotoxicity, γ-aminobutyric acid (GABA) agonists, antioxidant agents, inhibitors of nitric oxide synthesis, and immunoregulators. However, all these drugs failed to reach the market, since they showed no or limited therapeutic benefits for patients (Karsy M. *et al.*, 2017; Rajah G.B. and Ding Y., 2017). Thus, the further investigation of additional molecular mechanisms underlying the pathogenesis of brain ischemia is needed for the development of novel and more efficacious pharmacological tools able to prevent, or at least limit, the devastating consequences of this widespread neurological disorder.
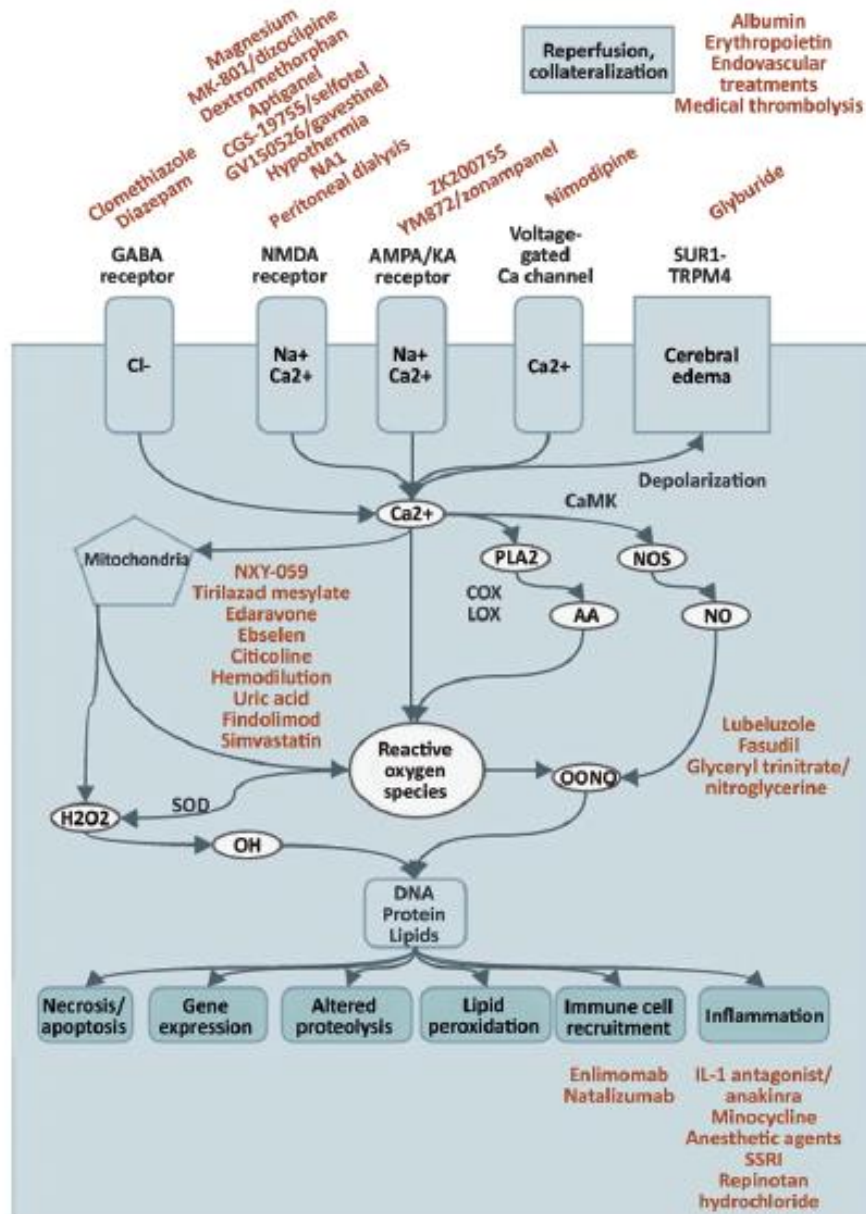
Fig.13 - Pathophysiology of ischemic stroke and neuroprotective strategies. The basic underlying pathology of ischemic stroke involves excitotoxicity and failure of cellular homeostatic functions, resulting in upregulation of Ca^{2+} and overproduction of free radicals. The end result involves cellular demise, maladaptive genetic expression, altered proteolysis, lipid peroxidation, recruitment of immune cells, and further inflammatory cascades. A variety of neuroprotective approaches (shown in red) have been tested in an attempt to target these various aspects (*modified from Karsy M. et al., 2017*).

2. AIM OF THE STUDY

Recent studies have demonstrated that a physical interaction between lysosomes and the endoplasmic reticulum (ER) occurs in different cell types under physiological conditions (Kilpatrick B.S. *et al.*, 2013; Kilpatrick B.S. *et al.*, 2016b; Aston D. *et al.*, 2017). Moreover, it has been shown that the tight apposition between the two compartments plays an important functional role, since these intracellular Ca^{2+}-storing organelles could communicate with the aim to regulate intracellular Ca^{2+} homeostasis, under both physiological and pathological conditions (Patel S. and Docampo R., 2010; Morgan A.J. *et al.*, 2011). This interaction has been well characterized in sea urchin eggs (Morgan A.J. *et al.*, 2013), human fibroblasts (Kilpatrick B.S. *et al.*, 2013; Kilpatrick B.S. *et al.*, 2016b), and rabbit ventricular cardiomyocytes (Aston D. *et al.*, 2017). However, the functional coupling between lysosomes and ER has not yet been properly investigated in the central nervous system (CNS). Furthermore, our research group has already shown that ER Ca^{2+} homeostasis is highly compromised under hypoxic conditions; this dysfunction occurs at neuronal level and leads to the activation of the ER stress pathway, thus triggering neuronal death (Sirabella R. *et al.*, 2009).

Considering these evidences, my thesis work has been focused on the study of the functional coupling between lysosomes and ER in primary cortical neurons under physiological conditions and under hypoxic conditions mimicking brain ischemia.

The first aim of my study has been to establish the possible contribution of the main lysosomal Ca^{2+} channel, TRPML1, in the regulation of lysosomal and ER Ca^{2+} homeostasis under physiological conditions. We started from the evidence that this channel can "chatter" with ER Ca^{2+} channels to trigger global Ca^{2+} signals in human fibroblasts (Kilpatrick B.S. *et al.*, 2016b).

Then, we evaluated the existence of a crosstalk between lysosomes and ER in anoxic neurons and the possible contribution of TRPML1 in this phenomenon. In order to reproduce

an *in vitro* model of brain ischemia, cortical neurons were exposed to 3 hours of oxygen and glucose deprivation (OGD) followed by 24 hours of reoxygenation; this model recapitulates the pathological events occurring during brain ischemia. In these cells, we analyzed the expression levels of TRPML1 during anoxia and the possible repercussion of the pharmacological modulation of the channel on neuronal survival and on the maintenance of lysosomal and ER Ca^{2+} homeostasis.

Since it has been reported that ER stress and apoptotic cell death play a key role in the neurodegeneration associated to brain ischemia (Paschen W. and Mengersdorf T., 2005), we also investigated the effect of TRPML1 modulation on the expression of some markers involved in the Unfolded Protein Response (UPR) and in the apoptotic cell death.

Finally, we also studied the possible effect of TRPML1 modulation during anoxia on the autophagic pathway, whose role is controversial in hypoxic conditions. We started from the evidence that Ca^{2+} released through this channel is able to activate the autophagic flux (Medina D.L. *et al.*, 2015; Zhang X. *et al.*, 2016).

To these aims, we performed some biochemical and functional experiments on cortical neurons under physiological conditions or in neurons exposed to oxygen and glucose deprivation followed by reoxygenation, by using some pharmacological and genetic tools able to modulate TRPML1 expression or function. Moreover, we also tested the effect of TRPML1 pharmacological modulation in an *in vivo* model of brain ischemia represented by rats subjected to the transient occlusion of the middle cerebral artery (tMCAO). Our conclusions seem to favor a detrimental role for autophagy in our experimental models of brain ischemia.

3. MATERIALS AND METHODS

3.1 Reagents and molecular structures of the pharmacological tools used in the present study

Media and sera for cell cultures were purchased from Life Technologies (Milan, Italy); antibiotics for cell cultures were from Sigma-Aldrich (Milan, Italy). Rabbit polyclonal antibodies against TRPML1 (#ACC-081) and STIM1 (STIM1-ATTO-550, #ACC-063-AO) were from Alomone Labs (Jerusalem, Israel); mouse monoclonal antibody against α-tubulin (#T5168), and rabbit polyclonal antibody against LAMP2 (#L0668) were from Sigma-Aldrich (Milan, Italy); mouse monoclonal antibody against STIM1 (#sc-166840) was from Santa Cruz Biotechnology, Inc. (Dallas, TX, USA); mouse monoclonal antibody against IP$_3$R-3 (#610313) was from BD Biosciences (San Jose, CA, USA); rabbit polyclonal antibody against LAMP1 (#AB2971) was from Merck Millipore (Darmstadt, Germany); rabbit polyclonal anti-GRP78 (#3183) antibody was from Cell Signaling Technology, Inc. (Danvers, MA, USA); rabbit polyclonal antibodies against beclin 1 (#NB500-249) and p62 (#NBP1-48320) were from Novus Biologicals (Littleton, CO, USA); rabbit polyclonal antibodies against caspase 9 (#GTX132331) and LC3B (#GTX127375) were from GeneTex Inc. (Irvine, CA, USA). ECL reagents and all chemicals for Western blotting were from GE Healthcare (Milan, Italy). Small interfering RNAs (siRNAs) against TRPML1 and siRNA-Control were purchased from Qiagen (Milan, Italy). (1R,3S)-1-[3-[[4-(2-Fluorophenyl)piperazin-1-yl]methyl]-4-methoxyphenyl]-2,3,4,9-tetrahydro-1H-pyrido[3,4-b]indole-3-carboxylic acid (*trans*-Ned19) was from Tocris Bioscience (Bio-Techne/R&D Systems, Minneapolis, MN, USA); 2-(2-Oxo-2-(2,2,4-trimethyl-3,4-dihydroquinolin-1(2H)-yl)ethyl)isoindoline-1,3-dione (ML-SA1) was from Merck Millipore (Darmstadt, Germany), while Gly-Phe β-naphthylamide (GPN) and YM201636 were purchased from Santa Cruz Biotechnology, Inc. (Dallas, TX, USA). Thapsigargin and bafilomycin A1 were from Sigma-Aldrich (Milan, Italy). 1-[2-(5-

Carboxyoxazol-2-yl)-6-aminobenzofuran-5-oxy]-2-(21-amino-51-methylphenoxy)-ethane-N,N,N1,N1-tetraacetic acid penta-acetoxymethyl ester (Fura-2/AM) was from Molecular Probes (Invitrogen, Milan, Italy).
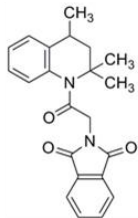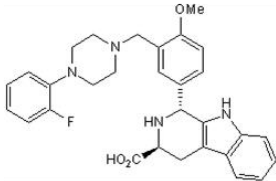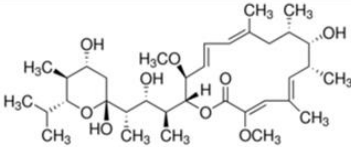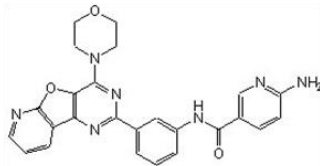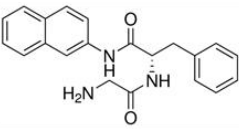
Pharmacological tool	Structure	Function
ML-SA1 (2-(2-Oxo-2-(2,2,4-trimethyl-3,4-dihydroquinolin-1(2H)-yl)ethyl)isoindoline-1,3-dione)		TRPML1 agonist
***trans*-Ned19** ((1*R*,3*S*)-1-[3-[[4-(2-Fluorophenyl)piperazin-1-yl]methyl]-4-methoxyphenyl]-2,3,4,9-tetrahydro-1*H*-pyrido[3,4-*b*]indole-3-carboxylic acid)		TRPML1 inhibitor
Bafilomycin A1		Lysosomal v-ATPase inhibitor
YM201636 (6-Amino-N-(3-(4-(4-morpholinyl)pyrido[3'2':4,5]furo[3,2-d]pyrimidin-2-yl)phenyl)-3-pyridine carboxamide)		Inhibitor of phosphatidylinositol phosphate kinase PIKfyve
GPN (Gly-Phe β-naphthylamide)		Lysosomotropic agent that induces the osmotic lysis of lysosomes

Table 2 - Pharmacological tools used in this study.

3.2 Primary cultures of rat cortical neurons

Cortical neurons-enriched cultures were obtained from brains of 14/16-day-old Wistar rat embryos (Charles River). Briefly, rats were first anesthetized and then decapitated to

minimize pain and distress. Dissection and dissociation were performed in Ca^{2+}/Mg^{2+}-free PBS (*Phosphate-Buffered Saline*) containing glucose (30 mM). Tissues were incubated with papain for 10 minutes at 37°C and dissociated by trituration in Earle's Balanced Salt Solution (EBSS) containing DNase (0,16 U/ml), bovine serum albumin (BSA) (10 mg/ml), and ovomucoid (10 mg/ml). Cells were plated at 15×10^6 in 100 mm plastic Petri dishes or on glass coverslips precoated with poly-D-lysine (20 μg/ml) in minimum Eagle's medium/F12 containing glucose, 5% fetal bovine serum (FBS), 5% horse serum (HS), glutamine (2 mmol/l), penicillin (50 U/ml), and streptomycin (5 μg/ml). Neurons were cultured at 37°C in a humidified 5% CO_2 atmosphere and used after 7 days of culture. Ara-C (cytosine arabinoside, 10 μM) was added within 72 hours of plating to prevent non-neuronal cell growth. All the experiments were performed according to the procedures described in the experimental protocols approved by the Ethical Committee of "Federico II" University of Naples, Italy.

3.3   Animal care

Male Sprague-Dawley rats (Charles River), weighting 200 g to 250 g, were housed under diurnal lighting conditions (12 hours darkness/light) and in a conditioned room (23°C). Experiments were performed according to the international guidelines for animal research and approved by the Animal Care Committee of "Federico II" University of Naples, Italy. To minimize suffering, animals, during any surgical or invasive procedure, were anesthetized using 2% sevofluorane, 60% N_2O, and 38% O_2, and the rectal temperature was maintained at 37±0.5°C with a heat-controlled mat (Harvard Apparatus).

3.4   Immunocytochemistry and confocal microscopy

Cortical neurons were rinsed twice in cold 0.01 M PBS at pH 7.4 and fixed in 4% paraformaldehyde for 20 minutes at room temperature. After three washes in PBS, cells were

blocked in PBS containing 3% BSA for 30 minutes and then incubated overnight at 4°C with anti-TRPML1 antibody (1:1000) (for experiments presented in Fig.14 A), or with anti-TRPML1 (1:1000) and anti-STIM1-ATTO-550 (1:400) antibodies (for experiments presented in Fig.19). Then, cells were washed with PBS and incubated with anti-rabbit Cy3-conjugated antibody (Jackson, 1:200) (for experiments presented in Fig.14 A), or with anti-rabbit Cy2-conjugated antibody (Jackson, 1:200) (for experiments presented in Fig.19) for 1 hour at room temperature under dark conditions and washed again with PBS. To allow visualization of cell nuclei in the fluorescent staining, cells were finally incubated for 5 minutes with Hoechst 1 μM. Finally, cover glasses were mounted with a SlowFade™ Antifade Kit (Molecular Probes, Invitrogen) and acquired by a 63X oil immersion objective using a Zeiss inverted 700 confocal microscope (Scorziello A. *et al.*, 2013). Quantitative analysis of co-localization of TRPML1 and STIM1-ATTO-550 (Fig.19) was conducted by using the co-localization plug-in *JACoP* (*Just Another Colocalization Plugin*) for *ImageJ* Software (NIH, Bethesda, MA, USA) (Bolte S. and Cordelières F.P., 2006). A correlation of signal intensity was calculated as a Pearson's coefficient (Rr). Rr is a quantitative measurement that estimates the degree of overlap between the fluorescence signals obtained from two channels.

3.5 Small interfering RNAs

TRPML1 knocking down was achieved by using three different FlexiTube small interfering RNAs (siRNAs) against the channel (Qiagen, Milan, Italy). Neurons were transfected in OptiMem medium by HiPerFect Transfection Reagent (Qiagen, Milan, Italy) with the non-targeting control and the following siRNAs (all at 10 nM):

(#1) Rn_LOC288371_4 (sense strand: 5'-GCAGAACGAGUUUGUUGUAUTT-3'; antisense strand: 5'-UACAACAAACUCGUUCUGCAG-3');

(#2) Rn_LOC288371_3 (sense strand: 5'-UGAUCACAUUUGACAAUAATT-3'; antisense strand: 5'UUAUUGUCAAAUGUGAUCAGG-3');

(#3) Rn_LOC288371_2 (sense strand: 5'-ACGAGAUCCCUGACUGUUATT-3'; antisense strand: 5'-UAACAGUCAGGGAUCUCGUTG-3').

The mixture containing the specific siRNA was added to cells and then, after 5 hours of incubation, the medium was replaced with fresh medium.

3.6   Western blotting

After treatments, cells were washed in PBS and collected by gentle scraping in ice-cold lysis buffer containing 20 mM Tris-HCl (pH 7.5), 10 mM NaF, 1 mM PMSF, 1% Nonidet P-40, 1 mM Na$_3$VO$_4$, 0.1% aprotinin, 0.7 mg/ml pepstatin and 1 µg/ml leupeptin. After centrifugation (12,000 rpm, 30 minutes, 4°C), the supernatants were collected and protein concentration was determined by the Bradford method (Bradford M.M., 1976). Proteins (20 µg) were loaded and separated on 10% sodium dodecyl sulphate (SDS)-polyacrylamide gels for TRPML1, LAMP1, LAMP2, beclin 1, p62, GRP78, and caspase 9 expression, and on 15% SDS-polyacrylamide gels for LC3 expression, and then transferred onto Hybond ECL nitrocellulose membranes (GE Healthcare, Milan, Italy). The membranes were blocked for 1 hour at room temperature with 5% non-fat dry milk (Bio-Rad, Milan, Italy) in Tris-Buffered Saline-TWEEN 20 (2 mM Tris-HCl, 50 mM NaCl, pH 7.5, plus 0.1% TWEEN 20), and then incubated overnight at 4°C in the blocking buffer containing the polyclonal antibodies against: TRPML1 (1:1000), LAMP1 (1:1000), LAMP2 (1:1000), beclin 1 (1:1000), p62 (1:1000), LC3 (1:1000), GRP78 (1:1000) or caspase 9 (1:1000). All membranes were re-blotted in the blocking buffer with the monoclonal antibody against α-tubulin (1:2000). Immunoreactive bands were detected using ECL reagent kits. The optical density of the bands, normalized to α-tubulin, was determined by a Chemi-Doc Imaging System (Bio-Rad, Hercules, CA, USA).

3.7 $[Ca^{2+}]_i$ measurements

$[Ca^{2+}]_i$ was measured by single-cell computer assisted video imaging (Secondo A. *et al.*, 2007). Briefly, neuronal cells plated on glass coverslips were loaded with 10 μM Fura-2/AM for 1 hour at 37°C in cell culture medium or in Normal Krebs solution containing 5.5 mM KCl, 160 mM NaCl, 1.2 mM $MgCl_2$, 1.5 mM $CaCl_2$, 10 mM glucose, and 10 mM HEPES-NaOH (pH 7.4). At the end of the Fura-2/AM loading period, coverslips were placed into a perfusion chamber (Medical System, Co. Greenvale, NY, USA) mounted onto a Zeiss Axiovert 200 microscope (Carl Zeiss, Zena, Germany) equipped with a FLUAR 40X oil objective lens. The experiments were carried out with a digital imaging system composed of MicroMax 512BFT cooled CCD camera (Princeton Instruments, Trenton, NJ, USA), LAMBDA 10-2 filter wheeler (Sutter Instruments, Novato, CA, USA) and Meta-Morph/MetaFluor Imaging System software (Universal Imaging, West Chester, PA, USA). All the results are presented as cytosolic Ca^{2+} concentration. Assuming that the Kd for Fura-2 was 224 nM, the equation of Grynkiewicz *et al.* (Grynkiewicz G. *et al.*, 1985; Urbanczyk J. *et al.*, 2006) was used for calibration.

3.8   Determination of mitochondrial function

Neuronal survival was assessed by the 3[4,5-dimethylthiazol-2-yl]-2,5-diphenyl-tetrazolium bromide (MTT) assay. The assay is based on the red-ox ability of living mitochondria to convert dissolved MTT into insoluble formazan. Briefly, after treatments, cells were incubated in 1 ml of MTT solution (0.5 mg/ml) for 1 hour at 37°C. To stop incubation, MTT solution was removed and 1 ml of dimethyl sulfoxide (DMSO) was added to solubilize the formazan product. The absorbance was monitored at 540 nm with a Perkin-Elmer LS 55 luminescence spectrometer (Perkin-Elmer Ltd, Beaconsfield, England). The data were expressed as a percentage of cell viability compared to control cultures.

3.9   Immunoprecipitation (IP)

Cells were homogenized in a lysis buffer containing 50 mM HEPES, 100 mM NaCl, 1.5 mM $MgCl_2$, 1 mM PMSF, 0.2% Nonidet P-40, 5 μg/ml aprotinin, 10 μg/ml leupeptin, and 2 μg/ml pepstatin. Lysates were cleared by centrifugation (12,000 rpm, 30 minutes, 4°C). 500 μg of cell lysate were immunoprecipitated with anti-STIM1 (1:200), anti-TRPML1 (1:200), anti-IP$_3$R-3 (1:200), or anti-LAMP1 (1:200) antibodies. Then the immunoprecipitated samples were resolved by sodium dodecyl sulphate-polyacrylamide gel electrophoresis (SDS-PAGE) and transferred onto a nitrocellulose membrane. Immunoblot analysis was performed using anti-TRPML1 (1:1000), anti-STIM1 (1:1000), or anti-LC3 (1:1000) antibodies.

3.10   Combined oxygen and glucose deprivation (OGD)

Anoxic conditions were reproduced *in vitro* by exposing cortical neurons to 3 hours of oxygen and glucose deprivation (OGD) followed by 24 hours of reoxygenation (Rx). In particular, OGD was achieved by incubating neurons for 3 hours in a glucose-free medium previously saturated with 95% N_2 and 5% CO_2 for 20 minutes and containing 116 mM NaCl, 5.4 mM KCl, 0.8 mM $MgSO_4$, 26.2 mM $NaHCO_3$, 1 mM NaH_2PO_4, 1.8 mM $CaCl_2$, 0.01 mM glycine and 0.001% phenol red (Goldberg M.P. and Choi D.W., 1990). Hypoxic conditions were maintained using a hypoxic chamber (atmosphere 5% CO_2 and 95% N_2, temperature 37°C). At the end of incubation, OGD was stopped by replacing the glucose-free medium with a culture medium containing normal levels of O_2 and glucose; thus, reoxygenation was achieved by returning neurons to normoxic conditions (5% CO_2 and 95% air, temperature 37°C) for 24 hours. For the experiments of Fig.20 B, also cortical glial cells were exposed to OGD/Rx. Ischemic preconditioning (IPC) was reproduced by pre-exposing neurons, 24 hours before OGD/Rx, which represent the lethal insult, to 30 minutes of OGD, a condition that is comparable to a sublethal ischemic insult.

3.11 Transient focal ischemia

Rats were subjected to transient middle cerebral artery occlusion (tMCAO), a surgical procedure that consists in the insertion of a suture filament into the internal carotid artery until to the middle cerebral artery (MCA) (Longa E.Z. *et al.*, 1989), modified and readapted in our laboratory (Pignataro G. *et al.*, 2008). Briefly, under an operating stereomicroscope (Nikon SMZ800, Nikon Instruments, Florence, Italy), the first step was the identification and the exposition of right carotid bifurcation, by using surgical pincers (Dumont #7, FST). Then, the external carotid artery near the bifurcation was cut and electrocauterized to create a stump on the artery. A silicon-coated nylon filament (Doccol, Ca, USA) was inserted through the stump and was gently advanced 19 mm into the right internal carotid artery until it blocks the origin of the MCA. At this point, the surgical wound was temporarily closed by surgical suture and the filament left in place for 100 minutes and kept still in place by using a braided silk suture (FST). When the time of occlusion was expired, the filament was gently removed in order to allow reperfusion. Induction of ischemia was confirmed by monitoring regional cerebral blood flow in the area of the right MCA through a disposable microtip fiber optic probe (diameter 0.5 mm), applied with a cyanoacrylate glue to the right temporo-parietal region of the rat skull, connected through a Master Probe to a laser Doppler computerized main unit (PF5001; Perimed, Sweden) and analyzed using PSW Perisoft 2.5 (Kawano T. *et al.*, 2006).

Animals were divided into three groups: (i) sham-operated rats receiving intracerebroventricular (icv) infusion of vehicle; (ii) ischemic rats receiving icv infusion of vehicle; (iii) ischemic rats receiving icv infusion of *trans*-Ned19 at the onset of reperfusion. All animals were sacrificed 24 hours after tMCAO.

3.12 Intracerebroventricular administration of *trans*-Ned19

Drug delivery into brain lateral ventricle was carried out in rats positioned on a stereotaxic apparatus at different time points after the induction of transient ischemia (onset, 3 hours, 6 hours, 12 hours, 24 hours). The drug was intracerebroventricularly (icv) infused through a stainless-steel cannula (brain infusion kit alzet® 3-5mm), positioned into the right lateral ventricle relating to the following stereotaxic coordinates from the bregma: 0.4 mm caudal, 2 mm lateral, and 2 mm below the dura, connected to a Hamilton syringe (10µl). *Trans*-Ned19 compound was dissolved in saline solution (NaCl 0,9%) and icv injected once at a volume of 5µl.

3.13 Evaluation of the infarct volume

The ischemic volume was evaluated by 2,3,5-triphenyl tetrazolium chloride (TTC) staining. Specifically, 24 hours after starting reperfusion from tMCAO, animals were euthanized and the brains were removed. *Trans*-Ned19 24 hours rats were sacrificed 48 hours after the induction of ischemia. After that, brains were cut into 1 mm coronal slices with a vibratome (Campden Instrument, 752 M). Coronal slices were incubated in 2% TTC for 20 minutes and in 4% paraformaldehyde overnight. The infarct area of the sections (about six in total) was calculated with image analysis software (Image-J 1.50c) (Bederson J.B. *et al.*, 1986). The total infarct volume, corrected for edema, was calculated as sum of the single infarcted areas and expressed as percentage of the volume of the hemisphere ipsilateral to the lesion. Edema was calculated by difference between the volume of hemisphere ipsilateral to the lesion and that of hemisphere contralateral to the lesion.

3.14 Evaluation of neurological deficit scores

Neurological scores were evaluated immediately before the sacrifice, at 24 hours from tMCAO, according to 2 scales: a general neurological scale and a focal neurological scale (Clark W.M. *et al.*, 1997). In the general score, the following 6 general deficits were measured: (1) hair conditions, (2) position of ears, (3) eye conditions, (4) posture, (5) spontaneous activity, and (6) epileptic behaviour. For each of the 6 general deficits measured, animals received a score ranging between 0 and 12 depending on the severity of signs. The scores of investigated items were then summed to provide a total general score ranging from 0 to 28. In the focal score, the following 7 areas were assessed: (1) body symmetry, (2) gait, (3) climbing, (4) circling behaviour, (5) front limb symmetry, (6) compulsory circling, and (7) whisker response. For each of these items, animals were rated between 0 and 4 depending on severity. The 7 items were then summed to give a total focal score ranging from 0 to 28.

3.15 Statistical analysis

Data are expressed as mean ± S.E.M. Statistical analysis was performed ad hoc with unpaired t-test or one-way analysis of variance (ANOVA) followed by Newman-Keuls test. Statistical significance was accepted at the 95% confidence level ($p < 0.05$).

4. RESULTS AND DISCUSSION

4.1 Immunocytochemical and biochemical characterization of TRPML1 expression in rat primary cortical neurons

Primary cultures of cortical neurons were obtained from brains of E14/E16 rat embryos, as described in the Materials and Methods section. By immunocytochemical analysis, we showed that the lysosomal Ca^{2+} channel TRPML1 was expressed at high levels in these cells under physiological conditions (**Fig.14 A**).

In order to downregulate TRPML1 protein expression, we transfected cortical neurons with three different siRNA (*small interfering RNA*) duplexes targeting TRPML1 mRNA (10 nM), or with a scrambled siRNA (siControl) (10 nM) as negative control. Then, to determine the transfection efficiency and in consideration of the turnover of the protein, TRPML1 protein levels were assessed at 24 hours after siRNAs transfection by means of Western blotting analysis. The results obtained showed that in our cellular model only siRNA #2 (siTRPML1 #2) efficiently downregulated TRPML1 protein expression at 24 hours after transfection (**Fig.14 B**). Moreover, to determine the duration of TRPML1 knocking down, we performed time-course experiments in which cells were harvested for Western blotting analysis at 24 and 48 hours after siTRPML1 #2 transfection. Our results indicated that this siRNA was able to downregulate TRPML1 expression only at 24 hours after transfection, since within 48 hours TRPML1 expression levels tended to increase, returning to the control values (**Fig.14 C**).
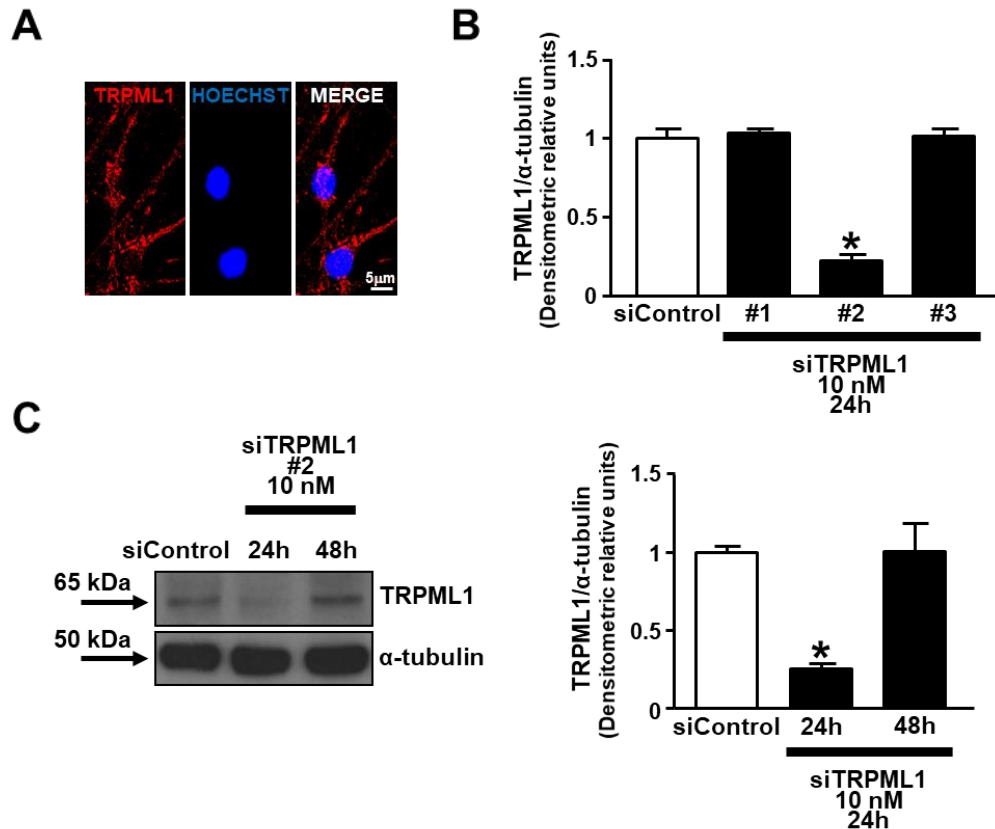
Fig.14 - TRPML1 immunolocalization and downregulation in rat primary cortical neurons. (**A**) Immunocytochemical analysis of TRPML1 (red immunosignal) in rat primary cortical neurons; nuclei were counterstained with Hoechst (blue). Scale bar: 5 μm. (**B**) Representative quantification of TRPML1 protein expression in cortical neurons transfected with 3 different siRNAs (10 nM) against TRPML1 mRNA, or with a non-targeting control (siControl). (**C**) Representative Western blotting (left) and quantification (right) of TRPML1 protein expression after time-course experiments with siTRPML1 #2 (10 nM) at 24 and 48 hours after transfection.
All the experiments were repeated 3 times with similar results. *$p < 0.05$ versus siControl.

This observation suggests a rapid turnover rate of TRPML1 at neuronal level. Interestingly, our data are in accordance with the results reported by Miedel *et al.*, who showed that in HeLa cells repeated siRNA applications were needed to successfully knock down the channel over longer periods (Miedel M.T. *et al.*, 2008).

4.2   Pharmacological characterization of TRPML1 activity in cortical neurons

To verify the role of TRPML1 in lysosomal Ca^{2+} homeostasis in cortical neurons, we performed single-cell Fura-2/AM microfluorimetry experiments under physiological conditions. In our experiments, Ca^{2+} efflux from lysosomes was elicited by the administration

of ML-SA1 (10 μM), a membrane-permeant synthetic chemical which acts as a specific agonist of TRPML1 (Shen D. *et al.*, 2012). The results obtained indicated that the pharmacological activation of the channel promoted an increase in intracellular Ca^{2+} concentration ($[Ca^{2+}]_i$) through TRPML1 of approximately 40% compared to basal values (**Fig.15 A**). Conversely, this effect was completely abrogated when the channel was silenced with the specific siRNA against TRPML1 mRNA (siTRPML1 #2). Considering the absence of response upon ML-SA1 stimulation in neurons silenced for TRPML1, at the end of this experiment the specific Ca^{2+} ionophore ionomycin (5 μM) was used to verify the efficiency of the fluorescent probe Fura-2/AM and the cell status in our experimental system (**Fig.15 B**).

It has been reported that in macrophages an increase in lysosomal pH, induced by the incubation with ammonium chloride (NH_4Cl) or by the administration of the lysosomal v-ATPase inhibitor bafilomycin A1, was able to elicit Ca^{2+} efflux from lysosomes, thus emptying lysosomal Ca^{2+} stores (Christensen K.A. *et al.*, 2002). Moreover, it has been proposed that in presenilin 1 knock out cells (PS1KO) a defective lysosomal acidification, due to a v-ATPase deficiency, could hyperactivate the lysosomal Ca^{2+} channel TRPML1, thus promoting an abnormal Ca^{2+} efflux from lysosomes (Lee J.H. *et al.*, 2015). Considering these evidences, we verified whether the alkalinization of lysosomal lumen could impair lysosomal Ca^{2+} homeostasis and activate TRPML1 channel in cortical neurons under physiological conditions. To this aim, we first analyzed the effect of bafilomycin A1 (100 nM) on lysosomal Ca^{2+} release in these cells. Interestingly, this drug was able to elicit Ca^{2+} efflux from lysosomes, thus inducing an increase in $[Ca^{2+}]_i$ of approximately 30% compared to basal values (**Fig.15 C**). Conversely, in neurons transfected with the specific siRNA against the channel this effect was totally abolished, thus suggesting that the alkalinization of lysosomal pH promoted Ca^{2+} efflux from lysosomes through TRPML1 (**Fig.15 D**). However, the concomitant administration of both ML-SA1 and bafilomycin A1 provoked the same effect as that observed with ML-SA1 or

bafilomycin A1 administered alone, both in cells exposed to control conditions and in cells
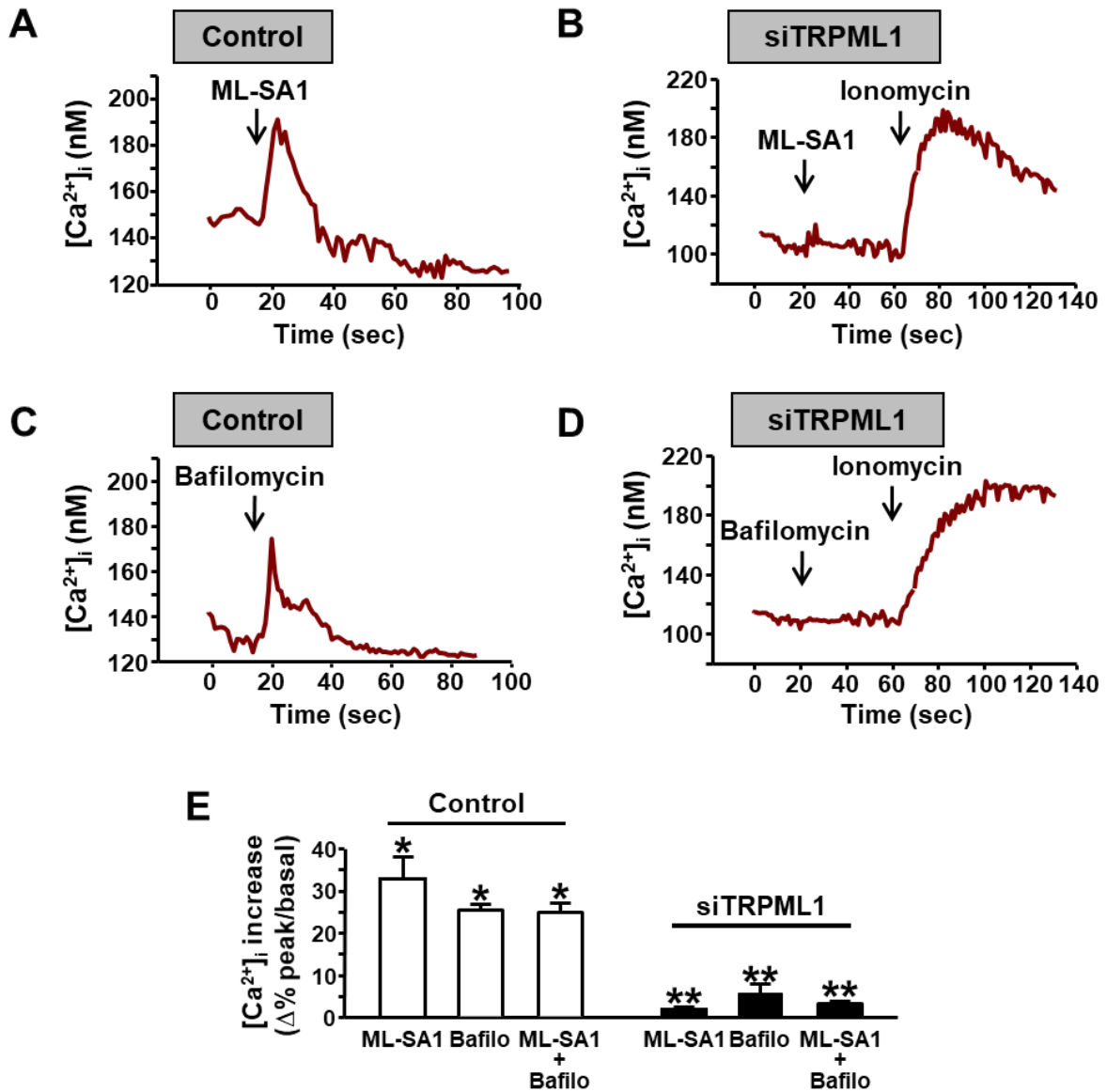
silenced for TRPML1 expression (**Fig.15 E**).

Fig.15 - Effect of ML-SA1 and bafilomycin A1 on intracellular Ca^{2+} levels. (**A-B**) Representative traces of the effect of ML-SA1 (10 μM) administration on intracellular Ca^{2+} levels in cortical neurons under control conditions (**A**) and in neurons transfected with the specific siRNA against TRPML1 mRNA (**B**). (**C-D**) Representative traces of the effect of bafilomycin A1 (100 nM) administration in cortical neurons under control conditions (**C**) and in neurons transfected with siTRPML1 #2 (**D**). (**E**) Bar graph depicts the quantification of the effect of the two pharmacological tools on intracellular Ca^{2+} levels under control conditions (left) and in neurons silenced for TRPML1 expression (right).
All the experiments were repeated 3 times on almost 40 cells with similar results.
* $p < 0.05$ versus basal levels; ** $p < 0.05$ versus control.

Collectively, these results suggest that TRPML1 plays a critical role in the maintenance

of lysosomal Ca^{2+} homeostasis in cortical neurons under physiological conditions. Moreover,

we showed that also an increase in lysosomal pH can promote TRPML1 activation, and this observation is in agreement with the results reported by other research groups (Christensen K.A. *et al.*, 2002; Lee J.H. *et al.*, 2015).

Since bafilomycin A1 disrupts lysosomal pH thus causing an impairment in cell homeostasis, we evaluated cell viability after the administration of this drug in order to rule out the possibility that it could affect neuronal survival during our functional experiments. To this aim, cells were incubated with 100 nM bafilomycin A1 for 2 minutes, 5 minutes and 1 hour under physiological conditions. At the end of treatments, cell viability was assessed in terms of mitochondrial function by MTT assay. Our data showed that the exposure to bafilomycin A1 100 nM for 2 and 5 minutes did not affect cell viability during our experiments; however, longer exposure reduced neuronal survival of ~30% compared to control (**Fig.16**).
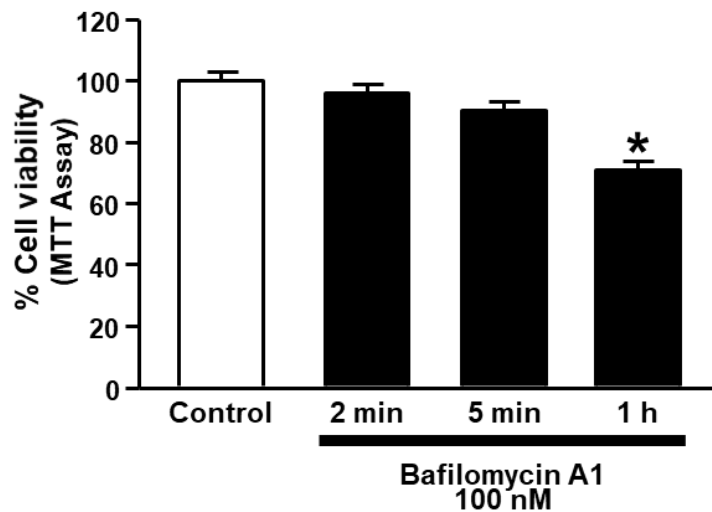

Fig.16 - Bafilomycin A1 effects on cell viability in cortical neurons. Cell viability rate was determined by MTT assay on cortical neurons exposed to 100 nM bafilomycin A1 for 2 minutes, 5 minutes and 1 hour. Cell viability of untreated controls was considered to be 100%.
The experiment was repeated 3 times with similar results.
* $p < 0.05$ versus control.

4.3 The pharmacological modulation of TRPML1 or its knocking down modifies intracellular Ca^{2+} homeostasis in cortical neurons

Recent experimental evidences demonstrated a tight coupling between lysosomes and the endoplasmic reticulum (ER), likely occurring at Ca^{2+} microdomains formed at membrane contact sites (MCSs) between the two organelles (Penny C.J. *et al.*, 2015). Accordingly, it has been proposed that the close apposition between acidic Ca^{2+} stores and ER could generate relevant global Ca^{2+} signals within the cell (Patel S. and Docampo R., 2010).

To verify the existence of a functional interplay between lysosomes and ER in cortical neurons, we performed single-cell Fura-2/AM microfluorimetry experiments under physiological conditions. We first measured cytosolic Ca^{2+} rise after the administration of the specific Ca^{2+} ionophore ionomycin (5 μM), used to elicit Ca^{2+} release from all internal, non-lysosomal Ca^{2+} stores, and in particular from ER. In neurons pre-treated for 1 hour with TRPML1 inhibitor *trans*-Ned19 (30 μM) (hereafter referred to as Ned19) and in neurons transfected with the specific siRNA against TRPML1 mRNA, ionomycin induced a significant increase in cytosolic Ca^{2+} levels compared to control (**Fig.17 A**). These results suggest that the pharmacological inhibition of the channel or its knocking down promoted an increase in Ca^{2+} content within the ER and other non-lysosomal Ca^{2+} stores.

Then, we measured ER Ca^{2+} content after the pharmacological or genetic knock down of TRPML1. To this aim we performed single-cell Fura-2/AM microfluorimetry experiments by using thapsigargin (Tg) in a Ca^{2+}-free solution; this pharmacological tool, by blocking the ER Ca^{2+} ATPase SERCA, induced a slow release of Ca^{2+} from ER that we measured as $[Ca^{2+}]_i$ increase in the cytosol. In our experiments, the pre-incubation with TRPML1 inhibitor Ned19 for 1 hour or TRPMLI knocking down by siRNA significantly increased ER Ca^{2+} content (**Fig.17 B**). By contrast, the preliminary Ca^{2+} leak from lysosomes obtained by the pre-

incubation with ML-SA1 for 1 hour determined a reduction in ER Ca^{2+} content of approximately 50% compared to control (**Fig.17 C**).
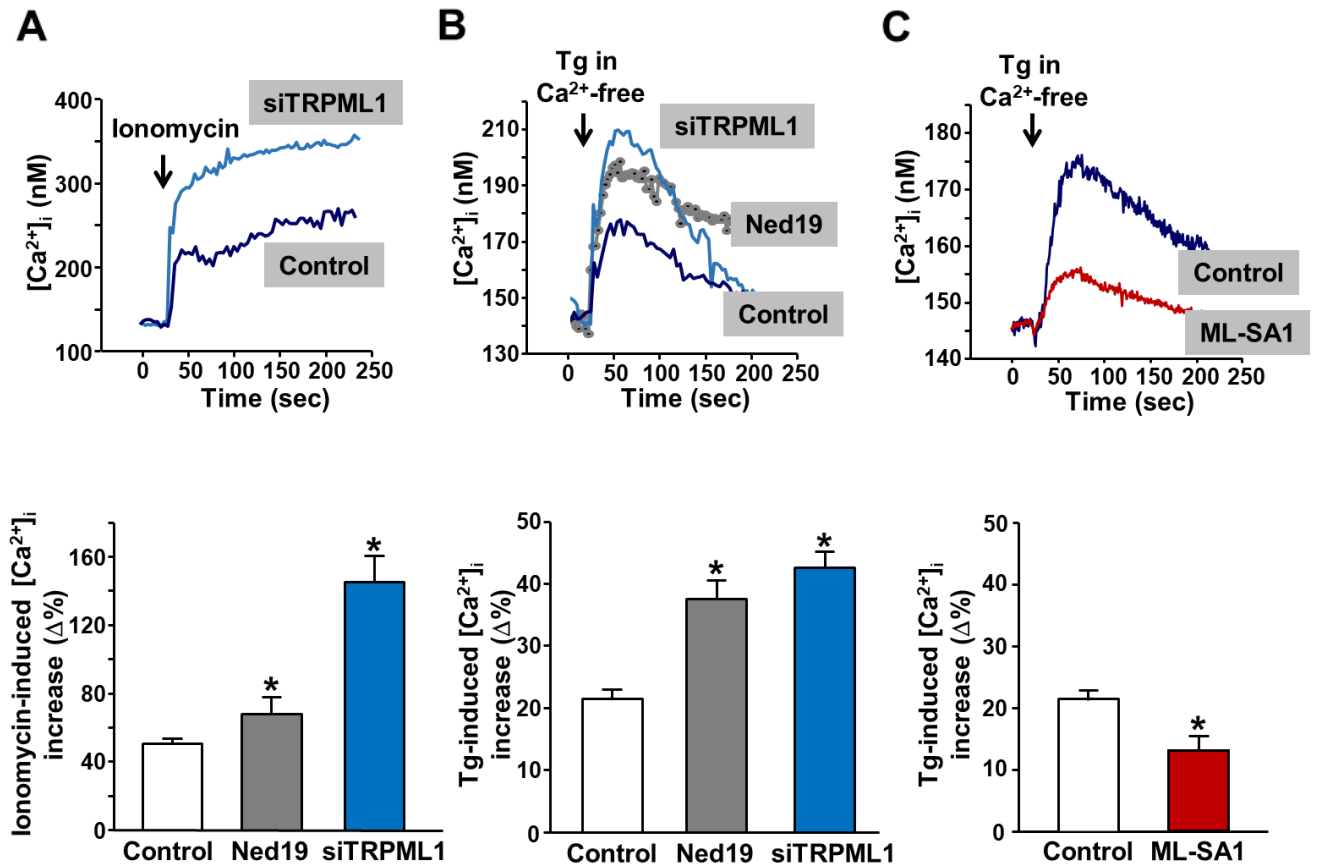

Fig.17 - Effect of the pharmacological modulation of TRPML1 or its knocking down on ER Ca^{2+} content in cortical neurons under physiological conditions. (**A**) Representative traces (top) and quantification (bottom) of the effect of Ned19 (30 μM) and siTRPML1 on intracellular Ca^{2+} release from ER induced by ionomycin (5 μM) in cortical neurons under physiological conditions. (**B**) Representative traces (top) and quantification (bottom) of the effect of Ned19 (30 μM) and siTRPML1 on ER Ca^{2+} content in cortical neurons. (**C**) Representative traces (top) and quantification (bottom) of the effect of ML-SA1 (10 μM) on ER Ca^{2+} content in cortical neurons.
All the experiments were repeated 3 times on almost 40 cells with similar results.
* $p < 0.05$ versus control.

These results suggest that ER Ca^{2+} homeostasis is controlled by lysosomal Ca^{2+} *via* TRPML1 in cortical neurons under physiological conditions.

4.4 Lysosomes are coupled to endoplasmic reticulum (ER) in the handling of intracellular Ca^{2+} concentration

Since in cortical neurons lysosomes and ER can communicate for the regulation of intracellular Ca^{2+} homeostasis under physiological conditions, we wondered about the molecular identity of the lysosomal and ER proteins promoting the interaction between the two organelles. In this respect, we hypothesized that Ca^{2+} exchanges between the two compartments could be controlled by the unique ER Ca^{2+} sensor actually known, namely STIM1 (*stromal interaction molecule 1*). STIM1 is a single transmembrane-spanning Ca^{2+}-binding protein resident in the ER membrane, where it senses intraluminal Ca^{2+} levels (Spassova M. *et al.*, 2006). It is well known that when ER Ca^{2+} concentration decreases, STIM1 moves to plasma membrane where it oligomerizes and activates ORAI1 Ca^{2+} channel (also known as CRACM1, *calcium release-activated calcium modulator 1*), thus mediating Ca^{2+} influx within the cell. This mechanism is termed "store-operated Ca^{2+} entry" (SOCE) (Várnai P. *et al.*, 2009). So, in order to verify whether STIM1 could mediate ER/lysosomes coupling, by means of co-immunoprecipitation experiments we analyzed the possible interaction between STIM1 and TRPML1 under physiological conditions. The results obtained showed that under normoxia the two proteins co-immunoprecipitated in primary cortical neurons (**Fig.18 A-B**). To further investigate the interplay between lysosomes and ER, we also examined the possible interaction between TRPML1 and IP$_3$R-3, one of the most abundant protein expressed at the level of ER membrane. Our co-immunoprecipitation experiments showed that the two proteins may interact (**Fig.18 C**), probably in order to promote Ca^{2+} exchanges between the two compartments.
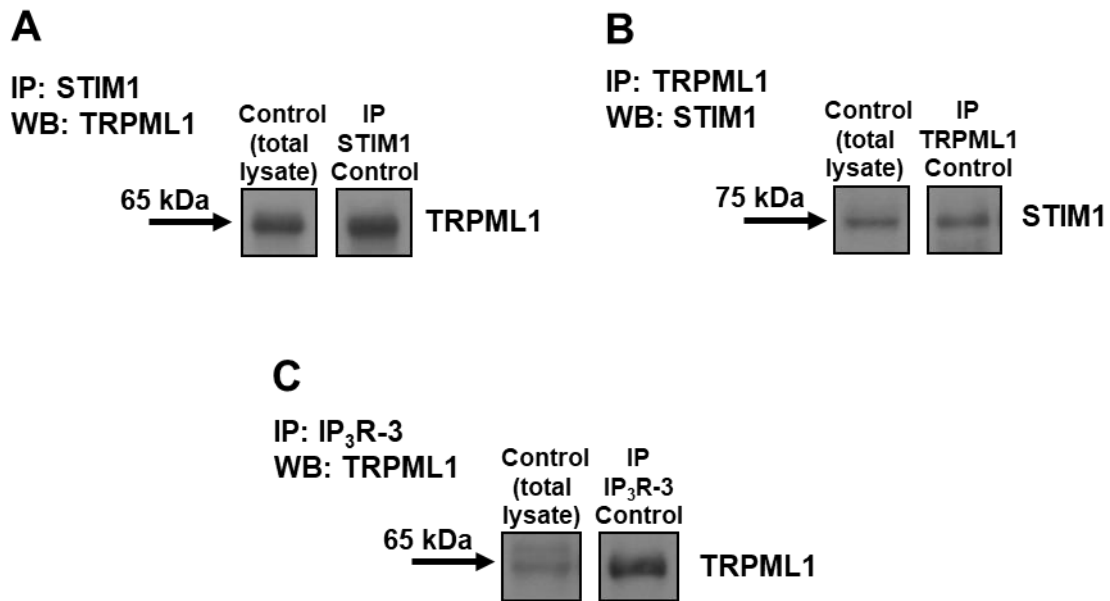
Fig.18 - Lysosome/ER coupling is mediated by the interaction between TRPML1 and some ER membrane proteins under physiological conditions. (**A-B**) Lysates from cortical neurons were subjected to immunoprecipitation (IP) using anti-STIM1 or anti-TRPML1 antibody. The presence of TRPML1 or STIM1 was analyzed by Western blotting (WB). (**C**) Lysates from cortical neurons were subjected to immunoprecipitation (IP) using anti-IP$_3$R-3 antibody. The presence of TRPML1 was analyzed by Western blotting (WB).
All the experiments were repeated 3 times with similar results.

Moreover, we also evaluated the co-localization between TRPML1 and STIM1 in our cells by means of immunocytochemical analysis. Our experiments revealed that the two proteins extensively co-localized in cortical neurons, in both soma and axons, under physiological conditions (**Fig.19**).
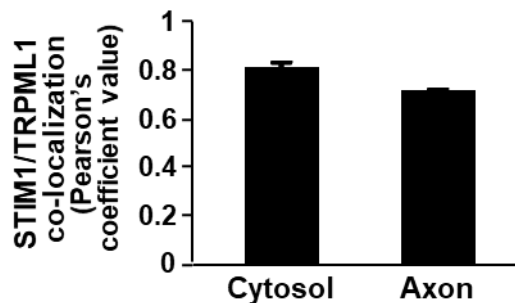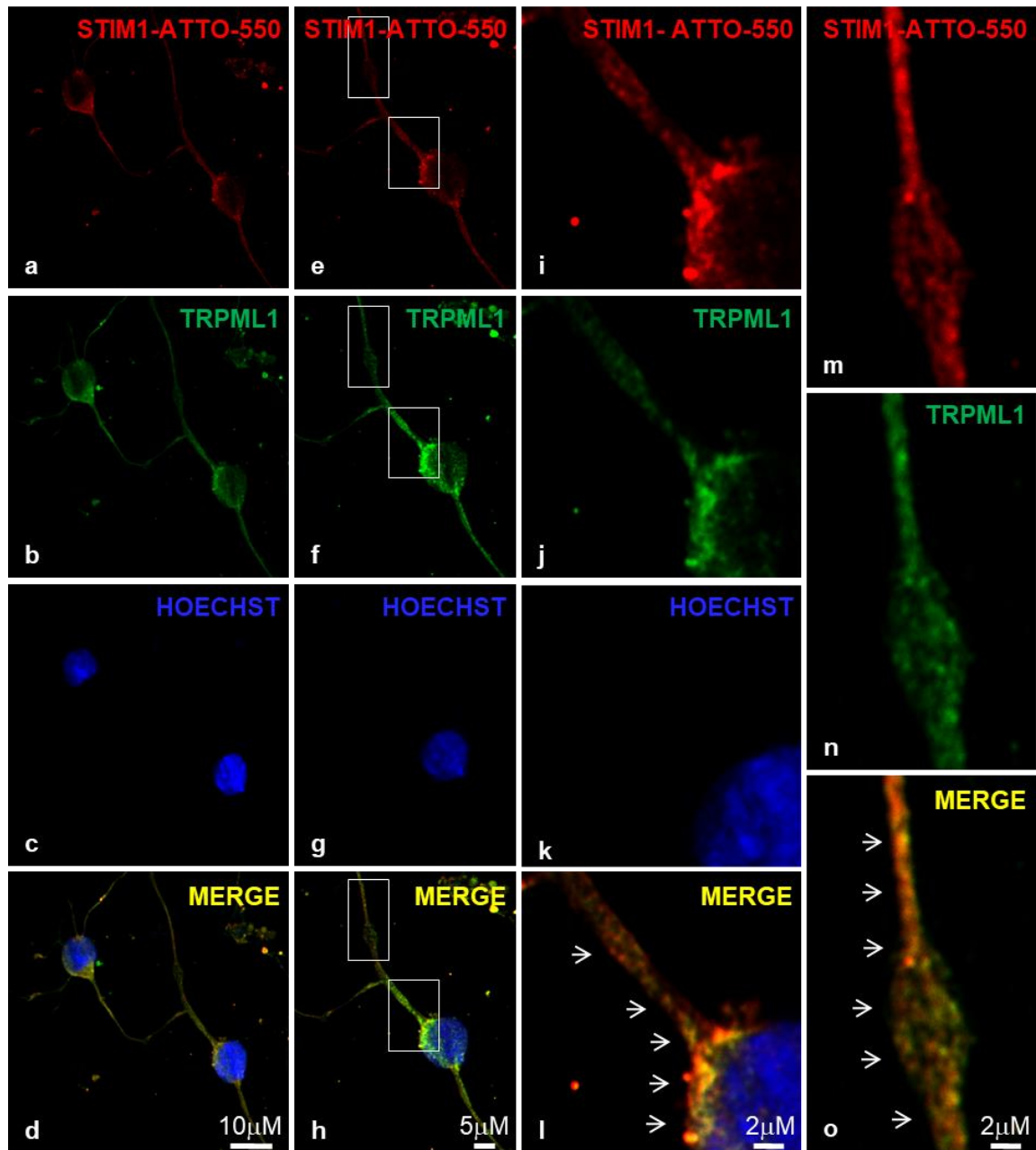
Fig.19 - Lysosome/ER coupling is mediated by STIM1/TRPML1 interaction under physiological conditions. STIM1 (STIM1-ATTO-550, red) and TRPML1 (green) immunosignals in cortical neurons under control conditions (a-h); nuclei were counterstained with Hoechst (blue). Higher magnifications of each frame illustrate STIM1/TRPML1 staining in the cell body (arrows, i-l) and along axons (arrows, m-o). Bar graph depicts the quantification of STIM1 and TRPML1 co-localization as Pearson's coefficient value. Scale bars: 10 μm (a-d), 5 μm (e-h), and 2 μm (i-o). The experiment was repeated 3 times with similar results.

On the basis of our results, we suggest that under physiological conditions STIM1 may interact with TRPML1 probably with the aim of allowing Ca^{2+} passage between the two organelles. This is an absolutely new evidence that will be corroborated by other experiments in the future.

4.5 Biochemical characterization of TRPML1 expression in cortical neurons and cortical glial cells exposed to anoxic conditions

Considering the existence of a physical and functional interplay between lysosomes and ER in cortical neurons under physiological conditions, we evaluated whether this interorganellar communication could be modified under hypoxic conditions reproducing brain ischemia. In order to obtain an *in vitro* model of the disease, primary cortical neurons were exposed to 3 hours of oxygen and glucose deprivation (OGD) followed by 24 hours of reoxygenation (Rx). In more detail, as already reported in the Materials and Methods section, neurons were incubated with a glucose-free medium and kept for 3 hours in a hypoxic chamber with a controlled atmosphere of N_2/CO_2 gases (95% N_2, 5% CO_2), to simulate the acute cerebral vessel occlusion that occurs *in vivo*. Cells were then exposed to normoxic, glucose-containing medium for 24 hours to reproduce the reperfusion phase occurring in pathological conditions (Scorziello A. *et al.*, 2001).

In our study, by means of Western blotting experiments, we analyzed the protein expression of TRPML1 in cortical neurons and in cortical glial cells exposed to 3 hours of OGD and 3 hours of OGD followed by 24 hours of reoxygenation. We observed that in cortical neurons TRPML1 expression levels were dramatically reduced during OGD; conversely, when OGD was followed by 24 hours of reoxygenation TRPML1 protein expression returned to control values (**Fig.20 A**). Interestingly, this phenomenon is neuron-specific, since anoxic conditions did not modulate the expression levels of the protein in cortical glial cells (**Fig.20**

B). Moreover, to demonstrate that anoxia did not induce a variation in the number of lysosomes within the cell, we also evaluated the expression of the lysosomal membrane protein LAMP2, which showed no significant modulation during anoxia in both cortical neurons and cortical glial cells (**Fig.20 A-B**).
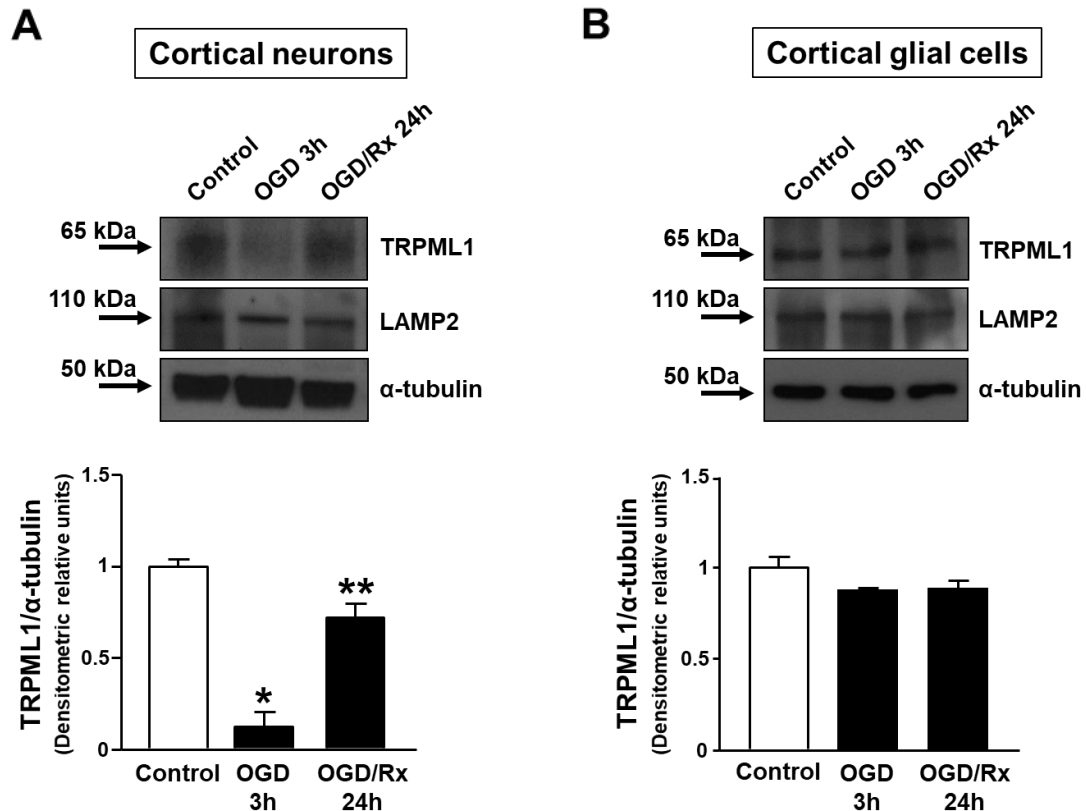

Fig.20 - Effect of OGD and OGD/Rx on TRPML1 protein expression in cortical neurons and in cortical glial cells. (**A**-**B**) Representative Western blotting (top) and quantification (bottom) of TRPML1 expression in cortical neurons (**A**) and in cortical glial cells (**B**) exposed to OGD and OGD/Rx. All the experiments were repeated 3 times with similar results.
* $p<0.05$ versus control; ** $p<0.05$ versus OGD 3h.

4.6 TRPML1 modification occurring during OGD triggers a dysfunction in lysosomal Ca²⁺ content

To assess whether anoxic conditions could induce a dysregulation in lysosomal Ca^{2+} homeostasis, we measured lysosomal Ca^{2+} content in cortical neurons exposed to OGD and OGD/Rx by means of Fura-2/AM single-cell microfluorimetry technique. In our experiments, to elicit lysosomal Ca^{2+} release into the cytosol we used the TRPML1 agonist ML-SA1 (10

μM). Our results showed that ML-SA1-induced lysosomal Ca^{2+} release significantly raised during OGD (**Fig.21 A**); in contrast, lysosomal Ca^{2+} efflux after ML-SA1 administration was strongly reduced when OGD was followed by 24 hours of reoxygenation (**Fig.21 B**). However, the pre-treatment for 10 minutes with the Ca^{2+} ionophore ionomycin, performed to elicit Ca^{2+} efflux from all intracellular non-lysosomal Ca^{2+} stores, and in particular from ER, caused a strong reduction in ML-SA1-induced lysosomal Ca^{2+} release during OGD (**Fig.21 A**), unmasking an experimental bias. Conversely, this pre-treatment failed to have the same effect on lysosomal Ca^{2+} release during OGD/Rx and under control conditions (**Fig.21 A-B**). Similar results were obtained when lysosomal Ca^{2+} release into the cytosol was promoted by using GPN (300 μM), a lysosomotropic agent that induces the osmotic lysis of lysosomes (data not shown).

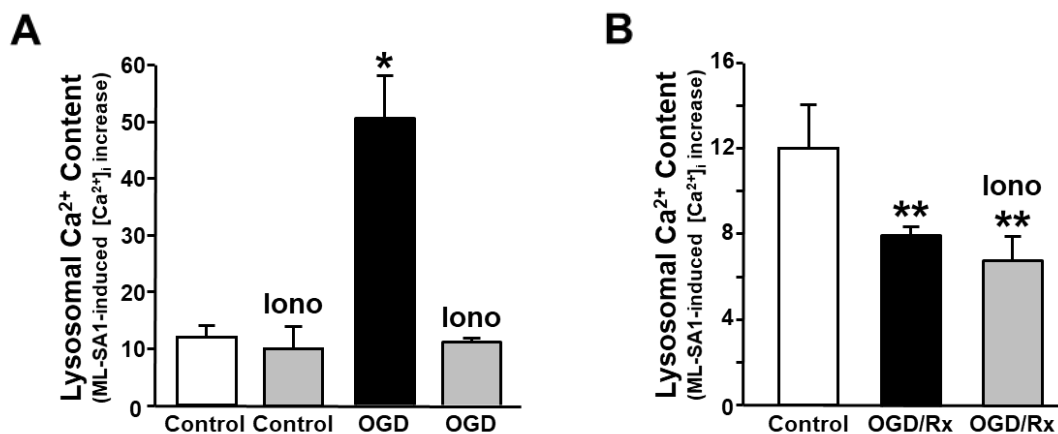**Fig.21 - Lysosomal Ca^{2+} content is dysregulated in hypoxic neurons.** (**A-B**) Quantification of the effect of ML-SA1-induced lysosomal Ca^{2+} release during OGD (**A**) and OGD/Rx (**B**), in the absence or presence of the Ca^{2+} ionophore ionomycin (**A-B**), in cortical neurons.
All the experiments were repeated 3 times on almost 40 cells with similar results.
* $p < 0.05$ versus control; ** $p < 0.05$ versus OGD and control.

These results suggest that, during OGD, lysosomal Ca^{2+} content remained unmodified, while ER Ca^{2+} content increased, as already demonstrated by our research group in a previous paper (Sirabella R. *et al.*, 2009). On the other hand, lysosomal Ca^{2+} strongly decreased during the reoxygenation phase, thus meaning that TRPML1 could be hyperfunctional during this phase, possibly due to an increased ROS production. That TRPML1 may be hyperactivated in a pathophysiological condition characterized by oxidative stress like anoxia is corroborated by

the recent findings by Zhang *et al.*, who demonstrated that TRPML1 could be activated upon elevations in ROS levels, thus promoting an excessive Ca^{2+} release from lysosomes (Zhang X. *et al.*, 2016).

4.7 The pharmacological modulation of TRPML1 during the reoxygenation phase determines cell fate of anoxic cortical neurons

Considering the biochemical and functional modifications of TRPML1 that we observed in cortical neurons exposed to anoxia and the strong reduction in cell viability occurring during OGD/Rx, we analyzed the effect of TRPML1 modulation under hypoxic conditions on neuronal survival. In this respect, we tested the effect of two pharmacological modulators of TRPML1 activity during anoxia: its agonist ML-SA1, and its inhibitor Ned19. We also verified the effect of the chemical YM201636 (10 μM), a potent inhibitor of the mammalian class III phosphatidylinositol phosphate kinase PIKfyve, which blocks the production of the endogenous activator of the channel, $PI(3,5)P_2$ (Jefferies H.B. *et al.*, 2008). Each drug was administered during OGD, at the onset of reoxygenation, or during both OGD and reoxygenation. In all the experiments, neuronal survival was evaluated by MTT assay at the end of the reoxygenation phase.

Our MTT experiments demonstrated that the activation of the channel by ML-SA1 failed to induce any effect on cell viability during anoxia, independently on the phase of administration (**Fig.22 A**). Similarly, no significant effect was observed when cells were treated with YM201636 during OGD or during the reoxygenation phase; however, when this drug was administered during both phases, it strongly affected neuronal survival compared to OGD/Rx (**Fig.22 B**). Moreover, at the cellular level, neurons treated with this chemical during anoxia displayed a vesiculation phenotype characterized by the presence of enlarged vacuolar

structures, thus suggesting a disruption in cell structure and function (data not shown). These data are consistent with an aspecific role of the phosphoinositide PI(3,5)P$_2$ at neuronal level.

In addition, no variation in cell viability was observed when cells were incubated with TRPML1 inhibitor Ned19 during OGD, in which TRPML1 expression was downregulated; conversely, the administration of this drug during the reoxygenation phase was able to promote a strong increase in neuronal survival compared to OGD/Rx (**Fig.22 C**). Interestingly, this neuroprotective effect was similar to that observed in ischemic preconditioning (IPC+OGD/Rx), a well-known model to induce neuroprotection in anoxic neurons (**Fig.22 C**). Indeed, it has been already reported that in cortical neurons exposed to the preconditioning insult (30 minutes of OGD that precede OGD/Rx), the impairment in mitochondrial activity was partially rescued compared to neurons exposed to OGD/Rx alone (Scorziello A. *et al.*, 2007).
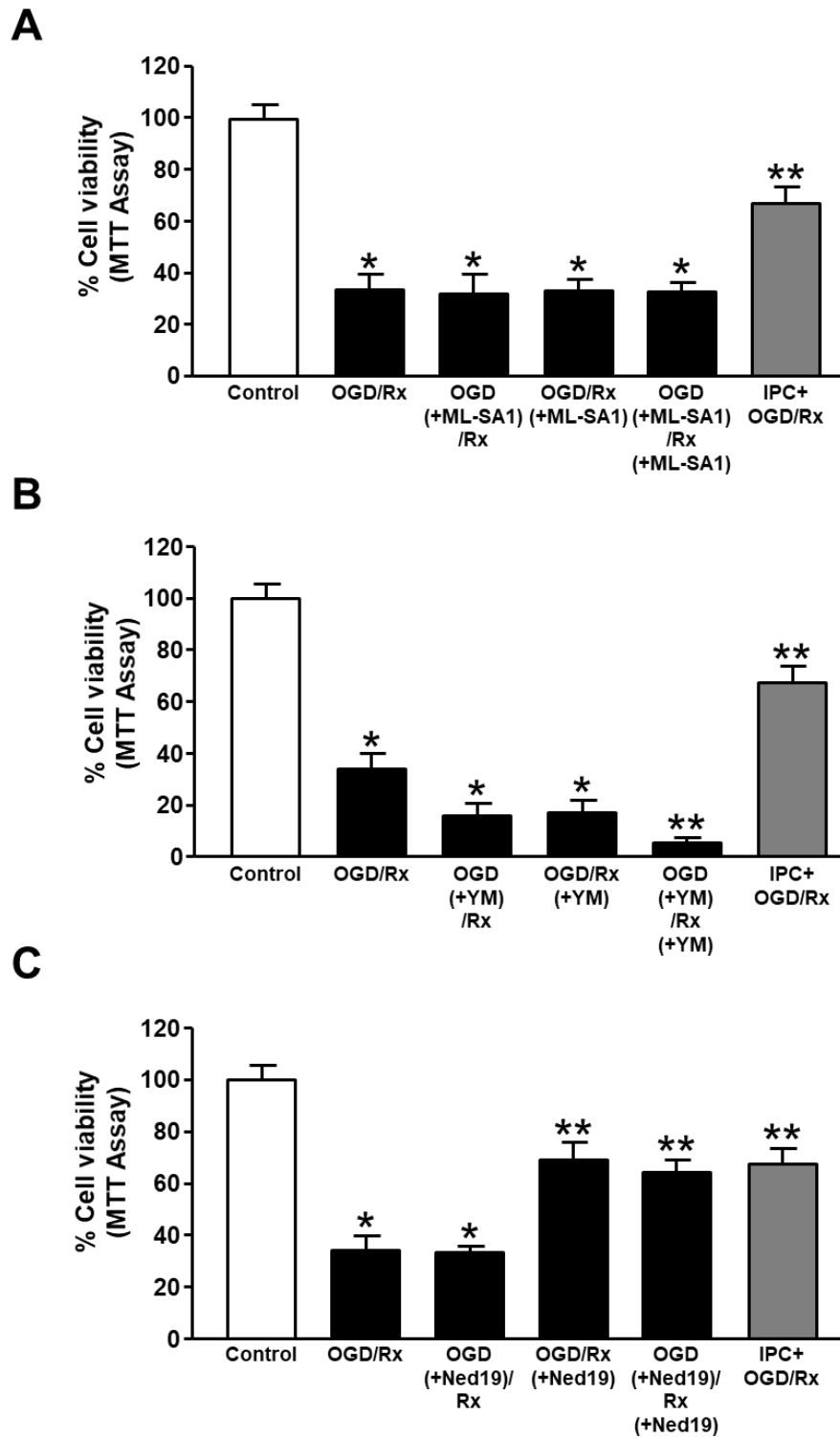
Fig.22 - Mitochondrial activity in cortical neurons exposed to anoxia and treated with three different drugs able to modulate TRPML1 function during OGD, during the reoxygenation, or during both phases. (A-C) Effect of ML-SA1 (10 μM) (**A**), YM201636 (10 μM) (**B**), and Ned19 (30 μM) (**C**) on cell viability in cortical neurons exposed to hypoxic conditions.
Cell viability of untreated controls was considered to be 100%.
All the experiments were repeated 3 times with similar results.
* p<0.05 versus control; ** p<0.05 versus OGD/Rx.

These results suggest that the pharmacological inhibition of the channel at the beginning of the reoxygenation phase may exert a neuroprotective effect in cortical neurons exposed to anoxia.

4.8 TRPML1 inhibition exerts a neuroprotective effect in hypoxic cortical neurons by modulating lysosomal Ca^{2+} homeostasis

Since the pharmacological inhibition of TRPML1 during the reoxygenation phase strongly improved cell survival in hypoxic neurons, we verified the effect of Ned19 on lysosomal and ER Ca^{2+} coupling during OGD/Rx. We first studied whether the anoxic stimulus could hamper the physical coupling between the two organelles promoted by STIM1/TRPML1 interaction. To this aim, we performed co-immunoprecipitation experiments followed by Western blotting analysis. Our results showed that the interaction between the two proteins observed under normoxia was maintained during OGD/Rx; interestingly, the pharmacological inhibition of TRPML1 during the reoxygenation phase did not block, but only slightly reduced, the physical coupling between lysosomes and ER (**Fig.23 A-B**).

Then, we analyzed the effect of TRPML1 inhibition on lysosomal and ER Ca^{2+} homeostasis during anoxia. We found that the administration of this drug during the reoxygenation phase was able to revert the dysfunction of lysosomal Ca^{2+} homeostasis observed during OGD/Rx, by restoring a proper lysosomal Ca^{2+} content (**Fig.23 C**). We hypothesized that this effect is possibly due to the blockade of a hyperfunctional TRPML1 channel, which, due to the high ROS levels produced during the reoxygenation, could promote massive Ca^{2+} release from lysosomes. However, the pharmacological inhibition of TRPML1 failed to exert any effect on ER Ca^{2+} concentration during OGD/Rx (**Fig.23 D**).
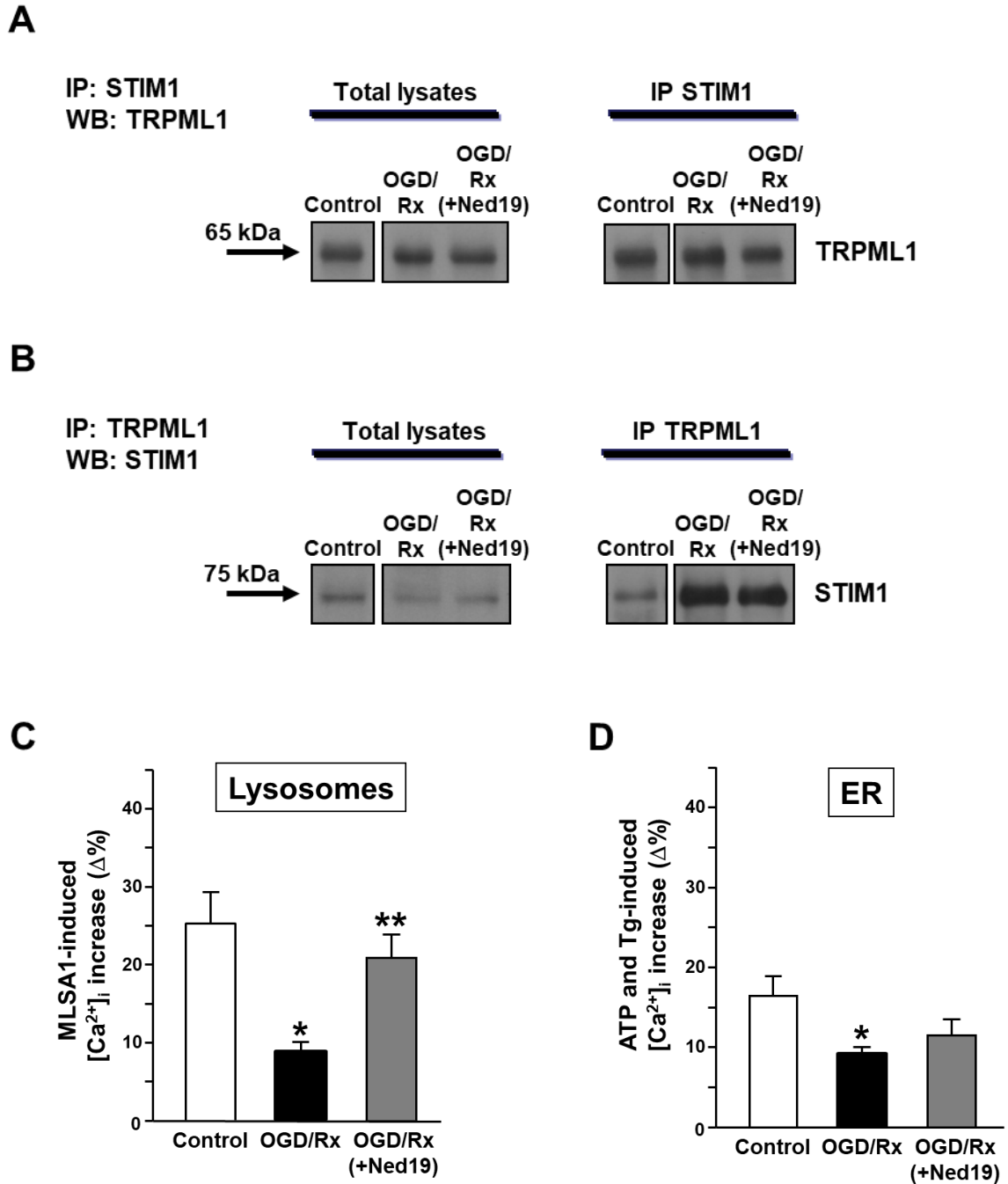
Fig.23 - Effect of TRPML1 inhibition on lysosome/ER coupling during OGD/Rx. (**A-B**) Lysates from cortical neurons exposed to anoxia were subjected to immunoprecipitation (IP) using anti-STIM1 or anti-TRPML1 antibodies. The presence of TRPML1 or STIM1 was analyzed by Western blotting (WB). The experiments were repeated 3 times with similar results. (**C-D**) Quantification of the effect of TRPML1 inhibition during the reoxygenation phase on lysosomal (**C**) and ER Ca^{2+} content (**D**) in cortical neurons exposed to OGD/Rx. All the experiments were repeated 3 times on almost 40 cells with similar results.

For C and D, * $p<0.05$ versus control; ** $p<0.05$ versus OGD/Rx.

Collectively, these data suggest that the Ca^{2+} coupling between lysosomes and ER is impaired during anoxia. In this respect, the lack of effect of Ned19 in restoring ER Ca^{2+} content

during the reoxygenation phase is possibly due to a disruption of lysosomes/ER membrane contact sites, or to an alteration in the functional coupling between the two organelles. These two putative events could both occur during the reoxygenation phase. However, our immunoprecipitation experiments revealed that a certain amount of interaction between the lysosomal channel TRPML1 and the ER Ca^{2+} sensor STIM1 was maintained in hypoxic neurons treated with TRPML1 inhibitor. On the basis of these evidences we suggest that the ineffectiveness of Ned19 on ER Ca^{2+} homeostasis during anoxia could be mainly linked to an impairment in the functional coupling occurring between lysosomes and ER.

4.9 Effect of TRPML1 inhibition on ER stress and apoptotic cell death in cortical neurons exposed to OGD/Rx

Since TRPML1 inhibition exerts a beneficial effect on neuronal survival and on lysosomal Ca^{2+} homeostasis in our *in vitro* model of brain ischemia, we tried to characterize the molecular mechanisms underlying Ned19-mediated neuroprotection.

Several experimental evidences showed that ER stress and apoptotic cell death play a key role in the neurodegeneration associated to brain ischemia (Paschen W. *et al.*, 2003; Shibata M. *et al.*, 2003; Paschen W. and Mengersdorf T., 2005; Pallast S. *et al.*, 2010). Thus, we verified whether the neuroprotective effect of Ned19 could be due to a reduction of the ER stress occurring during anoxia. To this aim, by means of Western blotting analysis, we evaluated the protein expression of GRP78 (also known as BiP), a molecular chaperone that activates the UPR (*Unfolded Protein Response*) in the presence of misfolded proteins in the lumen of ER (Malhotra J.D. and Kaufman R.J., 2007). Our results showed that GRP78 expression levels were increased after OGD/Rx, compared to control cells. Interestingly, the administration of Ned19 during the reoxygenation phase prevented the increase in GRP78 induced by anoxia

(**Fig.24 A**), thus suggesting that the pharmacological inhibition of TRPML1 protected cortical neurons exposed to hypoxic conditions by preventing ER stress.

Moreover, we also evaluated the effect of TRPML1 inhibition on the expression of caspase 9, a pro-apoptotic marker known to be activated after severe and prolonged ER stress. Indeed, it has been reported that this protein, mainly involved in the intrinsic (mitochondria-dependent) pathway of apoptosis, can also be activated by caspase 12, an ER-specific caspase that participates in apoptosis under ER stress (Morishima N. *et al.*, 2002; Rao R.V. *et al.*, 2002). Our results showed that OGD/Rx induced a strong increase in the expression levels of cleaved-caspase 9, that was efficiently reduced by TRPML1 inhibition during the reoxygenation phase (**Fig.24 B**).

Fig. 24 - Effect of TRPML1 inhibition on the expression of ER stress and apoptotic cell death markers during OGD/Rx. (A-B) Representative Western blotting (top) and quantification (bottom) of GRP78 (**A**) and cleaved-caspase 9 (**B**) expression in cortical neurons exposed to OGD/Rx and OGD/Rx (+Ned19).
All the experiments were repeated 3 times with similar results.
* p<0.05 versus control; ** p<0.05 versus OGD/Rx.

Collectively, our results indicate that Ned19 is able to prevent the induction of ER stress and protects cortical neurons from apoptotic cell death induced by anoxia.

4.10 Effect of TRPML1 inhibition on the autophagic pathway in cortical neurons exposed to OGD/Rx

The lysosomal Ca^{2+} channel TRPML1 is involved in the regulation of several Ca^{2+}-dependent functions within the cell and, in particular, it has been reported that Ca^{2+} released through this channel is responsible for the activation of autophagy (Medina D.L. *et al.*, 2015; Zhang X. *et al.*, 2016). So, starting from this evidence, by means of Western blotting experiments we studied the effect of the pharmacological inhibition of TRPML1 during anoxia on the expression of two proteins involved in the autophagic pathway: LC3-II, the autophagosome-associated form of LC3, and p62, an adaptor protein that recruits poly-ubiquitylated substrates to autophagosomes. Our results showed that this drug was able to induce a significant accumulation of these two autophagic markers, compared to OGD/Rx (**Fig.25 A-B**).
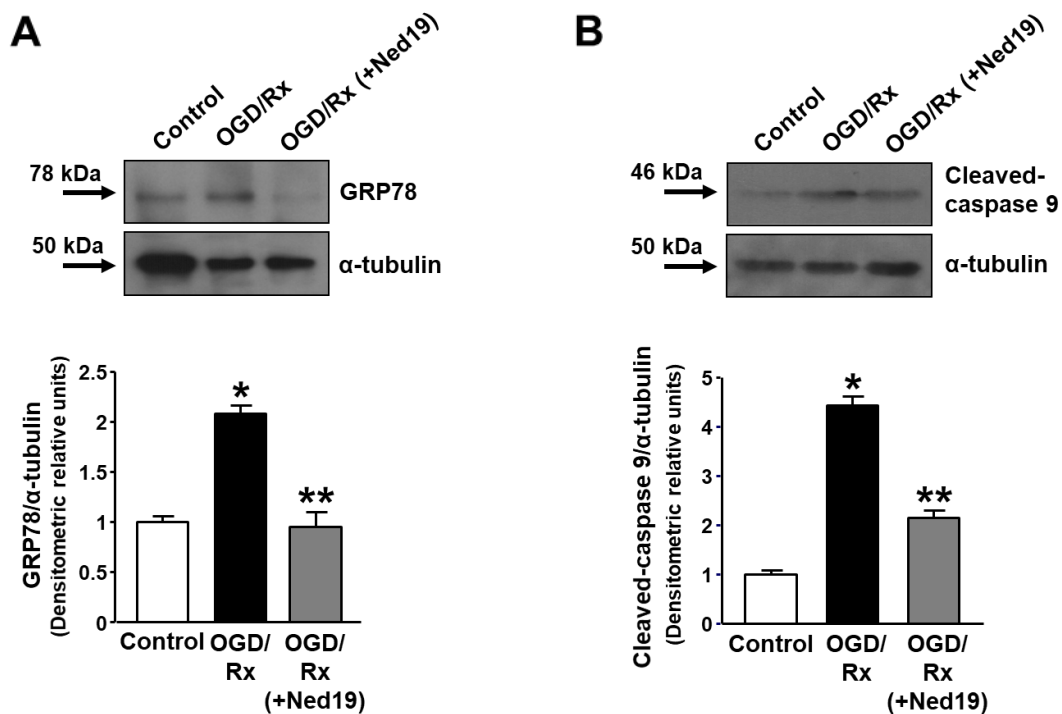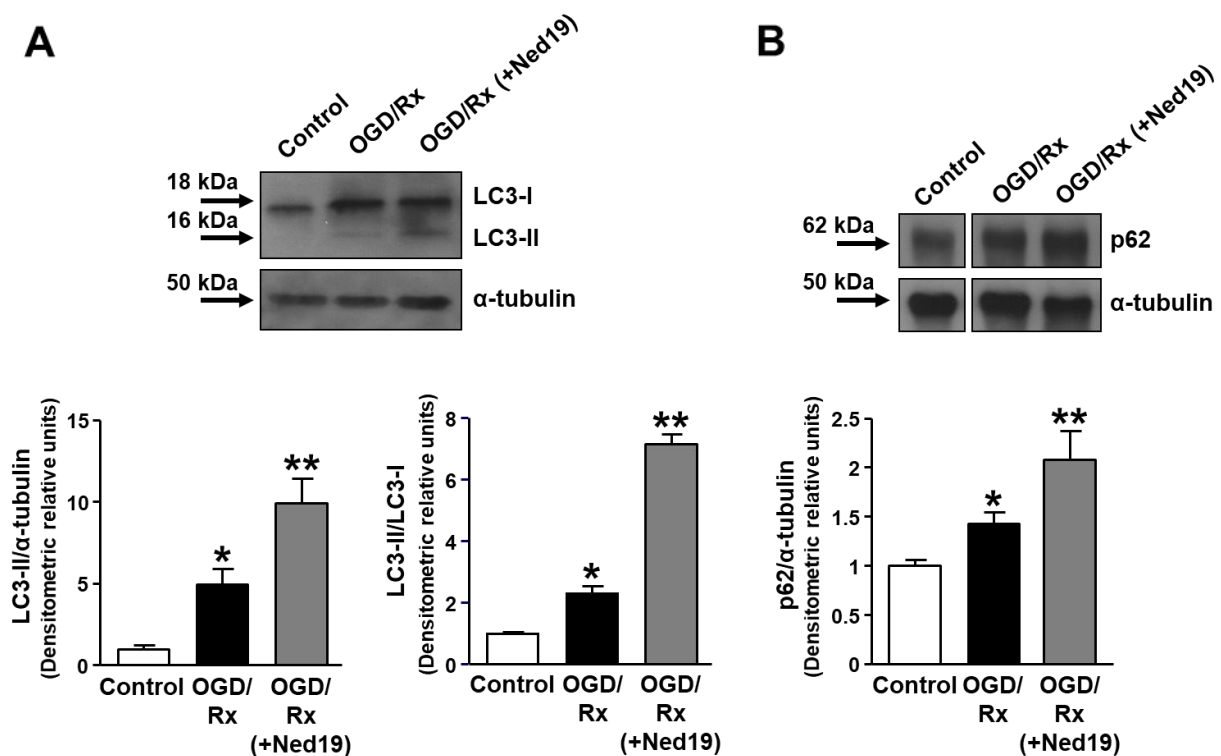

Fig. 25 - Effect of TRPML1 inhibition on the expression of autophagic markers during OGD/Rx.
(**A-B**) Representative Western blotting (top) and quantification (bottom) of LC3-II (**A**) and p62 (**B**) expression in cortical neurons exposed to OGD/Rx and OGD/Rx (+Ned19).
All the experiments were repeated 3 times with similar results.
* p<0.05 versus control; ** p<0.05 versus OGD/Rx.

We postulated that this accumulation could be due to a block in the autophagic flux, rather than an increase in the process, induced by Ned19 during the reoxygenation. To confirm our hypothesis, the expression of LC3-II was evaluated under anoxia also after the administration of bafilomycin A1 during the reoxygenation phase; indeed, this drug has been reported to inhibit autophagy (Yamamoto A. *et al.*, 1998; Mauvezin C. *et al.*, 2015). We observed that during OGD/Rx bafilomycin A1 induced an accumulation of LC3-II (**Fig.26**) similar to that observed after the administration of Ned19. This result suggests that during OGD/Rx the accumulation of the autophagic markers is due to a block, rather than an activation, of the autophagic flux.
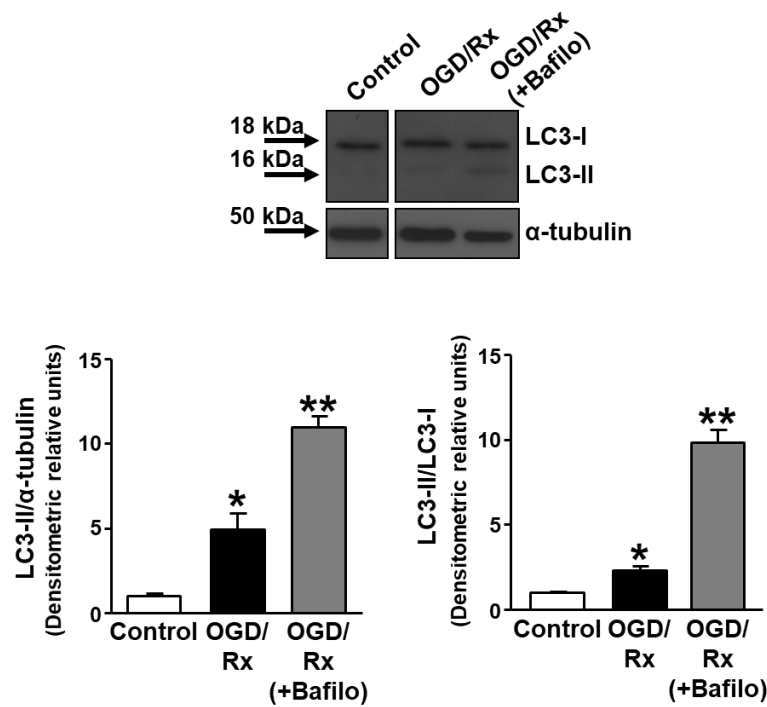
Fig.26 - Effect of bafilomycin A1 on the expression of LC3-II during OGD/Rx. Representative Western blotting (top) and quantification (bottom) of LC3-II in cortical neurons exposed to OGD/Rx and OGD/Rx (+Bafilomycin A1).
All the experiments were repeated 3 times with similar results.
* $p < 0.05$ versus control; ** $p < 0.05$ versus OGD/Rx.

Considering that the inhibition of the autophagic flux induced by bafilomycin A1 is due to a block in the fusion of autophagosomes with lysosomes (Yamamoto A. *et al.*, 1998; Mauvezin C. *et al.*, 2015), we hypothesized that Ned19 could inhibit autophagy through the same mechanism in our cellular model.

In order to analyze the block in the autophagic flux, we performed immunoprecipitation experiments in which we evaluated the possible interaction between the autophagosomal membrane protein LC3-II and the lysosomal membrane protein LAMP1. In order to verify that this technique could be suitable for our purpose, as positive control, we tested the effect of bafilomycin A1 on the interaction between the two proteins under physiological conditions. The results obtained demonstrated that under normoxia LAMP1 and LC3-II physically interacted; interestingly, the incubation for 1 hour with 100 nM bafilomycin A1 was able to reduce the interaction between the two proteins (**Fig.27**), thus confirming that this drug interferes with autophagosomes/lysosomes fusion.

Fig.27 - Effect of bafilomycin A1 on the interaction between lysosomal and autophagosomal proteins in cortical neurons under physiological conditions. Lysates from cortical neurons under physiological conditions were subjected to immunoprecipitation (IP) using anti-LAMP1 antibody. The presence of LC3-II was analyzed by Western blotting (WB).
The experiment was repeated 3 times with similar results.

Then, to verify the possibility that Ned19 could cause a similar defect in the fusion between autophagosomes and lysosomes, the interaction between LAMP1 and LC3-II was also evaluated after the administration of the pharmacological inhibitor of TRPML1 under both physiological and hypoxic conditions. We observed that in cortical neurons exposed to normoxia the incubation with Ned19 for 1 hour strongly decreased the co-immunoprecipitation of the two proteins. This interaction, preserved in neurons exposed to OGD/Rx, was also reduced by Ned19 in anoxic neurons (**Fig.28**).
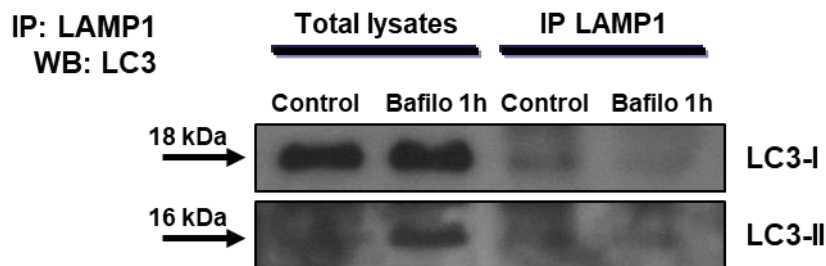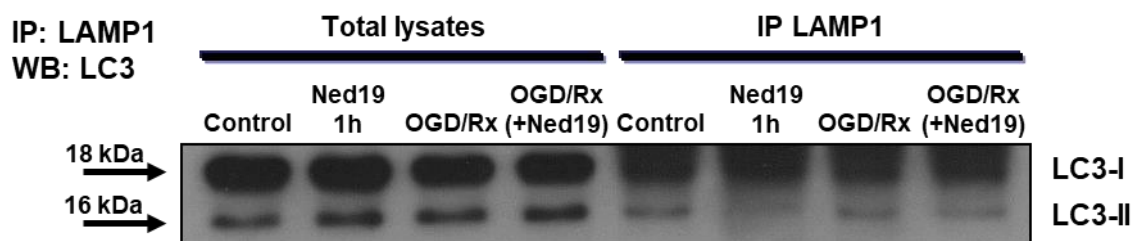
Fig.28 - Effect of Ned19 on the interaction between the lysosomal and autophagosomal proteins in cortical neurons under physiological conditions and in neurons exposed to anoxia. Lysates from cortical neurons exposed to anoxia were subjected to immunoprecipitation (IP) using anti-LAMP1 antibody. The presence of LC3-II was analyzed by Western blotting (WB).
The experiment was repeated 3 times with similar results.

Altogether, our results suggest that the neuroprotective effect of Ned19 in anoxic neurons was due to a blockade in the autophagic flux caused by an impaired fusion between autophagosomes and lysosomes. We hypothesize that this blockade could improve neuronal status by reducing the elimination of intracellular organelles (such as mitochondria) and components that are partially damaged, but still functional. Indeed, the degradation of these cellular constituents could represent a detrimental event for neuronal survival, already compromised during OGD/Rx. Moreover, by destroying partially impaired mitochondria, autophagy could also reduce the number of these compartments, and so produce a secondary energy failure in post-ischemic neurons.

4.11   The pharmacological inhibition of TRPML1 exerts a neuroprotective effect on ischemic damage in rats subjected to transient focal ischemia

Considering the neuroprotective effect of TRPML1 inhibition in anoxic neurons, we tested Ned19 in an *in vivo* rat model of transient cerebral ischemia (tMCAO), by evaluating the effect of this drug on both brain infarct volume and neurological deficits induced by brain ischemia. Interestingly, we observed that Ned19, intracerebroventricularly (icv) infused at the onset of reperfusion in ischemic rats, significantly reduced the extent of the ischemic damage

of ~40% compared to rats subjected to tMCAO and treated with vehicle (**Fig.29 A**). Furthermore, the reduction in the ischemic volume induced by Ned19 was accompanied by a marked improvement in general and focal neurological scores of animals subjected to cerebral ischemia (**Fig.29 B**).
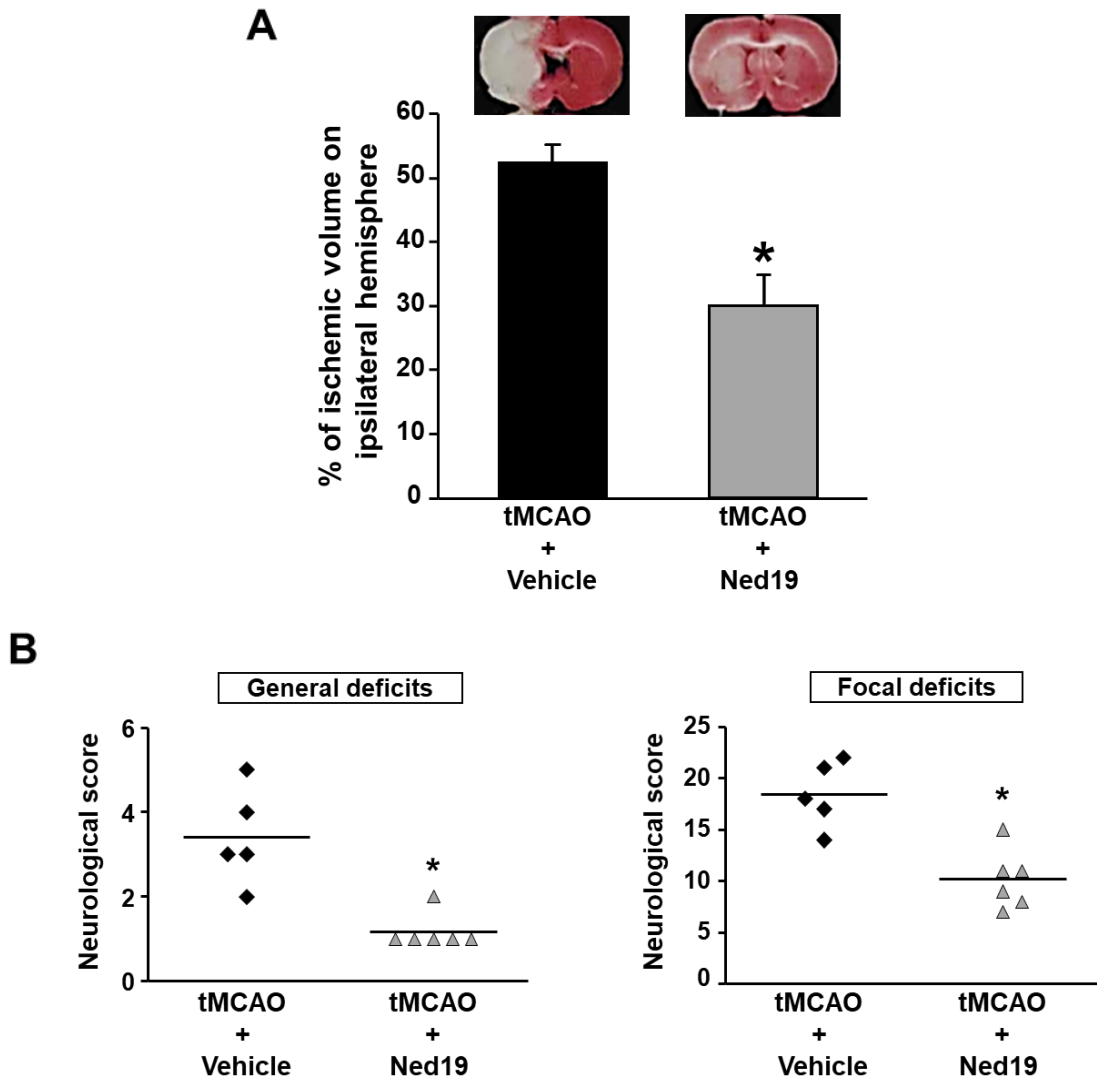
Fig.29 - Quantification of infarct volume after 100 minutes of tMCAO and administration of Ned19 coupled with performance of general and focal neurological deficits after TRPML1 inhibition in ischemic rats. (**A**) Effect of Ned19 on infarct volume of rats subjected to 100 minutes of tMCAO compared to ischemic rats treated with vehicle, all analyzed after 24 hours. On the top side representative coronal brain slices indicating the extension of the infarct area are reported. (**B**) Effect of Ned19 on general and focal neurological scores (horizontal line indicates the mean neurological score). For A and B:
n = 5-6 animals per group.
* p<0.05 versus tMCAO + vehicle.

Then, we also tested the effect of Ned19 infusion at different time points after the onset of reperfusion (3 hours, 6 hours, 12 hours, and 24 hours). Unfortunately, the results obtained indicated that TRPML1 inhibition at these time points failed to induce any significant reduction in the ischemic volume or amelioration in general and focal deficits in rats subjected to tMCAO (data not shown). This could be due to the coexistence of other mechanisms occurring during the reperfusion phase.

In addition, by means of Western blotting experiments, we evaluated the effect of Ned19 administration at the onset of reperfusion on the expression of the autophagic markers p62 and LC3-II in the ipsilateral cortex of rats subjected to brain ischemia. We observed that in this cerebral tissue affected by the ischemic insult, the pharmacological inhibition of TRPML1 was able to induce an increase of both the proteins (**Fig.30**), as it occurs in our *in vitro* model of the disease.
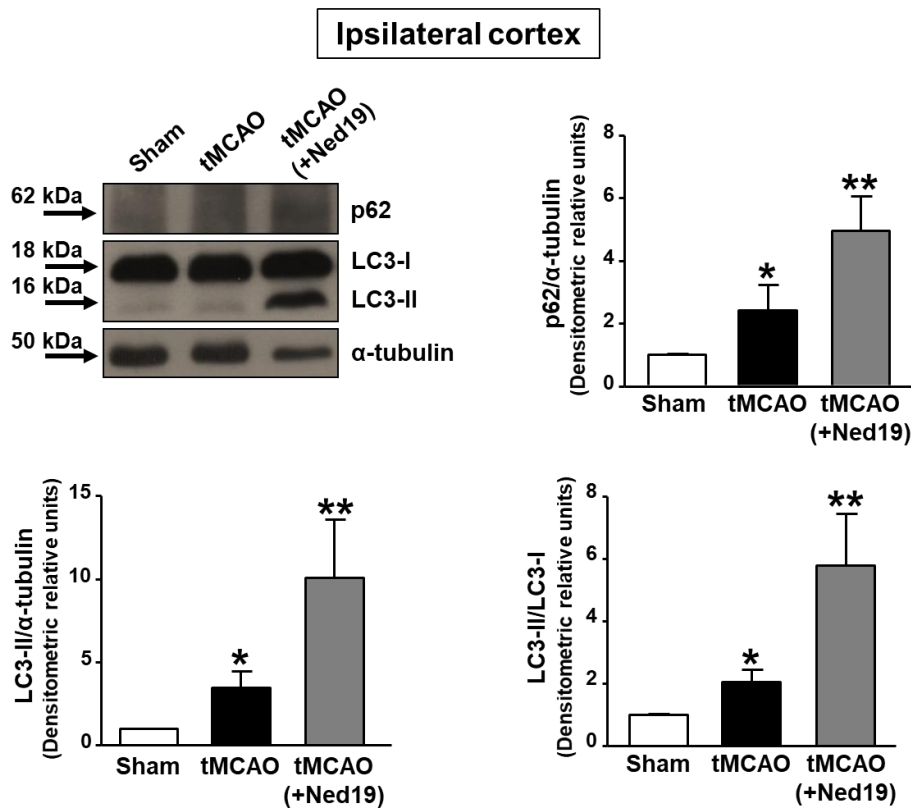
Fig. 30 - Effect of TRPML1 inhibition on the expression of autophagic markers in the ipsilateral cortex of ischemic rats. Representative Western blotting and quantification of p62 and LC3-II expression in the ipsilateral cortex of sham-operated (controls), ischemic (tMCAO), and Ned19-treated ischemic (tMCAO+Ned19) rats.
n = 5 animals per group.
* $p < 0.05$ versus sham-operated group; ** $p < 0.05$ versus tMCAO.

Moreover, we also analyzed the expression of p62 and LC3-II in the ipsilateral cortex of rats subjected to tMCAO and icv infused with Ned19 at three hours after the onset of reperfusion. As expected, the modulation in the expression of these two autophagic markers was not statistically significant (data not shown). Indeed, the infusion of the drug at this time point did not induce any significant reduction in the ischemic brain volume nor any amelioration in general and focal deficits in ischemic rats.

Collectively, our *in vivo* results demonstrate that the pharmacological inhibition of TRPML1 at the onset of the reperfusion is able to reduce the ischemic damage induced by tMCAO and suggest that the neuroprotective effect of Ned19 during the reperfusion phase may be linked to a block in the autophagy flux.

CONCLUSIONS

A physical and functional coupling between the endoplasmic reticulum (ER) and lysosomes has been recently reported to occur in different cell types under physiological conditions (Kilpatrick B.S. *et al.*, 2013; Kilpatrick B.S. *et al.*, 2016b; Aston D. *et al.*, 2017). Indeed, lysosomes, that participate in the regulation of intracellular Ca^{2+} homeostasis under both physiological and pathological conditions, can communicate with the ER for the handling of intracellular Ca^{2+} concentration (Patel S. and Docampo R., 2010; Morgan A.J. *et al.*, 2011). A recent study highlighted the involvement of TRPML1 in the communication between the two organelles in human fibroblasts (Kilpatrick B.S. *et al.*, 2016b). Despite being a non-selective cation channel, TRPML1 is the main Ca^{2+}-extruding system localized to lysosomal membrane. Loss-of-function mutations in *mcoln1*, the gene encoding for TRPML1, cause mucolipidosis type IV (MLIV), a devastating lysosomal storage disorder characterized by neurodegeneration (Bargal R. *et al.*, 2000; Bassi T.M. *et al.*, 2000; Sun M. *et al.*, 2000). So far, there is no evidence in literature about the possible contribution of this channel in the maintenance of intracellular Ca^{2+} homeostasis in the neurodegeneration associated to brain ischemia. However, it is well-known that dysfunctions in the ER play a key role in the neurodegenerative mechanisms underlying this neurological disorder (Paschen W. *et al.*, 2003; Shibata M. *et al.*, 2003; Paschen W. and Mengersdorf T., 2005; Sirabella *et al.*, 2009; Pallast S. *et al.*, 2010).

So far, many drugs have been tested for the treatment of acute ischemic stroke; however, none of them has been proven to be effective. At present, the only effective drug approved by the FDA and EMA for the treatment of brain ischemia is the recombinant tPA (tissue plasminogen activator), but its administration is characterized by some limitations, including the appearance of some adverse effects (Donnan G.A. et al., 2008; Brouns R. and De Deyn P.P., 2009; Haelewyn B. et al., 2010). Thus, the identification of novel molecular mechanisms

underlying this widespread neurological disease could help researchers in the development of new and more efficacious drugs for its pharmacological treatment.

My PhD thesis is mainly focused on the study of a novel role for TRPML1 in the regulation of intracellular Ca^{2+} homeostasis during brain ischemia. Indeed, we investigated for the first time the possible contribution of this channel in the functional coupling between lysosomes and ER for intracellular Ca^{2+} handing in some experimental models of the disease. Briefly, in the first part of my PhD work, TRPML1 involvement in lysosomes/ER Ca^{2+} coupling was evaluated in rat primary cortical neurons under physiological conditions. Our results showed that the pharmacological or genetic modulation of the channel was able to modify ER Ca^{2+} content, thus suggesting the existence of an interplay between the two Ca^{2+} stores at neuronal level controlled by TRPML1. In the second part of my thesis, considering the dysfunction of ER Ca^{2+} homeostasis occurring during brain ischemia, we verified whether the functional crosstalk between lysosomes and ER observed under physiological conditions could be impaired under pathological conditions. In particular, we showed that in our *in vitro* model of the disease, represented by cortical neurons exposed to oxygen and glucose deprivation (OGD) followed by reoxygenation (Rx), the protein expression of the channel was strongly modulated, with a significant downregulation during OGD and a return to the control levels after the reoxygenation. In addition, the anoxic stimulus not only led to neuronal death, but also strongly impaired the function of the channel, thus resulting in a disruption of the functional coupling between lysosomes and ER during anoxia. Interestingly, the results presented in this thesis work demonstrated that the pharmacological inhibition of TRPML1 by means of Ned19 during the reoxygenation phase exerted a neuroprotective effect in anoxic neurons by restoring lysosomal Ca^{2+} content, by preventing ER stress and apoptotic cell death, and by blocking the autophagic flux. Interestingly, in an *in vivo* model of brain ischemia represented by rats subjected to the transient middle cerebral artery occlusion (tMCAO), this drug, intracerebroventricularly infused at the onset of reperfusion, was able to improve the

neurological deficits and to reduce the extent of brain damage following the injury by blocking the hyperactive autophagic flux. Unfortunately, the administration of Ned19 at different time points after the onset of reperfusion, performed to establish a therapeutic time window for this drug, failed to exert any neuroprotective effect in ischemic rats. This failure could be due to the activation of other concomitant mechanisms during the reperfusion phase that will be further investigated in the future.

In conclusion, my PhD thesis highlights the detrimental role of TRPML1 dysfunction in the neurodegeneration associated to brain ischemia and identifies a novel potential therapeutic target that could be pharmacologically modulated, together with other relevant mechanisms, to promote neuroprotection. Furthermore, my study contributed to identify the exact time window in which the autophagic flux could be considered hyperactive and, therefore, potentially druggable.

REFERENCES

Abe K., Puertollano R. (2011) **Role of TRP Channels in the Regulation of the Endosomal Pathway**. *Physiology (Bethesda)*, 26:14-22. doi: 10.1152/physiol.00048.2010.

Alberts B., Bray D., Lewis J., Raff M., Roberts K., Watson J.D. (1994) **Molecular Biology of the Cell**. Garland Publishing, New York.

Allison A. (1967) **Lysosomes and disease**. *Sci Am*, 217:62-72.

Altarescu G., Sun M., Moore D.F., Smith J.A., Wiggs E.A., Solomon B.I., *et al.* (2002) **The neurogenetics of mucolipidosis type IV**. *Neurology*, 59:306-313. doi: 10.1212/WNL.59.3.306.

Amir N., Zlotogora J., Bach G. (1987) **Mucolipidosis type IV: clinical spectrum and natural history**. *Pediatrics*, 79:953-959.

Appelqvist H., Wäster P., Kågedal K., Öllinger K. (2013) **The lysosome: from waste bag to potential therapeutic target**. *J Mol Cell Biol*, 5:214-226. doi: 10.1093/jmcb/mjt022.

Arumugam T.V., Okun E., Mattson M.P. (2009) **Basis of ionic dysregulation in cerebral ischemia**. In: Annunziato L. (Ed.), New Strategies in Stroke Intervention. Contemporary Neuroscience, Humana Press (Springer), New York, pp. 1-10. doi: 10.1007/978-1-60761-280-3_1.

Aston D., Capel R.A., Ford K.L., Christian H.C., Mirams G.R., Rog-Zielinska E.A., *et al.* (2017) **High resolution structural evidence suggests the Sarcoplasmic Reticulum forms microdomains with Acidic Stores (lysosomes) in the heart**. *Sci Rep*, 7:40620. doi: 10.1038/srep40620.

Bach G., Cohen M.M., Kohn G. (1975) **Abnormal ganglioside accumulation in cultured fibroblasts from patients with mucolipidosis IV**. *Biochem Biophys Res Commun*, 66:1483-1490. doi: 10.1016/0006-291X(75)90526-4.

Bach G., Ziegler M., Kohn G., Cohen M.M. (1977) **Mucopolysaccharide accumulation in cultured skin fibroblasts derived from patients with mucolipidosis IV**. *Am J Hum Genet*, 29:610-618.

Bach G. (2001) **Mucolipidosis type IV**. *Mol Genet Metab*, 73:197-203. doi: 10.1006/mgme.2001.3195.

Bach G., Webb M.B., Bargal R., Zeigler M., Ekstein J. (2005) **The frequency of mucolipidosis type IV in the Ashkenazi Jewish population and the identification of 3 novel MCOLN1 mutations**. *Hum Mutat*, 26:591. doi: 10.1002/humu.9385.

Bainton D.F. (1981) **The discovery of lysosomes**. *J Cell Biol*, 91:66s-76s.

Bargal R., Bach G. (1988) **Phospholipids accumulation in mucolipidosis IV cultured fibroblasts**. *J Inherit Metab Dis*, 11:144-150. doi: 10.1007/BF01799863.

Bargal R., Bach G. (1997) **Mucolipidosis type IV: abnormal transport of lipids to lysosomes**. *J Inherit Metab Dis*. 20:625-632. doi: 10.1023/A:1005362123443.

Bargal R., Avidan N., Ben-Asher E., Olender Z., Zeigler M., Frumkin A., *et al.* (2000) **Identification of the gene causing mucolipidosis type IV**. *Nat Genet*, 26:118-123. doi: 10.1038/79095.

Bassi M.T., Manzoni M., Monti E., Pizzo M.T., Ballabio A., Borsani G. (2000) **Cloning of the gene encoding a novel integral membrane protein, mucolipidin-and identification of the two major founder mutations causing mucolipidosis type IV**. *Am J Hum Genet*, 67:1110-1120. doi: 10.1016/S0002-9297(07)62941-3.

Bederson J.B., Pitts L.H., Germano S.M., Nishimura M.C., Davis R.L., Bartkowski H.M. (1986) **Evaluation of 2,3,5-triphenyltetrazolium chloride as a stain for detection and quantification of experimental cerebral infarction in rats**. *Stroke*, 17:1304-1308.

Berman E.R., Livni N., Shapira E., Merin S., Levij I.S. (1974) **Congenital corneal clouding with abnormal systemic storage bodies: a new variant of mucolipidosis**. *J Pediatr*, 84:519-526. doi: 10.1016/S0022-3476(74)80671-2.

Bolte S., Cordelières F.P. (2006) **A guided tour into subcellular colocalization analysis in light microscopy**. *J Microsc*, 224:213-232. doi: 10.1111/j.1365-2818.2006.01706.x.

Bootman M.D., Chehab T., Bultynck G., Parys J.B., Rietdorf K. (2018) **The regulation of autophagy by calcium signals: Do we have a consensus?** *Cell Calcium*, 70:32-46. doi: 10.1016/j.ceca.2017.08.005.

Bradford M.M. (1976) **A rapid and sensitive method for the quantification of microgram quantities of protein utilizing the principle of protein-dye binding**. *Ann Biochem*, 72:248-254. doi: 10.1016/0003-2697(76)90527-3.

Brailoiu E., Churamani D., Cai X., Schrlau M.G., Brailoiu G.C., Gao X., *et al.* (2009) **Essential requirement for two-pore channel 1 in NAADP-mediated calcium signaling**. *J Cell Biol*, 186:201-219. doi: 10.1083/jcb.200904073.

Brailoiu E., Hooper R., Cai X., Brailoiu G.C., Keebler M.V., Dun N.J., *et al.* (2010) **An ancestral deuterostome family of two-pore channels mediates nicotinic acid adenine dinucleotide phosphate-dependent calcium release from acidic organelles**. *J Biol Chem*, 285:2897-2901. doi: 10.1074/jbc.C109.081943.

Brailoiu G.C., Brailoiu E. (2016) **Modulation of Calcium Entry by the Endo-lysosomal System**. In: Rosado J. (eds), Calcium Entry Pathways in Non-excitable Cells. *Adv Exp Med Biol*, vol 898. Springer, Cham. doi: 10.1007/978-3-319-26974-0_18.

Brouns R., De Deyn P.P. (2009) **The complexity of neurobiological processes in acute ischemic stroke**. *Clin Neurol Neurosurg*, 111:483-495. doi: 10.1016/j.clineuro.2009.04.001.

Brown W.J., Goodhouse J., Farquhar M.G. (1986) **Mannose-6-phosphate receptors for lysosomal enzymes cycle between the Golgi complex and endosomes**. *J Cell Biol*, 103:1235-1247.

Burgoyne T., Patel S., Eden E.R. (2015) **Calcium signaling at ER membrane contact sites**. *Biochim Biophys Acta*, 1853:2012-2017. doi: 10.1016/j.bbamcr.2015.01.022.

Burman C., Ktistakis N.T. (2010) **Regulation of autophagy by phosphatidylinositol 3-phosphate**. *FEBS Lett*, 584:1302-1312. doi: 10.1016/j.febslet.2010.01.011.

Bygrave F.L., Benedetti A. (1996) **What is the concentration of calcium ions in the endoplasmic reticulum?** *Cell Calcium*, 19:547-551.

Calcraft P.J., Ruas M., Pan Z., Cheng X., Arredouani A., Hao X., *et al.* (2009) **NAADP mobilizes calcium from acidic organelles through two-pore channels**. *Nature*, 459:596-600. doi: 10.1038/nature08030.

Cancela J.M., Churchill G.C., Galione A. (1999) **Coordination of agonist-induced Ca2+-signalling patterns by NAADP in pancreatic acinar cells**. *Nature*, 398:74-76.

Cang C., Zhou Y., Navarro B., Seo Y.J., Aranda K., Shi L., *et al.* (2013) **mTOR regulates lysosomal ATP-sensitive two-pore Na(+) channels to adapt to metabolic state**. *Cell*, 152:778-790. doi: 10.1016/j.cell.2013.01.023.

Cao Q., Yang Y., Zhong X.Z., Dong X.P. (2017) **The lysosomal Ca2+ release channel TRPML1 regulates lysosome size by activating calmodulin**. *J Biol Chem*, 292:8424-8435. doi: 10.1074/jbc.M116.772160.

Carloni S., Girelli S., Scopa C., Buonocore G., Longini M., Balduini W. (2010) **Activation of autophagy and Akt/CREB signaling play an equivalent role in the neuroprotective effect of rapamycin in neonatal hypoxia-ischemia**. *Autophagy*, 6:366-377.

Carlsson S.R., Simonsen A. (2015) **Membrane dynamics in autophagosome biogenesis**. *J Cell Sci*, 128:193-205. doi: 10.1242/jcs.141036.

Chandrachud U., Walker M.W., Simas A.M., Heetveld S., Petcherski A., Klein M., *et al.* (2015) **Unbiased Cell-based Screening in a Neuronal Cell Model of Batten Disease Highlights an Interaction between Ca2+ Homeostasis, Autophagy, and CLN3 Protein Function**. *J Biol Chem*, 290:14361-14380. doi: 10.1074/jbc.M114.621706.

Chao Y.K., Schludi V., Chen C.C., Butz E., Nguyen O.N.P., Müller M., *et al.* (2017) **TPC2 polymorphisms associated with a hair pigmentation phenotype in humans result in gain of channel function by independent mechanisms**. *Proc Natl Acad Sci U S A*, 114:E8595-E8602. doi: 10.1073/pnas.1705739114.

Chen C.C., Keller M., Hess M., Schiffmann R., Urban N., Wolfgardt A., *et al.* (2014) **A small molecule restores function to TRPML1 mutant isoforms responsible for mucolipidosis type IV**. *Nat Commun*, 5:4681. doi: 10.1038/ncomms5681.

Chen C.S., Bach G., Pagano R.E. (1998) **Abnormal transport along the lysosomal pathway in mucolipidosis, type IV disease**. *Proc Natl Acad Sci U S A*, 95:6373-6378. doi: 10.1073/pnas.95.11.6373.

Chen Q., She J., Zeng W., Guo J., Xu H., Bai XC., *et al.* (2017) **Structure of mammalian endolysosomal TRPML1 channel in nanodiscs**. *Nature*, 550:415-418. doi: 10.1038/nature24035.

Chen Y., Garcia G.E., Huang W., Constantini S. (2014) **The involvement of secondary neuronal damage in the development of neuropsychiatric disorders following brain insults**. *Front Neurol*, 5:22. doi: 10.3389/fneur.2014.00022.

Chen W., Sun Y., Liu K., Sun X. (2014) **Autophagy: a double-edged sword for neuronal survival after cerebral ischemia**. *Neural Regen Res*, 9:1210-1216. doi: 10.4103/1673-5374.135329.

Cheng X., Shen D., Samie M., Xu H. (2010) **Mucolipins: Intracellular TRPML1-3 channels**. *FEBS Lett*, 584:2013-2021. doi: 10.1016/j.febslet.2009.12.056.

Christensen K.A., Myers J.T., Swanson J.A. (2002) **pH-dependent regulation of lysosomal calcium in macrophages**. *J Cell Sci*, 115:599-607.

Churchill G.C., Galione A. (2001) **NAADP induces Ca2+ oscillations via a two-pool mechanism by priming IP3- and cADPR-sensitive Ca2+ stores**. *EMBO J*, 20:2666-2671.

Clark W.M., Lessov N.S., Dixon M.P., Eckenstein F. (1997) **Monofilament intraluminal middle cerebral artery occlusion in the mouse**. *Neurol Res*, 19:641-648.

Coen K., Flannagan R.S., Baron S., Carraro-Lacroix L.R., Wang D., Vermeire W., *et al.* (2012) **Lysosomal calcium homeostasis defects, not proton pump defects, cause endo-lysosomal dysfunction in PSEN-deficient cells**. *J Cell Biol*, 198:23-35. doi: 10.1083/jcb.201201076.

Collins T.P., Bayliss R., Churchill G.C., Galione A., Terrar D.A. (2011) **NAADP influences excitation-contraction coupling by releasing calcium from lysosomes in atrial myocytes**. *Cell Calcium*, 50:449-458. doi: 10.1016/j.ceca.2011.07.007.

Csordás G., Renken C., Várnai P., Walter L., Weaver D., Buttle K.F., *et al.* (2006) **Structural and functional features and significance of the physical linkage between ER and mitochondria**. *J Cell Biol*, 174:915-921. doi: 10.1083/jcb.200604016.

Cuervo A.M. (2010) **Chaperone-mediated autophagy: selectivity pays off**. *Trends Endocrinol Metab*, 21:142-150. doi: 10.1016/j.tem.2009.10.003.

Cullen P.J., Steinberg F. (2018) **To degrade or not to degrade: mechanisms and significance of endocytic recycling**. *Nat Rev Mol Cell Biol*, 19:679-696. doi: 10.1038/s41580-018-0053-7.

Curcio-Morelli C., Zhang P., Venugopal B., Charles F.A., Browning M.F., Cantiello H.F., *et al.* (2010a) **Functional multimerization of mucolipin channel proteins**. *J Cell Physiol*, 222:328-335. doi: 10.1002/jcp.21956.

Curcio-Morelli C., Charles F.A., Micsenyi M.C., Cao Y., Venugopal B., Browning M.F., *et al.* (2010b) **Macroautophagy is defective in mucolipin-1-deficient mouse neurons**. *Neurobiol Dis*, 40:370-377. doi: 10.1016/j.nbd.2010.06.010.

Czibener C., Sherer N.M., Becker S.M., Pypaert M., Hui E., Chapman E.R., *et al.* (2006) **Ca2+ and synaptotagmin VII-dependent delivery of lysosomal membrane to nascent phagosomes**. *J Cell Biol*, 174:997-1007. doi: 10.1083/jcb.200605004.

de Duve C., Pressman B.C., Gianetto R., Wattiaux R., Appelmans F. (1955) **Tissue fractionation studies. 6. Intracellular distribution patterns of enzymes in rat-liver tissue**. *Biochem J*, 60:604-617.

de Duve C. (2005) **The lysosome turns fifty**. *Nat Cell Biol*, 7:847-849. doi: 10.1038/ncb0905-847.

Di Palma F., Belyantseva I.A., Kim H.J., Vogt T.F., Kachar B., Noben-Trauth K. (2002) **Mutations in Mcoln3 associated with deafness and pigmentation defects in varitint-waddler (Va) mice**. *Proc Natl Acad Sci U S A*, 99:14994-14999. doi: 10.1073/pnas.222425399.

Di Paola S., Scotto-Rosato A., Medina D.L. (2018) **TRPML1: The Ca(2+)retaker of the lysosome**. *Cell Calcium*, 69:112-121. doi: 10.1016/j.ceca.2017.06.006.

Dong X.P., Cheng X., Mills E., Delling M., Wang F., Kurz T., *et al.* (2008) **The type IV mucolipidosis-associated protein TRPML1 is an endolysosomal iron release channel**. *Nature*, 455:992-996. doi: 10.1038/nature07311.

Dong X.P., Wang X., Shen D., Chen S., Liu M., Wang Y., *et al.* (2009) **Activating mutations of the TRPML1 channel revealed by proline-scanning mutagenesis**. *J Biol Chem*, 284:32040-32052. doi: 10.1074/jbc.M109.037184.

Dong X.P., Shen D., Wang X., Dawson T., Li X., Zhang Q., *et al.* (2010) **PI(3,5)P(2) controls membrane trafficking by direct activation of mucolipin Ca(2+) release channels in the endolysosome**. *Nat Commun*, 1:38. doi: 10.1038/ncomms1037.

Donnan G.A., Fisher M., Macleod M., Davis S.M. (2008) **Stroke**. *Lancet*, 371:1612-1623. doi: 10.1016/S0140-6736(08)60694-7.

Earley S., Brayden J.E. (2015) **Transient receptor potential channels in the vasculature**. *Physiol Rev*, 95:645-690. doi: 10.1152/physrev.00026.2014.

Efe J.A., Botelho R.J., Emr S.D. (2005) **The Fab1 phosphatidylinositol kinase pathway in the regulation of vacuole morphology**. *Curr Opin Cell Biol*, 17:402-428. doi: 10.1016/j.ceb.2005.06.002.

Eichelsdoerfer J.L., Evans J.A., Slaugenhaupt S.A., Cuajungco M.P. (2010) **Zinc dyshomeostasis is linked with the loss of mucolipidosis IV-associated TRPML1 ion channel**. *J Biol Chem*, 285:34304-34308. doi: 10.1074/jbc.C110.165480.

Eskelinen E.L., Tanaka Y., Saftig P. (2003) **At the acidic edge: emerging functions for lysosomal membrane proteins**. *Trends Cell Biol*, 13:137-145. doi: 10.1016/S0962-8924(03)00005-9.

Finbow M.E., Harrison M.A. (1997) **The vacuolar H+-ATPase: a universal proton pump of eukaryotes**. *Biochem J*, 324:697-712.

Garrity A.G., Wang W., Collier C.M., Levey S.A., Gao Q., Xu H. (2016) **The endoplasmic reticulum, not the pH gradient, drives calcium refilling of lysosomes**. *Elife*, 5. pii: e15887. doi: 10.7554/eLife.15887.

Goldberg M.P., Choi D.W. (1990) **Intracellular free calcium increases in cultured cortical neurons deprived of oxygen and glucose**. *Stroke*, 21:III75-77.

Grimm C., Hassan S., Wahl-Schott C., Biel M. (2012) **Role of TRPML and two-pore channels in endolysosomal cation homeostasis**. *J Pharmacol Exp Ther*, 342:236-244. doi: 10.1124/jpet.112.192880.

Grimm C., Cuajungco M.P. (2014) **TRPML Channels and Mucolipidosis Type IV** In: Weiss N. and Koschak A. (Eds.), *Pathologies of Calcium Channels*, Springer-Verlag Berlin Heidelberg. doi: 10.1007/978-3-642-40282-1_19.

Grimm C., Butz E., Chen C.C., Wahl-Schott C., Biel M. (2017) **From mucolipidosis type IV to Ebola: TRPML and two-pore channels at the crossroads of endo-lysosomal trafficking and disease**. *Cell Calcium*, 67:148-155. doi: 10.1016/j.ceca.2017.04.003.

Grynkiewicz G., Poenie M., Tsien R.Y. (1985) **A new generation of Ca^{2+} indicators with greatly improved fluorescence properties**. *J Biol Chem*, 260:3440-3450.

Guse A.H., Lee H.C. (2008) **NAADP: a universal Ca2+ trigger**. *Sci Signal*, 1:re10. doi: 10.1126/scisignal.144re10.

Hacke W., Kaste M., Bluhmki E., Brozman M., Dávalos A., Guidetti D., *et al.* (2008) **Thrombolysis with alteplase 3 to 4.5 hours after acute ischemic stroke**. *N Engl J Med.* 359:1317-1329. doi: 10.1056/NEJMoa0804656.

Haelewyn B., Risso J.J., Abraini J.H. (2010) **Human recombinant tissue-plasminogen activator (alteplase): why not use the 'human' dose for stroke studies in rats?** *J Cereb Blood Flow Metab*, 30:900-903. doi: 10.1038/jcbfm.2010.33.

Huang P., Zou Y., Zhong X.Z., Cao Q., Zhao K., Zhu M.X., *et al.* (2014) **P2X4 forms functional ATP-activated cation channels on lysosomal membranes regulated by luminal pH**. *J Biol Chem*, 289:17658-17667. doi: 10.1074/jbc.M114.552158.

Huotari J., Helenius A. (2011) **Endosome maturation**. *EMBO J*, 30:3481-3500. doi: 10.1038/emboj.2011.286.

Ishibashi K., Suzuki M., Imai M. (2000) **Molecular cloning of a novel form (two-repeat) protein related to voltage-gated sodium and calcium channels**. *Biochem Biophys Res Commun*, 270:370-376.

Jansen S.M., Groener J.E., Bax W., Poorthuis B.J. (2001) **Delayed lysosomal metabolism of lipids in mucolipidosis type IV fibroblasts after LDL-receptor-mediated endocytosis**. *J Inherit Metab Dis*, 24:577-586. doi: 10.1023/A:1012467827719.

Jefferies H.B., Cooke F.T., Jat P., Boucheron C., Koizumi T., Hayakawa M., *et al.* (2008) **A selective PIKfyve inhibitor blocks PtdIns(3,5)P(2) production and disrupts**

endomembrane transport and retroviral budding. *EMBO Rep*, 9:164-170. doi: 10.1038/sj.embor.7401155.

Karsy M., Brock A., Guan J., Taussky P., Kalani M.Y., Park M.S. (2017) **Neuroprotective strategies and the underlying molecular basis of cerebrovascular stroke**. *Neurosurg Focus*, 42:E3. doi: 10.3171/2017.1.FOCUS16522.

Kawano T., Anrather J., Zhou P., Park L., Wang G., Frys K.A., *et al.* (2006) **Prostaglandin E2 EP1 receptors: downstream effectors of COX-2 neurotoxicity**. *Nat Med*, 12:225-229.

Kilpatrick B.S., Eden E.R., Schapira A.H., Futter C.E., Patel S. (2013) **Direct mobilisation of lysosomal Ca2+ triggers complex Ca2+ signals**. *J Cell Sci*, 126:60-66. doi: 10.1242/jcs.118836.

Kilpatrick B.S. (2016a) **Connecting Ca2+ and lysosomes to Parkinson disease**. *Messenger (Los Angel)*, 5:76-86. doi: 10.1166/msr.2016.1059.

Kilpatrick B.S., Yates E., Grimm C., Schapira A.H., Patel S. (2016b) **Endo-lysosomal TRP mucolipin-1 channels trigger global ER Ca2+ release and Ca2+ influx**. *J Cell Sci*, 129:3859-3867. doi: 10.1242/jcs.190322.

Kim I., Xu W., Reed J.C. (2008) **Cell death and endoplasmic reticulum stress: disease relevance and therapeutic opportunities**. *Nat Rev Drug Discov*, 7:1013-1030. doi: 10.1038/nrd2755.

Kim J., Kundu M., Viollet B., Guan K.L. (2011) **AMPK and mTOR regulate autophagy through direct phosphorylation of Ulk1**. *Nat Cell Biol*, 13:132-141. doi: 10.1038/ncb2152.

Kinnear N.P., Wyatt C.N., Clark J.H., Calcraft P.J., Fleischer S., Jeyakumar L.H., *et al.* (2008) **Lysosomes co-localize with ryanodine receptor subtype 3 to form a trigger zone for calcium signalling by NAADP in rat pulmonary arterial smooth muscle**. *Cell Calcium*, 44:190-201. doi: 10.1016/j.ceca.2007.11.003.

Kintzer A.F., Stroud R.M. (2018) **On the structure and mechanism of two-pore channels**. *FEBS J,* 285:233-243. doi: 10.1111/febs.14154.

Kiselyov K., Chen J., Rbaibi Y., Oberdick D., Tjon-Kon-Sang S., Shcheynikov N., *et al.* (2005) **TRP-ML1 is a lysosomal monovalent cation channel that undergoes proteolytic cleavage**. *J Biol Chem*, 280:43218-43223. doi: 10.1074/jbc.M508210200.

Klionsky D.J., Abdelmohsen K., Abe A., Abedin M.J., Abeliovich H., Acevedo Arozena A., *et al.* (2016) **Guidelines for the use and interpretation of assays for monitoring autophagy (3rd edition)**. *Autophagy*, 12:1-222. doi: 10.1080/15548627.2015.1100356.

Lange I., Yamamoto S., Partida-Sanchez S., Mori Y., Fleig A., Penner R. (2009) **TRPM2 functions as a lysosomal Ca2+-release channel in beta cells**. *Sci Signal*, 2:ra23. doi: 10.1126/scisignal.2000278.

LaPlante J.M., Falardeau J., Sun M., Kanazirska M., Brown E.M., Slaugenhaupt S.A., *et al.* (2002) **Identification and characterization of the single channel function of human**

mucolipin-1 implicated in mucolipidosis type IV, a disorder affecting the lysosomal pathway. *FEBS Lett*, 532:183-187. doi: 10.1016/S0014-5793(02)03670-0.

LaPlante J.M., Sun M., Falardeau J., Dai D., Brown E.M., Slaugenhaupt S.A., *et al.* (2006) **Lysosomal exocytosis is impaired in mucolipidosis type IV**. *Mol Genet Metab*, 89:339-348. doi: 10.1016/j.ymgme.2006.05.016.

La Rovere R.M.L., Roest G., Bultynck G., Parys J.B. (2016) **Intracellular Ca(2+) signaling and Ca(2+) microdomains in the control of cell survival, apoptosis and autophagy**. *Cell Calcium*, 60:74-87. doi: 10.1016/j.ceca.2016.04.005.

Lee H.C. (2012) **Cyclic ADP-ribose and nicotinic acid adenine dinucleotide phosphate (NAADP) as messengers for calcium mobilization**. *J Biol Chem*, 287:31633-31640. doi: 10.1074/jbc.R112.349464.

Lee J.H., McBrayer M.K., Wolfe D.M., Haslett L.J., Kumar A., Sato Y., *et al.* (2015) **Presenilin 1 Maintains Lysosomal Ca(2+) Homeostasis via TRPML1 by Regulating vATPase-Mediated Lysosome Acidification**. *Cell Rep*, 12:1430-1444. doi: 10.1016/j.celrep.2015.07.050.

Li X., Rydzewski N., Hider A., Zhang X., Yang J., Wang W., *et al.* (2016) **A molecular mechanism to regulate lysosome motility for lysosome positioning and tubulation**. *Nat Cell Biol*, 18:404-417. doi: 10.1038/ncb3324.

Li M., Zhang W.K., Benvin N.M., Zhou X., Su D., Li H., *et al.* (2017) **Structural basis of dual Ca2+/pH regulation of the endolysosomal TRPML1 channel**. *Nat Struct Mol Biol*, 24:205-213. doi: 10.1038/nsmb.3362.

Liebl M.P., Hoppe T. (2016) **It's all about talking: two-way communication between proteasomal and lysosomal degradation pathways via ubiquitin**. *Am J Physiol Cell Physiol*, 311:C166-78. doi: 10.1152/ajpcell.00074.2016.

Lloyd-Evans E., Morgan A.J., He X., Smith D.A., Elliot-Smith E., Sillence D.J., *et al.* (2008) **Niemann-Pick disease type C1 is a sphingosine storage disease that causes deregulation of lysosomal calcium**. *Nat Med*, 14:1247-1255. doi: 10.1038/nm.1876.

Lloyd-Evans E., Platt F.M. (2011) **Lysosomal Ca(2+) homeostasis: role in pathogenesis of lysosomal storage diseases**. *Cell Calcium*, 50:200-205. doi: 10.1016/j.ceca.2011.03.010.

Lloyd-Evans E. (2016a) **On the move, lysosomal CAX drives Ca^{2+} transport and motility**. *J Cell Biol*, 212:755-757. doi: 10.1083/jcb.201603037.

Lloyd-Evans E. (2016b) **Acidic Ca2+ stores in neurodegeneration**. *Messenger (Los Angel)*, 5:37-55. doi: 10.1166/msr.2016.1054.

Longa E.Z., Weinstein P.R., Carlson S., Cummins R. (1989) **Reversible middle cerebral artery occlusion without craniectomy in rats**. *Stroke*, 20:84-91.

Luzio J.P., Pryor P.R., Bright N.A. (2007) **Lysosomes: fusion and function**. *Nat Rev Mol Cell Biol*, 8:622-632. doi: 10.1038/nrm2217.

Luzio J.P., Parkinson M.D., Gray S.R., Bright N.A. (2009) **The delivery of endocytosed cargo to lysosomes**. *Biochem Soc Trans*, 37:1019-1021. doi: 10.1042/BST0371019.

Malhotra J.D., Kaufman R.J. (2007) **The Endoplasmic Reticulum and the Unfolded Protein Response**. *Semin Cell Dev Biol*, 18:716-731. doi: 10.1016/j.semcdb.2007.09.003.

Manzanero S., Santro T., Arumugam T.V. (2013) **Neuronal oxidative stress in acute ischemic stroke: sources and contribution to cell injury**. *Neurochem Int*, 62:712-718. doi: 10.1016/j.neuint.2012.11.009.

Marks D.L., Holicky E.L., Wheatley C.L., Frumkin A., Bach G., Pagano R.E. (2012) **Role of protein kinase d in Golgi exit and lysosomal targeting of the transmembrane protein, Mcoln1**. *Traffic*. 13:565-575. doi: 10.1111/j.1600-0854.2012.01331.x.

Mauvezin C., Nagy P., Juhász G., Neufeld T.P. (2015) **Autophagosome-lysosome fusion is independent of V-ATPase-mediated acidification**. *Nat Commun*, 6:7007. doi: 10.1038/ncomms8007.

Medina D.L., Fraldi A., Bouche V., Annunziata F., Mansueto G., Spampanato C., *et al.* (2011) **Transcriptional activation of lysosomal exocytosis promotes cellular clearance**. *Dev Cell*, 21:421-430. doi: 10.1016/j.devcel.2011.07.016.

Medina D.L., Di Paola S., Peluso I., Armani A., De Stefani D., Venditti R., *et al.* (2015) **Lysosomal calcium signalling regulates autophagy through calcineurin and TFEB**. *Nat Cell Biol*, 17:288-299. doi: 10.1038/ncb3114.

Melchionda M., Pittman J.K., Mayor R., Patel S. (2016) **Ca^{2+}/H^+ exchange by acidic organelles regulates cell migration in vivo**. *J Cell Biol*, 212:803-813. doi: 10.1083/jcb.201510019.

Miedel M.T., Weixel K.M., Bruns J.R., Traub L.M., Weisz O.A. (2006) **Posttranslational cleavage and adaptor protein complex-dependent trafficking of mucolipin-1**. *J Biol Chem*, 281:12751-12759. doi: 10.1074/jbc.M511104200.

Miedel M.T., Rbaibi Y., Guerriero C.J., Colletti G., Weixel K.M., Weisz O.A., *et al.* (2008) **Membrane traffic and turnover in TRP-ML1-deficient cells: a revised model for mucolipidosis type IV pathogenesis**. *J Exp Med*, 205:1477-1490. doi: 10.1084/jem.20072194.

Mindell J.A. (2012) **Lysosomal acidification mechanisms**. *Annu Rev Physiol*, 74:69-86. doi: 10.1146/annurev-physiol-012110-142317.

Morgan A.J., Platt F.M., Lloyd-Evans E., Galione A. (2011) **Molecular mechanisms of endolysosomal Ca^{2+} signalling in health and disease**. *Biochem J*, 439:349-374. doi: 10.1042/BJ20110949.

Morgan A.J., Davis L.C., Wagner S.K., Lewis A.M., Parrington J., Churchill G.C., *et al.* (2013) **Bidirectional Ca^{2+} signaling occurs between the endoplasmic reticulum and acidic organelles**. *J Cell Biol*, 200:789-805. doi: 10.1083/jcb.201204078.

Morishima N., Nakanishi K., Takenouchi H., Shibata T., Yasuhiko Y. (2002) **An endoplasmic reticulum stress-specific caspase cascade in apoptosis. Cytochrome c-independent**

activation of caspase-9 by caspase-12. *J Biol Chem*, 277:34287-34294. doi: 10.1074/jbc.M204973200.

Neiss W.F. (1984) **A coat of glycoconjugates on the inner surface of the lysosomal membrane in the rat kidney**. *Histochemistry*, 80:603-688.

Nilius B., Owsianik G., Voets T., Peters J.A. (2007) **Transient receptor potential cation channels in disease**. *Physiol Rev*, 87:165-217. doi: 10.1152/physrev.00021.2006.

Nixon R.A., Yang D.S. (2012) **Autophagy and neuronal cell death in neurological disorders**. *Cold Spring Harb Perspect Biol*, 4.pii: a008839. doi: 10.1101/cshperspect.a008839.

Nixon R.A. (2013) **The role of autophagy in neurodegenerative disease**. *Nat Med*, 19:983-997. doi: 10.1038/nm.3232.

Ohkuma S., Moriyama Y., Takano T. (1982) **Identification and characterization of a proton pump on lysosomes by fluorescein-isothiocyanate-dextran fluorescence**. *Proc Natl Acad Sci U S* A, 79:2758-2762.

Pallast S., Arai K., Pekcec A., Yigitkanli K., Yu Z., Wang X., *et al*. (2010) **Increased nuclear apoptosis-inducing factor after transient focal ischemia: a 12/15-lipoxygenase-dependent organelle damage pathway**. *J Cereb Blood Flow Metab*, 30:1157-1167. doi: 10.1038/jcbfm.2009.281.

Palmieri M., Impey S., Kang H., di Ronza A., Pelz C., Sardiello M., *et al.* (2011) **Characterization of the CLEAR network reveals an integrated control of cellular clearance pathways**. *Hum Mol Genet,* 20:3852-3866. doi: 10.1093/hmg/ddr306.

Pandya R.S., Mao L., Zhou H., Zhou S., Zeng J., Popp A.J., *et al.* (2011) **Central nervous system agents for ischemic stroke: neuroprotection mechanisms**. *Cent Nerv Syst Agents Med Chem*, 11:81-97.

Paschen W., Aufenberg C., Hotop S., Mengesdorf T. (2003) **Transient cerebral ischemia activates processing of xbp1 messenger RNA indicative of endoplasmic reticulum stress**. *J Cereb Blood Flow Metab*, 23:449-461. doi: 10.1097/01.WCB.0000054216.21675.AC.

Paschen W., Mengesdorf T. (2005) **Endoplasmic reticulum stress response and neurodegeneration**. *Cell Calcium*, 38:409-415. doi: 10.1016/j.ceca.2005.06.019

Patel S., Docampo R. (2009) **In with the TRP channels: intracellular functions for TRPM1 and TRPM2**. *Sci Signal*, 2:pe69. doi: 10.1126/scisignal.295pe69.

Patel S., Docampo R. (2010) **Acidic calcium stores open for business: expanding the potential for intracellular Ca^{2+} signaling**. *Trends Cell Biol*, 20:277-286. doi: 10.1016/j.tcb.2010.02.003.

Patel S., Cai X. (2015) **Evolution of acidic Ca^{2+} stores and their resident Ca^{2+}-permeable channels**. *Cell Calcium*, 57:222-230. doi: 10.1016/j.ceca.2014.12.005.

Penny C.J., Kilpatrick B.S., Eden E.R., Patel S. (2015) **Coupling acidic organelles with the ER through Ca²⁺ microdomains at membrane contact sites**. *Cell Calcium* 58:387-396. doi: 10.1016/j.ceca.2015.03.006.

Perraud A.L., Fleig A., Dunn C.A., Bagley L.A., Launay P., Schmitz C., *et al.* (2001) **ADP-ribose gating of the calcium-permeable LTRPC2 channel revealed by Nudix motif homology**. *Nature*, 411:595-599. doi: 10.1038/35079100.

Pignataro G., Meller R., Inoue K., Ordonez A.N., Ashley M.D., Xiong Z., *et al.* (2008) **In vivo and in vitro characterization of a novel neuroprotective strategy for stroke: ischemic postconditioning**. *J Cereb Blood Flow Metab*, 28:232-241. doi: 10.1038/sj.jcbfm.9600559.

Pittman J.K. (2011) **Vacuolar Ca(2+) uptake**. *Cell Calcium*, 50:139-146. doi: 10.1016/j.ceca.2011.01.004.

Pryor P.R., Reimann F., Gribble F.M., Luzio J.P. (2006) **Mucolipin-1 is a lysosomal membrane protein required for intracellular lactosylceramide traffic**. *Traffic*, 7:1388-1398. doi: 10.1111/j.1600-0854.2006.00475.x.

Puertollano R., Kiselyov K. (2009) **TRPMLs: in sickness and in health**. *Am J Physiol Renal Physiol*, 296:F1245-F1254. doi: 10.1152/ajprenal.90522.2008

Qureshi O.S., Paramasivam A., Yu J.C., Murrell-Lagnado R.D. (2007) **Regulation of P2X4 receptors by lysosomal targeting, glycan protection and exocytosis**. *J Cell Sci*, 120:3838-3849. doi: 10.1242/jcs.010348.

Raas-Rothschild A., Bargal R., Della Pergola S., Zeigler M., Bach G. (1999) **Mucolipidosis type IV: the origin of the disease in the Ashkenazi Jewish population**. *Eur J Hum Genet*, 7:496-498. doi: 10.1038/sj.ejhg.5200277.

Rajah G.B., Ding Y. (2017) **Experimental neuroprotection in ischemic stroke: a concise review**. *Neurosurg Focus*, 42:E2. doi: 10.3171/2017.1.FOCUS16497.

Rao R.V., Castro-Obregon S., Frankowski H., Schuler M., Stoka V., del Rio G., *et al.* (2002) **Coupling endoplasmic reticulum stress to the cell death program. An Apaf-1-independent intrinsic pathway**. *J Biol Chem*, 277:21836-21842. doi: 10.1074/jbc.M202726200.

Ravikumar B., Sarkar S., Davies J.E., Futter M., Garcia-Arencibia M., Green-Thompson Z.W., *et al.* (2010) **Regulation of mammalian autophagy in physiology and pathophysiology**. *Physiol Rev*, 90:1383-1435. doi: 10.1152/physrev.00030.2009.

Reggiori F., Klumperman J. (2016) **Lysosome biogenesis and autophagy**. In: Maxfield F.R., Willard J.M., Lu S. (Eds.), Lysosomes: Biology, Diseases, and Therapeutics. John Wiley & Sons, Inc., Hoboken, New Jersey, pp. 7-31. doi: 10.1002/9781118978320.ch2.

Rosenbaum A.I., Maxfield F.R. (2011) **Niemann-Pick type C disease: molecular mechanisms and potential therapeutic approaches**. *J Neurochem*, 116:789-795. doi: 10.1111/j.1471-4159.2010.06976.x.

Saftig P., Klumperman J. (2009) **Lysosome biogenesis and lysosomal membrane proteins: trafficking meets function**. *Nat Rev Mol Cell Biol,* 10:623-635. doi: 10.1038/nrm2745.

Saftig P., Schröder B., Blanz J. (2010) **Lysosomal membrane proteins: life between acid and neutral conditions**. *Biochem Soc Trans*, 38:1420-1423. doi: 10.1042/BST0381420.

Samie M., Wang X., Zhang X., Goschka A., Li X., Cheng X., *et al.* (2013) **A TRP channel in the lysosome regulates large particle phagocytosis via focal exocytosis**. *Dev Cell*, 26:511-524. doi: 10.1016/j.devcel.2013.08.003.

Sardiello M., Palmieri M., di Ronza A., Medina D.L., Valenza M., Gennarino V.A., *et al.* (2009) **A gene network regulating lysosomal biogenesis and function**. *Science*, 325:473-7. 47doi: 10.1126/science.1174447.

Schmiege P., Fine M., Blobel G., Li X. (2017) **Human TRPML1 channel structures in open and closed conformations**. *Nature*, 550:366-370. doi: 10.1038/nature24036.

Schulze H., Kolter T., Sandhoff K. (2009) **Principles of lysosomal membrane degradation: Cellular topology and biochemistry of lysosomal lipid degradation**. *Biochim Biophys Acta*, 1793:674-683. doi: 10.1016/j.bbamcr.2008.09.020.

Scorziello A., Pellegrini C., Forte L., Tortiglione A., Gioielli A., Iossa S., *et al.* (2001) **Differential vulnerability of cortical and cerebellar neurons in primary culture to oxygen glucose deprivation followed by reoxygenation**. *J Neurosci Res*, 63:20-26.

Scorziello A., Savoia C., Sisalli M.J., Adornetto A., Secondo A., Boscia F., *et al* (2013) **NCX3 regulates mitochondrial Ca(2+) handling through the AKAP121-anchored signaling complex and prevents hypoxia-induced neuronal death**. *J Cell Sci*, 126:5566-5577. doi: 10.1242/jcs.129668.

Secondo A., Staiano R.I., Scorziello A., Sirabella R., Boscia F., Adornetto A., *et al.* (2007) **BHK cells transfected with NCX3 are more resistant to hypoxia followed by reoxygenation than those transfected with NCX1 and NCX2: possible relationship with mitochondrial membrane potential**. *Cell Calcium*, 42:521-535. doi: 10.1016/j.ceca.2007.01.006.

Settembre C., Fraldi A., Medina D.L., Ballabio A. (2013) **Signals from the lysosome: a control centre for cellular clearance and energy metabolism**. *Nat Rev Mol Cell Biol*, 14:283-296. doi: 10.1038/nrm3565.

Settembre C., Ballabio A. (2014) **Lysosomal adaptation: how the lysosome responds to external cues**. *Cold Spring Harb Perspect Biol*, pii: a016907. doi: 10.1101/cshperspect.a016907.

Shen D., Wang X., Li X., Zhang X., Yao Z., Dibble S., *et al.* (2012) **Lipid storage disorders block lysosomal trafficking by inhibiting a TRP channel and lysosomal calcium release**. *Nat Commun*, 3:731. doi: 10.1038/ncomms1735.

Shibata M., Hattori H., Sasaki T., Gotoh J., Hamada J., Fukuuchi Y. (2003) **Activation of caspase-12 by endoplasmic reticulum stress induced by transient middle cerebral artery occlusion in mice**. *Neuroscience*, 118:491-499.

Sirabella R., Secondo A., Pannaccione A., Scorziello A., Valsecchi V., Adornetto A., *et al.* (2009) **Anoxia-induced NF-kappaB-dependent upregulation of NCX1 contributes to Ca2+**

refilling into endoplasmic reticulum in cortical neurons. *Stroke*, 40:922-929. doi: 10.1161/STROKEAHA.108.531962.

Slaugenhaupt S.A., Acierno J.S. Jr., Helbling L.A., Bove C., Goldin E., Bach G., *et al.* (1999) **Mapping of the Mucolipidosis Type IV Gene to Chromosome 19p and Definition of Founder Haplotypes**. *Am J Hum Genet*, 65:773-778.

Spassova M.A., Soboloff J., He L.P., Xu W., Dziadek M.A., Gill D.L. (2006) **STIM1 has a plasma membrane role in the activation of store-operated Ca(2+) channels**. *Proc Natl Acad Sci U S A*, 103:4040-4045.

Spooner E., McLaughlin B.M., Lepow T., Durns T.A., Randall J., Upchurch C., *et al.* (2013) **Systematic screens for proteins that interact with the mucolipidosis type IV protein TRPML1**. *PLoS One*, 8:e56780. doi: 10.1371/journal.pone.0056780.

Sterea A.M., Almasi S., El Hiani Y. (2018) **The hidden potential of lysosomal ion channels: A new era of oncogenes**. *Cell Calcium*, 72:91-103. doi: 10.1016/j.ceca.2018.02.006.

Styrt B., Pollack C.R., Klempner M.S. (1988) **An abnormal calcium uptake pump in Chediak-Higashi neutrophil lysosomes**. *J Leukoc Biol*, 44:130-135.

Stolz A., Ernst A., Dikic I. (2014) **Cargo recognition and trafficking in selective autophagy**. *Nat Cell Biol*, 16:495-501. doi: 10.1038/ncb2979.

Sumoza-Toledo A., Penner R. (2011) **TRPM2: a multifunctional ion channel for calcium signalling**. *J* Physiol, 589:1515-1525. doi: 10.1113/jphysiol.2010.201855.

Sun L., Hua Y., Vergarajauregui S., Diab H.I., Puertollano R. (2015) **Novel Role of TRPML2 in the Regulation of the Innate Immune Response**. *J Immunol*, 195:4922-4932. doi: 10.4049/jimmunol.1500163.

Sun M., Goldin E., Stahl S., Falardeau J.L., Kennedy J.C., Acierno J.S. Jr, *et al.* (2000) **Mucolipidosis type IV is caused by mutations in a gene encoding a novel transient receptor potential channel**. *Hum Mol Genet*, 9:2471-2478. doi: 10.1093/hmg/9.17.2471.

Sun T., Wang X., Lu Q., Ren H., Zhang H. (2011) **CUP-5, the C. elegans ortholog of the mammalian lysosomal channel protein MLN1/TRPML1, is required for proteolytic degradation in autolysosomes**. *Autophagy*, 7:1308-1315. doi: 10.4161/auto.7.11.17759.

Suurväli J., Boudinot P., Kanellopoulos J., Rüütel Boudinot S. (2017) **P2X4: A fast and sensitive purinergic receptor**. *Biomed* J, 40:245-256. doi: 10.1016/j.bj.2017.06.010.

Traystman R.J. (2003) **Animal models of focal and global cerebral ischemia**. *ILAR* J, 44:85-95.

Treusch S., Knuth S., Slaugenhaupt S.A., Goldin E., Grant B.D., Fares H. (2004) **Caenorhabditis elegans functional orthologue of human protein h-mucolipin-1 is required for lysosome biogenesis**. *Proc Natl Acad Sci U S A*, 101:4483-4488. doi: 10.1073/pnas.0400709101.

Urbanczyk J., Chernysh O., Condrescu M., Reeves J.P. (2006) **Sodium-calcium exchange does not require allosteric calcium activation at high cytosolic sodium concentrations**. *J Physiol*, 575:693-705. doi: 10.1113/jphysiol.2006.113910.

Várnai P., Hunyady L., Balla T. (2009) **STIM and Orai: the long-awaited constituents of store-operated calcium entry**. *Trends Pharmacol Sci*, 30:118-128. doi: 10.1016/j.tips.2008.11.005.

Venkatachalam K., Long A.A., Elsaesser R., Nikolaeva D., Broadie K., Montell C. (2008) **Motor deficit in a Drosophila model of mucolipidosis type IV due to defective clearance of apoptotic cells**. *Cell*, 135:838-851. doi: 10.1016/j.cell.2008.09.041.

Venkatachalam K., Wong C.O., Zhu M.X. (2015) **The role of TRPMLs in endolysosomal trafficking and function**. *Cell Calcium*, 58:48-56. doi: 10.1016/j.ceca.2014.10.008.

Venugopal B., Browning M.F., Curcio-Morelli C., Varro A., Michaud N., Nanthakumar N., *et al.* (2007) **Neurologic, Gastric, and Opthalmologic Pathologies in a Murine Model of Mucolipidosis Type IV**. *Am J Hum Genet*, 81: 1070-1083. doi: 10.1086/521954.

Venugopal B., Mesires N.T., Kennedy J.C., Curcio-Morelli C., Laplante J.M., Dice J.F., *et al.* (2009) **Chaperone-mediated autophagy is defective in mucolipidosis type IV**. *J Cell Physiol*, 219:344-353. doi: 10.1002/jcp.21676.

Vergarajauregui S., Puertollano R. (2006) **Two di-leucine motifs regulate trafficking of mucolipin-1 to lysosomes**. *Traffic*, 7:337-353. doi: 10.1111/j.1600-0854.2006.00387.x.

Vergarajauregui S., Oberdick R., Kiselyov K., Puertollano R. (2008a) **Mucolipin 1 channel activity is regulated by protein kinase A-mediated phosphorylation**. *Biochem J*, 410:417-425. doi: 10.1042/BJ20070713.

Vergarajauregui S., Connelly P.S., Daniels M.P., Puertollano R. (2008b) **Autophagic dysfunction in mucolipidosis type IV patients**. *Hum Mol Genet*, 17:2723-2737. doi: 10.1093/hmg/ddn174.

Vergarajauregui S., Martina J.A., Puertollano R. (2009) **Identification of the penta-EF-hand protein ALG-2 as a Ca2+-dependent interactor of mucolipin-1**. *J Biol Chem*, 284:36357-36366. doi: 10.1074/jbc.M109.047241.

Vergarajauregui S., Martina J.A., Puertollano R. (2011) **LAPTMs regulate lysosomal function and interact with mucolipin 1: new clues for understanding mucolipidosis type IV**. *J Cell Sci*, 124:459-468. doi: 10.1242/jcs.076240.

Wakabayashi K., Gustafson A.M., Sidransky E., Goldin E. (2011) **Mucolipidosis type IV: an update**. *Mol Genet Metab*, 104:206-213. doi: 10.1016/j.ymgme.2011.06.006.

Wang X., Zhang X., Dong X.P., Samie M., Li X., Cheng X., *et al.* (2012) **TPC proteins are phosphoinositide- activated sodium-selective ion channels in endosomes and lysosomes**. *Cell*, 151:372-383. doi: 10.1016/j.cell.2012.08.036.

Wen Y.D., Sheng R., Zhang L.S., Han R., Zhang X., Zhang X.D., *et al.* (2008) **Neuronal injury in rat model of permanent focal cerebral ischemia is associated with activation of autophagic and lysosomal pathways**. *Autophagy*, 4:762-769.

Wong E., Cuervo A.M. (2010) **Integration of clearance mechanisms: the proteasome and autophagy**. *Cold Spring Harb Perspect Biol*, 2:a006734. doi: 10.1101/cshperspect.a006734.

Xin X.Y., Pan J., Wang X.Q., Ma J.F., Ding J.Q., Yang G.Y., *et al.* (2011) **2-methoxyestradiol attenuates autophagy activation after global ischemia**. *Can J Neurol Sci*, 38:631-638.

Xu H., Ren D. (2015) **Lysosomal physiology**. *Annu Rev* Physiol, 77:57-80. doi: 10.1146/annurev-physiol-021014-071649.

Yamaguchi S., Jha A., Li Q., Soyombo A.A., Dickinson G.D., Churamani D., *et al.* (2011) **Transient receptor potential mucolipin 1 (TRPML1) and two-pore channels are functionally independent organellar ion channels**. *J Biol Chem*, 286:22934-22942. doi: 10.1074/jbc.M110.210930.

Yamamoto A., Tagawa Y., Yoshimori T., Moriyama Y., Masaki R., Tashiro Y. (1998) **Bafilomycin A1 prevents maturation of autophagic vacuoles by inhibiting fusion between autophagosomes and lysosomes in rat hepatoma cell line, H-4-II-E cells**. *Cell Struct Funct*, 23:33-42.

Yang Z., Klionsky D.J. (2009) **An overview of the molecular mechanism of autophagy**. *Curr Top Microbiol Immunol*, 335:1-32. doi: 10.1007/978-3-642-00302-8_1.

Yin Y., Sun G., Li E., Kiselyov K., Sun D. (2017) **ER stress and impaired autophagy flux in neuronal degeneration and brain injury**. *Ageing Res Rev*, 34:3-14. doi: 10.1016/j.arr.2016.08.008.

Zeevi D.A., Frumkin A., Bach G. (2007) **TRPML and lysosomal function**. *Biochim Biophys Acta*, 1772:851-858. doi: 10.1016/j.bbadis.2007.01.004.

Zeevi D.A., Frumkin A., Offen-Glasner V., Kogot-Levin A., Bach G. (2009) **A potentially dynamic lysosomal role for the endogenous TRPML proteins**. *J Pathol*, 219:153-162. doi: 10.1002/path.2587.

Zhang F., Li P.L. (2007) **Reconstitution and characterization of a nicotinic acid adenine dinucleotide phosphate (NAADP)-sensitive Ca2+ release channel from liver lysosomes of rats**. *J Biol Chem*, 282:25259-25269. doi: 10.1074/jbc.M701614200.

Zhang F., Jin S., Yi F., Li P.L. (2009) **TRP-ML1 functions as a lysosomal NAADP-sensitive Ca2+ release channel in coronary arterial myocytes**. *J Cell Mol Med*, 13:3174-3185. doi: 10.1111/j.1582-4934.2008.00486.x.

Zhang F., Xu M., Han W.Q., Li P.L. (2011) **Reconstitution of lysosomal NAADP-TRP-ML1 signaling pathway and its function in TRP-ML1(-/-) cells**. *Am J Physiol Cell Physiol*, 301:C421-C430. doi: 10.1152/ajpcell.00393.2010.

Zhang X., Li X., Xu H. (2012) **Phosphoinositide isoforms determine compartment-specific ion channel activity**. *Proc Natl Acad Sci U S A*, 109:11384-11389. doi: 10.1073/pnas.1202194109.

Zhang X., Cheng X., Yu L., Yang J., Calvo R., Patnaik S., *et al.* (2016) **MCOLN1 is a ROS sensor in lysosomes that regulates autophagy**. *Nat Commun*, 7:12109. doi: 10.1038/ncomms12109.

Zhang S., Li N., Zeng W., Gao N., Yang M. (2017) **Cryo-EM structures of the mammalian endo-lysosomal TRPML1 channel elucidate the combined regulation mechanism**. *Protein Cell*, 8:834-847. doi: 10.1007/s13238-017-0476-5.

Zhong X.Z., Dong X.P. (2015) **Lysosome electrophysiology**. *Methods Cell Biol*, 126:197-215. doi: 10.1016/bs.mcb.2014.10.022.

Zhou Z.B., Meng L., Gelb A.W., Lee R., Huang W.Q. (2016) **Cerebral ischemia during surgery: an overview**. *J Biomed Res*, 30:83-87. doi: 10.7555/JBR.30.20150126.

Zong X., Schieder M., Cuny H., Fenske S., Gruner C., Rötzer K., *et al.* (2009) **The two-pore channel TPCN2 mediates NAADP-dependent Ca(2+)-release from lysosomal stores**. *Pflugers Arch*, 458:891-899. doi: 10.1007/s00424-009-0690-y.